University of Washington
Department of Civil and Environmental Engineering

HYDROLOGIC RESPONSE OF RESIDENTIAL-SCALE LAWNS ON TILL CONTAINING VARIOUS AMOUNTS OF COMPOST AMENDMENT

Kyle F. Kolsti
Stephen J. Burges
Bruce W. Jensen

Water Resources Series
Technical Report No. 147
September 1995

Seattle, Washington
98195

Department of Civil Engineering
University of Washington
Seattle, Washington 98195

HYDROLOGIC RESPONSE OF RESIDENTIAL SCALE-LAWNS ON TILL CONTAINING VARIOUS AMOUNTS OF COMPOST AMENDMENT

Kyle F. Kolsti
Stephen J. Burges
Bruce W. Jensen

Water Resources Series
Technical Report No. 147

September 1995

Department of Civil Engineering
University of Washington
Seattle, Washington 98195 - 2700

Hydrologic response of residential-scale lawns on till containing various amounts of compost amendment

by

Kyle F. Kolsti
Stephen J. Burges
Bruce W. Jensen

Water Resources Series
Technical Report No. 147

September 1995

Project Title: Improved Residential Onsite Stormwater Management

Grant Source: Washington Department of Ecology
Centennial Clean Water Fund Program FY 1993

Grant Number: G9400029

Matching Funds: City of Redmond, Washington.
King County Department of Public Works.

Project Period: July 20, 1993 - December 31, 1995

Department of Civil Engineering
University of Washington
Seattle, Washington 98195 - 2700

Hydrologic response of residential-scale lawns on till containing various amounts of compost amendment

by

Kyle F. Kolsti
Stephen J. Burges
Bruce W. Jensen

Water Resources Series
Technical Report No. 147

September 1995

Project Title:	Improved Residential Onsite Stormwater Management
Grant Source:	Washington Department of Ecology Centennial Clean Water Fund Program FY 1993
Grant Number:	G9400029
Matching Funds:	City of Redmond, Washington. King County Department of Public Works.
Project Period:	July 20, 1993 - December 31, 1995
Principal Investigator:	Stephen J. Burges Professor of Civil Engineering

ABSTRACT

In the Puget Sound lowlands of Washington State, the conversion of forested land to residential use may produce a wide range of detrimental effects due to changes in the hydrologic behavior of the catchment. The common practice for residential lawn construction is to plant grass or place sod on shallow soil overlying till. For the suburban land use condition, the increase in runoff from these lawns, as well as from impervious areas, results in a greater frequency of channel-changing runoff rates and volumes. This study examined the hydrologic response of residential-scale lawns on till containing various amounts of compost amendment. The working hypothesis was that amended soils were likely to have potential for reducing runoff-related problems of residential catchments.

Seven 24-m^2 test plots were built at the Center for Urban Horticulture at the University of Washington Seattle campus to examine the hydrologic effects of various forms of compost amendments on till soils at the hillslope scale. An instrumentation system which included piezometers, runoff collectors, and a weather station was used to monitor the rainfall, runoff, and storage of each plot from December, 1994, to June, 1995. From these data, hydrographs and statistical measures were generated to compare response behavior between plots and to infer the dominant hydrologic mechanisms. Artificial rainfall from sprinklers was used to examine the areal average response of each plot for a range of synthetic storm patterns and depths.

Beneficial effects on runoff response behavior were observed from plots with higher amounts of fine, well-aged compost. During natural storms, these plots generated 53% and 70% of the runoff volume observed from the unamended control plots. The reason for this reduction in storm runoff was the increased hydraulic conductivity of the amended soils, which allowed rain water to infiltrate and be detained. Between storms this

detained water was released as baseflow. In one amended soil the increase in conductivity relative to the till control altered the flow-generating mechanisms, with saturation overland flow becoming the prime mechanism rather than Horton infiltration-limited overland flow. There were few if any beneficial hydrologic effects from plots with coarse compost (containing visible wood fragments) or plots with leaner mixes of compost.

The results demonstrate that using compost to amend a lawn on till can, under some circumstances, significantly enhance the ability of the lawn to infiltrate, store, and release water as baseflow. Basin-wide soil amendment warrants further exploration as a stormwater management mitigation practice.

ACKNOWLEDGEMENT

This report is based on the Master's Degree thesis of the first author. Christopher Konrad provided critical assistance with the construction of the test plots. Dr. Robert Harrison of the College of Forest Resources provided many helpful discussions during the course of the project.

Many people contributed to this project. Phil Cohen, City of Redmond Department of Public Works, was instrumental in motivating and funding the project. Dr. Lorin Reinelt, King County Department of Public Works Surface Water Management, provided critical assistance in obtaining the grant. Compost for amending the till was donated by Jan Allen of Cedar Grove, Inc., and Leonard Winebrenner of Groco, Inc. Till was delivered to the field site by the Hoss Brothers and J. R. Hayes trucking companies. We thank Terra Hegy, our Department of Ecology project officer, for her interest and enthusiastic support.

The assistance provided by the director and staff of the University of Washington Center for Urban Horticulture was crucial. We thank Dr. Clem Hamilton, Director, Center for Urban Horticulture, for granting permission to use the Center's grounds for the field study, and to Fred Hoyt, Grounds/Greenhouse Supervisor, for his collegiality, advice, and help in coordinating equipment at the site.

Table of Contents

List of Figures

List of Tables

Chapter 1 - Introduction

1.1 Problem statement

Most natural hillslopes in King County in Western Washington are forested, with dense understory vegetation and a permeable, absorbent layer of organic material (forest duff) and permeable mineral soil at the ground surface [*Bain*, 1989]. The topsoil is shallow and underlain by Vashon Till, a "very dense, gray, silty to very silty, gravely, fine to coarse sand with scattered cobbles and boulders and a trace of clay" [*Olmsted*, 1969]. Approximately 15,000 years ago this till was overlain by 1000 meters of ice, and is therefore highly compacted. Bulk densities range to 2.6 g/cm^3 and hydraulic conductivities range from 10^{-7} to 10^{-5} cm/sec, making the till an "excellent material for dikes and dams." [*Olmsted*, 1969] Conversely, and for the same reasons, the till performs poorly as a rainwater storage medium.

Land use change associated with urbanization alters the hydrologic behavior of the catchment. Most of the trees are removed and the layers of duff and loose soil are scraped off to reveal the solid till, which provides a good base for road and building foundations. The newly impervious areas of roofs, driveways, and roads contribute runoff to stream channels which was previously absorbed by the catchment. Of comparable significance, however, is the runoff contribution by lawns. For landscaping, turf is established on a 2 to 5 cm layer of topsoil or sod over compacted till [*Bain*, 1989]. The resulting lawns collectively have a greatly reduced stormwater retention capacity relative to the natural state. Over a three-year study of a residential 17-ha catchment near Seattle, between 39% (1993) and 60% (1991) of the measured runoff originated from the 70% of the catchment which was principally pervious lawn [*Wigmosta et al*, 1994]. These results indicate that the ability of poorly constructed lawns to store water is only slightly better than that of the roads, streets, and roofs, counter to widespread local views and research in other parts of the country [*Striebe*, 1994]. The observed urban catchment behavior is also due to the relatively long duration of storms in the Puget Sound region which keep the soils wet for extended periods.

In the United States, a common stormwater management effort consists of conveyance systems (storm sewers, swales, and gutters) which transport site runoff to management structures or reservoirs located towards the bottom of the catchment. Stormwater has been viewed as "a form of refuse to be collected and disposed of as rapidly and as thoroughly as possible." [*Argue*, 1988] Accordingly, Puget Sound counties have historically attempted to mitigate the increased stormwater flows with extensive capital improvement projects such as detention ponds, wetlands, and channel improvements [*Bain*, 1989]. These attempts have been marginally successful. Additionally, the large land area required for such mitigation facilities is a liability for residential property developers.

As the population of Puget Sound continues to grow, the drainage problems associated with increased suburbanization of the previously forested hillsides will become more severe unless paradigms of stormwater management are re-examined and new technologies are evaluated, developed, and employed.

1.2 Research objectives

The current stormwater management practice described above contains the implicit concession that development in a catchment cannot be performed without adversely affecting its hydrologic response. Recently, a more optimistic approach of alternative stormwater management techniques has begun to interest the engineering and scientific communities: source control, or on-site management. On-site management techniques presume to make the urbanized catchment behave in a more similar manner to the natural state. Existing on-site systems include pervious pavements, infiltration structures, cisterns to store water for future use, and other local treatments. By controlling the runoff at its source rather than at a collection point, the following benefits may be realized:

1. Less costly downstream works
2. More area for profitable development (due to smaller control structures)
3. Improved groundwater recharge
4. Improved moisture retention of the soils resulting in lower summer irrigation demand

This study investigates the hydrologic effects of amending glacial till soil plots with different types and amounts of compost by mixing the compost into the existing till soil to a depth of about 0.3 meters. It is hypothesized that amending the soil in this manner will make the soil more effective in storing and releasing rain water, more permeable and better able to transmit water through the soil, and more suitable for turf establishment due to improved structure and nutrient availability. A ready supply of compost is available given the existing King County and City of Seattle curb pick-up programs for compostable material. This method holds promise because research has indicated that when a catchment is deforested and urbanized, the changes in the upper soil layers and structure may have a greater effect on the overall hydrology than the loss of the vegetation [*Striebe*, 1994]. It appears that soil amendment has not been investigated as a mitigation possibility. Therefore, this study investigates the potential for using compost as a soil amendment to aid stormwater mitigation by managing stormwater runoff at the source. The results are generally applicable to any geographic location where the climatological and geological setting is similar to the Puget Sound Lowlands.

This soil amendment study is part of the Improved On-Site Residential Stormwater Management Study performed at the University of Washington Center for Urban Water

Resources Management. Soil amendment is one of six on-site technologies examined. Other on-site mitigation techniques examined separately from the work reported here include (1) Permeable/porous pavements, (2) Stormwater detention (cisterns or vessels), (3) Stormwater retention for reuse, (4) Infiltration basins and trenches, and (5) Landscaping practices which decrease runoff (terracing, vegetal cover, etc.)

1.3 Report structure

The following chapters present the development, implementation, and results of the soil amendment study up to August, 1995. Chapter 2 is a literature review which provides background on pertinent geology, soil science, hydrologic processes, and previous soil amendment research. Chapter 3 describes the objectives and design of the field experiment. Chapter 4 provides discussions of measured runoff hydrographs from natural storms. Chapter 5 details statistical procedures used to create measures of plot response during the study period. Chapter 6 describes the program of producing artificial storms to generate responses from the research plots. Finally, Chapter 7 provides summaries of observations and conclusions.

Chapter 2 - The influence of a soil on the hydrologic response of hillslopes

2.1 Physical and hydrologic characteristics of till

Glaciation produces soils by a number of processes, usually classified according to the portion of the glacier which drives the process. First the glacier erodes rock or mineral by scouring as it migrates. Then it transports the material either by grinding it along the base (basal transport), incorporating it in the glacial ice (englacial transport), or carrying it atop the surface (superglacial transport) [*Dreimanis*, 1976]. Finally it deposits the transported material by dropping it during retreat, washing it away in melt water, or by some other mechanism. Thus the materials which make up a glacial deposit are determined by the location from which they were plucked by the glacier, which can be many miles from the point of deposition. The structure is determined by the mechanism which resulted in deposition and weathering, fluvial effects, or other process which occur following the glacial deposition.

Because the mechanisms by which glaciers deposit sediment vary significantly, the term "till" encompasses a wide variety of soils. *Dreimanis* [1976] reviewed works by other authors and derived a general set of characteristics by which tills are identified:

1. glacial origin (making the term "glacial till" redundant)
2. presence of a variety of rock and mineral fragments
3. wide range of particle sizes (poorly sorted)
4. lack of stratification
5. compactness

This list is a general guide to identifying whether a given soil fits the broadest of all till types, and therefore is neither complete nor does it identify all tills precisely.

Our concerns deal with the hydrologic effects of a shallow layer of basal till upon which housing and landscaping (sod) are placed. There are numerous sub-classifications of basal till, each fitting the 5-part description above, particularly the criterion of compactness. This high degree of compaction is attributed to the large pressures of the overlying ice combined with the wide range of particle sizes [*Dreimanis*, 1976]. Additional common characteristics of basal till include a lack of structure, particularly if the till contains clay, and rounded and possibly striated clasts. As a result of the compactness and lack of structure, basal tills often display high bulk densities, high shear strength, low porosity, and low void ratios. It is these characteristics which also make basal till desirable from a geotechnical standpoint [*Lutenegger et al*, 1983], inducing developers to scrape down to shallow, dense till when building new developments. It is also these characteristics which produce undesirable runoff generation behavior from residential lawns constructed on till.

2.2 Subsurface water storage and flux

The subsurface of a hillslope is divided into two general zones by the water table. Below the water table is the phreatic zone, where the soil is saturated and the pore water pressures are above atmospheric pressure. Above the water table is the vadose zone, where the soil is generally unsaturated with negative pore water pressures. These zones are also called the saturated and unsaturated zones, respectively.

Several parameters are used to characterize the storage behavior of a soil. Moisture content (θ) is defined as the volume fraction of water in a given volume of soil. Moisture content at saturation (θ_{sat}) occurs when a soil is saturated and is equal to the soil's active porosity *n*. (The active porosity does not include pores which are isolated from the flow paths and do not fill with water.) When the soil drains due to gravity a certain amount of water is retained in a film over the particles. The moisture content at this stage (θ_{fc}) is called the field capacity. The porosity available for storage during storms is equal to

(θ_{sat} - θ_{fc}) and is termed the "dynamic" or "effective" porosity. During long dry periods the vegetation will continue to draw water from the soil and transport it out of the soil through the roots and stems. The moisture content then falls below the field capacity. As water is withdrawn and suction heads increase, more energy is required to withdraw additional moisture. At moisture content θ_w this energy exceeds that which the vegetation can muster and the plants may die. At the irreducible water content (θ_n) no more water can be removed from the soil unless it is oven dried.

The saturation of a soil, S, is the percent of the voids filled by water. Thus S is zero if no moisture is present (in an oven-dried sample) and equals 100% when the soil is saturated.

$$S = (\text{volume of water}/\text{volume of voids})*100$$

The storage mechanism changes depending on the amount of water available. At low water content the water is bound to the soil particles as a film by electrical and molecular forces. As more water is introduced it is held in place between particles by capillary forces. Close to saturation non-bound free water is able to move more rapidly through the soil by passing through interconnected pores.

A soil structure is complicated further by biological activity, a process which is at least as significant as geological or morphological mechanisms. Hydraulic conductivity (a measure of the rate at which water moves through soil) has been shown to be at least as sensitive to structure as to particle size distribution [*Nyborg*, 1989]. The field-scale properties of a soil mass can often vary by orders of magnitude due to root channels, earthworm and rodent burrows, etc. [*Megahan and Clayton*, 1983]. Earthworms, for example, work the shallow soils and bring the digested dirt and organic materials to the surface at rates of up to approximately 4 kg/m^2 (18 tons per acre) per year [*Conniff*, 1993]. The biological activity in forests is credited for making the upper layers of soil highly permeable [*Whipkey*, 1965].

The heterogeneity of soil prompted research on the characterization of soil by a few parameters. *Binley, et al* [1989] investigated the effects of hydraulic conductivity variation on a simulated 150 m x 100 m hillslope on a slope of 6 horizontal:1 vertical. Results indicated that in high-permeability soils (where most flow was subsurface) the soil parameters were effectively integrated over the hillslope, while in low-permeability soils the effect of spatial variability on the runoff hydrographs is more pronounced and cannot be represented by a spatially averaged quantity.

After reviewing a number of studies, *Beven* [1981] noted that vertical and lateral hydraulic conductivity decreased with depth. Though he provides no hypothesis for this phenomenon, one can assume that compaction due to overburden increases with depth, resulting in structural collapse of the soil matrix and producing a reduction of pore space with depth. This assumption is supported by an increase in bulk density with depth in three of the cases Beven reviewed [*Dunne and Black*, 1970; *Harr*, 1977; *Whipkey*, 1965]. In addition, biological and chemical activities which break up the soil and enhance water storage and movement occur at shallower depths.

The difficulty in characterizing soil-water systems complicates the design of instrumentation and the analysis of data. *Koide and Wheater* [1992] performed a hydrologic study on a hillslope 18 meters long, 8 meters wide, and with a 25 degree slope. A network of tensiometers from 14 to 95 cm deep monitored soil moistures, a throughflow pit indicated flux at the lower slope boundary in each of five soil horizons, and tree throughfall and stemflow were monitored. Attempts to predict the response of the hillslope to rainfall with flow modeling were unsuccessful, illustrating the complex nature of the natural system. This work also exemplified the difficulty of examining hydrologic mechanisms, even on small, heavily-instrumented hillslopes.

Soil properties vary temporally as well as spatially. *Gupta, et al* [1992] measured hydraulic conductivities for three seasons in an agricultural field. Infiltrometer tests were performed every 5 m along a transect, and the results demonstrated that while saturated hydraulic conductivity varies with each season it remains spatially correlated.

2.3 Hydrology of small hillslopes in the Puget Sound region

The mechanical, chemical, and biological processes which take place after rain reaches the land surface are complex both in conceptual development and in experimental observation. However, these processes must be understood at least at an operational level if the response of a catchment to rainfall is to be investigated. The fundamental problem of hydrology is the water balance, or a study of the inputs, outputs, and storage of a given volume of land (the control volume). The water balance concept is summarized in the continuity equation:

$$dS/dt = I - O$$

where dS/dt = rate of change of storage inside the control volume

I = volume flux into the control volume

O = volume flux from the control volume

Each term in Equation 2-2 has dimensions of volume/time (L^3/T). If the control volume is defined for a small hillslope with a shallow soil, the water balance in terms of volumes over a given time step Δt can be formulated as

$$P + Q_{in} = \Delta S + ET + R + Q_{sub} + Q_{surf}$$

where P = precipitation

Q_{in} = inflow

ΔS = change in volume of water stored in control volume

ET = evapotranspiration

R = recharge, or percolation downwards out of the control volume

Q_{sub} = subsurface runoff (by lateral flux through saturated zone)

Q_{surf} = surface runoff

In Equation 2-3, all terms are in units of depth (average depth over the area of the catchment). The science of hydrology involves understanding the mechanisms which dictate the absolute and relative values of the terms in this equation. In particular, hydrologists strive to predict the terms on the right side of the equation given the terms on the left. For a general review of hillslope hydrology processes see *Freeze* [1974], *Chow et al* [1988], or *Linsley et al* [1982].

2.3.1 Precipitation

Winter storms in the Puget Sound basin are typically long-duration, low-intensity events. During spring the storms become more dynamic with shorter durations, more intense rainfall rates, and longer periods between storms.

General climate and storm frequency statistics of the Puget Sound basin are described in detail in Chapter 4.

2.3.2 Storage of water

On hillslopes the principle medium of rain (or snowmelt) water storage is the soil. The soil storage in response to a storm depends on the ability of water to enter the soil through infiltration and the speed with which the soil transports and releases the water. These processes are dictated by the pore structure (including the presence of plants and effects of biological activity), porosity, particle size, and soil chemistry. The principle parameters which characterize the soil's storage behavior are the porosity, field capacity, and saturated moisture content. The free water stored in the soil eventually leaves as lateral subsurface flow, percolates downwards to a deep aquifer, or is removed by surface evaporation or by vegetation through respiration processes.

Other mechanisms cause water to be stored temporarily by the hillslope. Interception occurs when rain drops land on vegetation and can be significant up to the point where the leaves become wet and shed rain. Thus interception is a storage mechanism which is significant only in small events or at the annual time scale [*Linsley et al*, 1982, page 235]. In more significant rain events the vegetation is wetted quickly and no longer prevents rain from reaching the soil surface. Interception storage capacity is determined by the type of vegetation and the wind speed. In grasses, interception has been related to grass height and extent of grass cover [*Dunne and Leopold*, 1978]. Intercepted rainfall eventually evaporates.

Depression storage occurs when water ponds but does not flow along the surface. Divots, rills, furrows, burrows, and other features of uneven topography cause depression storage. Depending on the atmospheric conditions and the ground surface properties, water stored in depressions will eventually infiltrate or evaporate. When a catchment is urbanized it is often graded to permit drainage, thereby eliminating a large amount of depression storage; the rain water which would have been stored in depressions becomes runoff.

2.3.3 Evapotranspiration

Evapotranspiration is the pathway by which water held on or within the land surface returns to the atmosphere. Because evaporation from foliage and soil and transpiration processes from vegetation are difficult to separate in practice, evapotranspiration encompasses both mechanisms. Water evaporates from the surface of vegetation, water-filled depressions, the soil, streams, and ponds. Transpiration is the release of water into the atmosphere by plants. The roots draw in the soil moisture, transport it through the stems, and expel it into the atmosphere through the stomata. Transpiration is the primary path by which moisture returns to the atmosphere from vegetated soil [*Linsley et al*, 1982]. Evapotranspiration is primarily dictated by atmospheric conditions [*Dunne and Leopold*, 1978]. Contributing factors include solar radiation, air (or leaf) temperature, air vapor pressure, and wind speed. The nature of the vegetation also affects evapotranspiration through the vegetation's albedo (tendency to reflect radiant energy), height above the ground, and root structure.

2.3.4 Percolation and aquifer recharge

In areas with thin layers of permeable soils overlying hardpan till, most water travels laterally along and above the till layer. Some of the water seeps into fissures of the till and percolates downwards to the local (lower) water table. This water eventually reaches the outlet of the catchment along deep flow paths. While the fast surface and near surface hydrologic responses from storms are analyzed on the order of hours or days, deeply percolated water can take months or years to reach the outlet. Only in cases of large areal expanse (river basins) or long time scales does deep percolation become pertinent to local small-scale mass balance calculations except as a storm "loss." Water which percolates is important ecologically and is the source for natural streams which have their headwaters below till plateau regions in the Puget Sound lowlands.

2.3.5 Subsurface runoff

Subsurface runoff is the lateral flux of water through the upper horizon of the soil column to the catchment outlet. In forested non-mountainous slopes of the Puget Sound lowlands the typical soil column consists of a highly permeable layer of soil underlain by nearly impermeable till. Precipitation which is not intercepted, or throughfall, infiltrates into the unsaturated zone and travels downwards to the perched water table above the till. Most lateral subsurface flow takes place in the saturated zone just above the till layer [*Whipkey*, 1965; *Harr*, 1977]. The high hydraulic conductivities of the shallow topsoil and steep hydraulic gradients are conditions conducive to significant hillslope response from subsurface flow [*Beven*, 1981].

Jamison and Peters [1967] investigated the effects of slope length on discharge hydrographs and concluded that recession flow is more significant in longer slopes. The slopes investigated were from 23 meters (76 feet) to 98 meters (323 feet) in length with a 3% grade. For long-duration or low-intensity storms, runoff per unit area decreased with longer slopes due to increased losses along the flow path due to evaporation and increased opportunity for deep percolation . In more intense storms, runoff per unit area increased with slope length due to return flow at the base of the slope.

2.3.6 Surface Runoff

Surface runoff is produced by three principal mechanisms: Horton overland flow, partial source areas, and variable source areas [*Freeze*, 1974]. Horton overland flow occurs when the rainfall intensity exceeds the infiltration capacity of the soil. Often located in humid areas with relatively high-permeability soil, partial source areas are fairly fixed regions of a catchment which supply most of the runoff from the catchment while making up less than 10% of its area. In highly permeable soil, variable source areas likewise contribute the bulk of a catchment's runoff, but they are created by subsurface flow which saturates soil near channels (a result of seepage mechanisms and a rise in the water table following infiltration). The saturated areas are impervious to rainfall which is shed quickly into the channels. The resulting hydrographs are then directly related to the precipitation on the downslope saturated areas. The terms "partial" and "variable" are sometimes used interchangeably, according to *Harr* [1977].

In steep forested slopes in Vermont, *Dunne and Black* [1970a] found that overland flow is produced only by surface runoff from direct precipitation onto areas saturated by a rising water table. These conclusions support the partial source area concept. Also, the authors concluded that the storm runoff potential of a hillslope depends on the amount of overland flow produced. Only surface runoff substantially contributed to channel flows.

Harr [1977] investigated steep forested slopes in the western Cascades in Oregon, and concluded that overland flow rarely results from storms. Harr cited the results of *Dunne and Black* [1970a] as unindicative of mechanisms in the Western Cascades region, where though the saturated zones expand upslope from seepage faces (variable source area concept) no overland flow is evident and channels do not expand. The ability of the thin layer of permeable soil at the surface to retain moisture, coupled with the less intense rainfall rates in the Western Cascades, precluded the occurrence of Horton infiltration rate-limited overland flow in steep forested slopes.

2.4 Soil amendment research

Soil amendment has historically been viewed as a method for improving plant growth, with agricultural considerations motivating exploration. The studies in Table 2-1 had similar motivations, as indicated by the trends in their investigations. Soils were typically sandy, since sandier soils drain more completely, and ways were sought to add nutrients to and improve moisture retention of the soil to support plant growth. Also, the most commonly studied amendments are sewage sludge and manure. Amendments were applied no deeper than the expected root zone (15 cm).

Table 2-1: Summary of selected soil amendment studies

Study	Soil	Tillage	Treatment	Vegetation
Epstein [1976]	silt loam	rototilled	sewage sludge/compost	corn
Gupta [1976]	90% sand	rototilled 15 cm	sewage sludge	vegetables
Pagliai [1981]	sandy loam	"plowed in"	sewage sludge	corn
Tester [1990]	97% sand	rototilled 15 cm	comp. sewage sludge	fescue
			complete fertilizer	fescue
			comp. sewage sludge	vegetables
			beef manure	vegetables

There is little published in the literature concerning compost soil amendments and their influence on hillslope hydrology. Even with regards to basic soil properties the research scope has been narrow. *Tester* [1990] noted "there are limited reports describing the effects of sewage-sludge compost on soil properties." However, the results of these reports can be used to deduce likely effects of soil amendment on hydrologic processes.

According to the authors of the reports listed in Table 2-1, the amendment of a soil with organic matter such as compost generally increases water retention and saturated hydraulic conductivity, and decreases bulk density and unsaturated conductivity.

The major hydraulic characteristics of a soil mass are functions of its pore structure. Porosity is a simple measure of the highly irregular pore space in a soil matrix. However, this single parameter does not characterize the hydro-biologic nature of the soil pore structure. *Pagliai et al* [1981] found the pore size distribution to be more of a controlling factor than porosity. Pore sizes are classified based on physical mechanisms they support (Pagliai credits *Greenland*, [1977]). Storage pores (0.5-50 μm) have the greatest agronomic function. Transmission pores (50 to 500 μm) control the flux of water and gases. Fissures (> 500 μm) affect root structure as well as water/gas flux. Lower fissure percentage is indicative of good soil structure. In their study, *Pagliai et al* noted that while the pore size distribution varied little between different types and amounts (mass/area) of amendment, the drop in fissure proportion between the controls and the amended soils was pronounced. The resulting conclusion was that organic amendments improved the soil structure from an agricultural point of view.

Contrary to *Pagliai et al* [1981], *Tester* [1990] and *Gupta et al* [1976] found that the amount of compost applied affected the ultimate properties of the amended material. Tester concurrently conducted two studies on amendment with sewage sludge. In the first study, the more relevant study here, the soil was amended once; in the second study the soils were amended annually. After five years, the repeated amending of the soil in the second study led to reduced bulk densities, increased the soil water retention, and increased particle surface area. Likewise, *Gupta et al* found that bulk density decreased and soil water content at 15 bars increased with the amount of amendment applied. The relationships were linear for the range of bulk density and water content investigated.

Organic material in compost will decompose over time. *Gupta et al* showed that after one and two years, 58% and 50% of the mass (respectively) of the original sludge organic matter remained. *Pagliai et al* credit other researchers for the conclusion that microbial activity, the regulator of organic decomposition, is generally greatest for a few weeks after amendment of the soil. Settlement of the soil due to loss of organic mass was not described.

2.5 Summary

In the Puget Sound lowlands, in the absence of wetlands and lakes, soil provides the largest component of stormwater storage in a natural forested catchment. High organic content, root channels from vegetation, and animal and insect action provide means for water to enter the soil where it is detained and slowly released. When a catchment is developed for pasture or urban or suburban infrastructure much of the upper soil is removed, effectively eliminating the primary stormwater storage reservoir. The remaining soil column fills with water after smaller volumes of rainfall and quickly generates surface runoff through overland flow processes. The flow production behavior is therefore altered, often to the detriment of the receiving streams and channels which now convey higher volumes of runoff.

To attempt to mitigate the hydrologic changes of urbanization, one needs to replace the storage and natural infiltration capacity of the soils which were removed during construction. Traditional stormwater management techniques such as detention ponds attempt to fulfill this role. Soil amendment could possibly provide an alternative means of managing stormwater throughout a catchment. Previous research indicates that amending a soil with organic material effectively alters the parent soil's water storage and flux behavior. Such practice on a catchment-wide basis could recreate a portion of the subsurface storage that was removed during construction, and more closely reproduce the catchment's hydrologic behavior prior to development.

Chapter 3 - Experimental design and implementation

3.1 Background

The objective of this work is to examine the difference in hydrologic behavior of a small area of a hillslope when organic material is added to the underlying till. Mechanisms of infiltration, storage, surface flow, and subsurface flow are each affected by changes in the composition or condition of the soil. The combined influence of these mechanisms throughout a hillslope produce an integral hillslope response. The field component of this study was performed to provide data which illustrate the potential differences in this aggregate hillslope behavior between amended and unamended soils.
Three questions to be addressed in this work include:

1. How does a lawn growing in till amended with compost respond to rain relative to a lawn growing in unamended till?
2. Does soil amendment appear to produce similar effects with different types of compost, different parent tills, or different relative loose volumes of till and compost?
3. Could soil amendment potentially provide benefits to residential catchments in terms of stormwater management?

These questions are addressed by field observations where water inputs to and outputs from small hillslope plots are measured. The internal mechanisms which generate the outputs are inferred rather than examined directly.

Matters beyond the scope of this work include:

1. Detailed analysis of microscale soil-water-biological processes.
2. Economic evaluation of widespread application of soil amendment.
3. Determination of design parameters, coefficients, or other numerical guidelines.

3.2 Plot design considerations

The research plots were designed to replicate typical residential lawns in the Puget Sound lowlands with respect to slope length, slope, and vegetation. A slope length of 9.75 meters (32 feet) was used as a compromise between lawn size replication and construction manageability. The slope was 5%. To establish turf, Problend™ broadcast seed was applied to the plots. This seed blend is the most widely used in the Seattle area. Sod was not used for turf establishment because the thin, high clay-content sod layer on top of the specimen soils might control the infiltration rates. The grass was mowed periodically with a mechanical push-mower to maintain the grass at a height of approximately 5 cm. Grass clippings were left on the plots to minimize supplemental fertilizer requirements.

The width of the plots, 2.44 meters (8 ft), was considered large enough to minimize any flow effects along the side walls of the plots. Also, given the plot length of 9.75 meters this width provided a plot area of sufficient size to produce integral plot response which is relatively unaffected by local variations in soil properties or vegetation. However, this width was small enough to allow an adequate number of plots to be constructed side-by-side in the small land area available for the study.

Because the experimental concept called for fabricating the plots rather than locating existing hillslopes, a liner could be installed which prevented seepage laterally and vertically through the sides and bottom of each plot. This liner therefore defined the boundary conditions of the control volume of each plot, eliminating unaccountable water flux into or out of the control volume. The depth from the liner bottom to the soil surface was selected to be 0.30 meters (12 inches) based on advice from landscape architects regarding effective rototilling depths. Thus the liner defined a soil mass 9.75 meters long, 2.44 meters wide, and 0.30 meters deep at a 5% slope (32 feet x 8 feet x 12 inches).

Other design considerations for all components of the study included constructability, cost, security, and appearance. Constructability involved recognizing the limited amount of labor available for construction and the lack of opportunity for the use of large power tools for earthwork or carpentry. Cost was minimized by designing the plots to use readily available, inexpensive components. Security was required of the instruments, with padlocks for below-ground vaults and a chain-linked fence for a storage and weather station enclosure. Appearance was important because the site was located in an ecological area frequented by the public.

The final issue involved selecting the soil amendments to be examined. With the size of the site limiting the number of plots to seven, we decided to examine a variety of compost types and mixing ratios. Three types of compost were donated by two local companies. Cedar Grove, Inc. provided two compost products from its plant in Maple Valley, Washington: 7/16-inch Pure Compost and 3/4-inch Cathcart. The sizes in the product names refer to the screen sizes used in producing the composts. The 7/16-inch compost consists of recycled yard waste (grass clippings, leaves, and prunings), produce trimmings, and cellulose products. It is composted for one year and screened for delivery with screen sizes as indicated by the product name. The batch delivered for this study was highly composted with small, moist organic particles and an earthy odor. The 3/4-inch compost, which consisted of 75% mulch and 25% 7/16-inch Pure Compost, was drier than the 7/16-inch compost and contained noticeable wood and bark particles. The third compost, derived from sawdust (67%) and sewage sludge (33%), was supplied by Groco, Inc. The Groco compost was moister and more odorous than the Cedar Grove compost.

3.3 Plot construction

The experimental plots are located on the grounds of the University of Washington Center for Urban Horticulture, in Seattle, Washington. The site was selected due to proximity to the University and supply vendors (especially hardware stores), accessibility, availability of water for irrigation and rainfall simulation, slope, and cost. The site is located on a hard clay cap which covers a solid waste landfill. Currently the area around the site is promoted as an ecological research area and is home to an abundance of ring-neck pheasants, California quail, Canada geese, various ducks, rabbits, the occasional bird of prey, and numerous other species of birds. Trails through the area are used extensively by university employees, students, and the general public. Evidence of illegal dumping and loitering adjacent to the site prompted concerns about security. The location of the site is shown in Figure 3-1, and the layout of the site is shown in Figure 3-2.

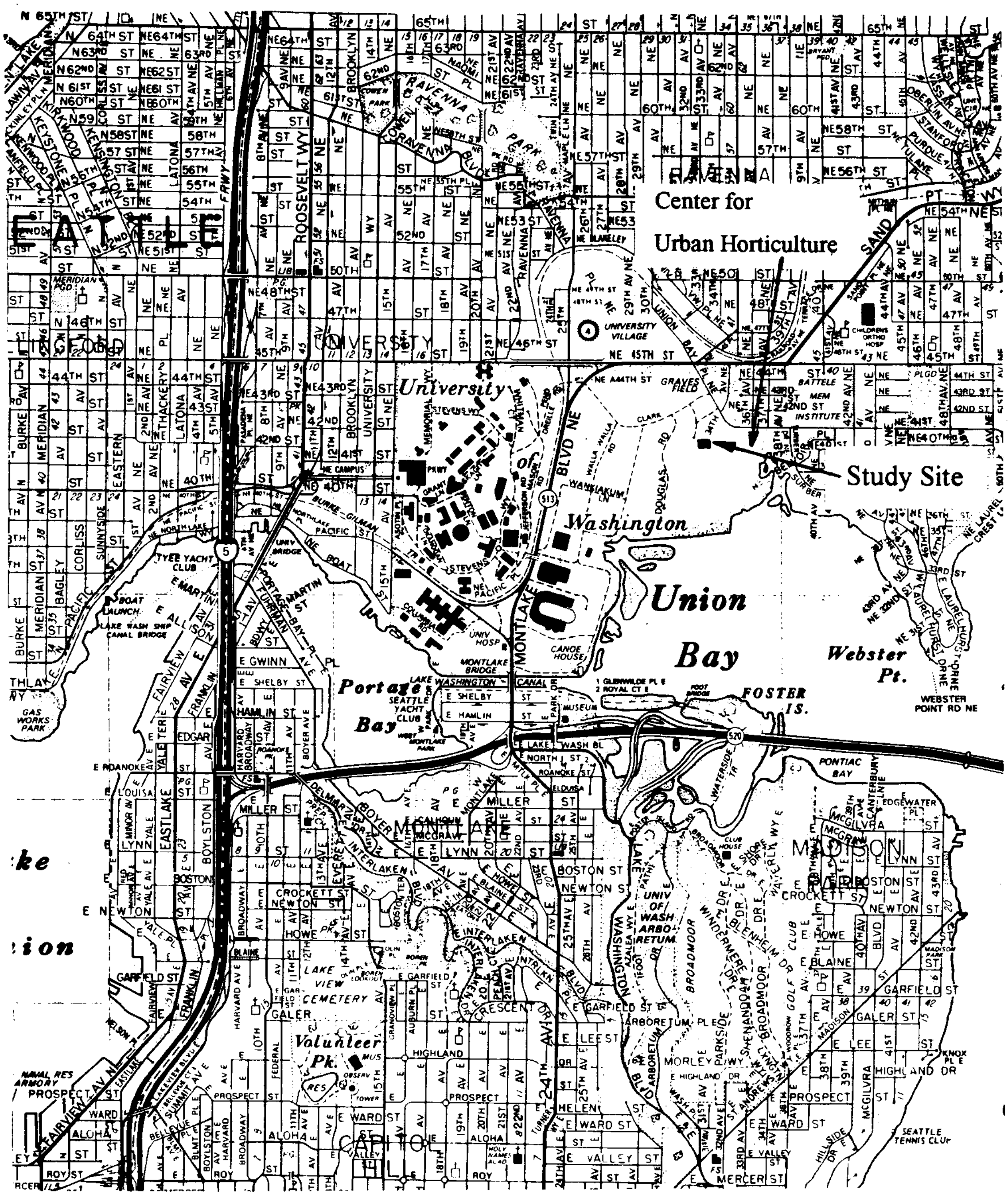

*From The Thomas Guide, King County Street Guide and Directory (© 1987 by Thomas Bros. Maps)

Figure 3-1: Map showing location of study site

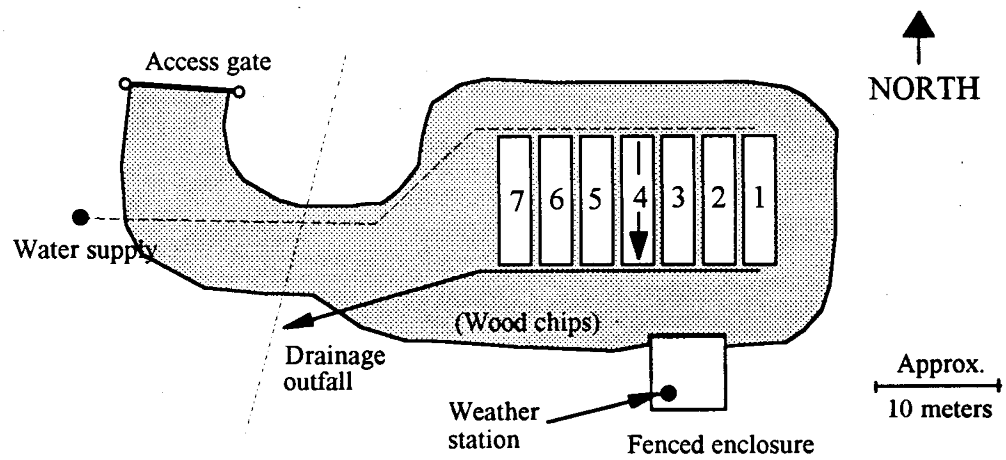

Figure 3-2: Site layout schematic

An area of approximately 15 meters by 45 meters (50 ft by 150 ft) was cleared of brush and grass about 45 meters from where an asphaltic concrete service road terminates at a padlocked gate. Wood chips provide ground cover for esthetics and control of dust and erosion on the site and on the path from the gate to the site. To provide drainage, a three-inch PVC pipe was buried one to 1.5 meters (3 to 5 ft) deep along the bottom edge of the proposed plot locations. This PVC pipe outfalls into an existing drainage swale. A buried two-inch PVC pipe was run from an existing city water outlet to the site to provide water for irrigation and rainfall simulation. Because the water line operates under high pressures, an adjustable pressure relief valve was placed in the line to prevent damage to sprinklers.

The plots were constructed sequentially beginning with Plot 1, the eastern-most plot. When a new plot was to be constructed, the first step was to grade the location with a tractor to a 5% downslope grade. Hand tools were used to grade the hard ground surface to a planar 5% slope. Next, 16-mm (5/8-inch) plywood was used to form a box-shaped form 9.75 meters (32 feet) long, 2.44 meters (8 feet) wide, and 0.30 meters (12 inches) tall. The longest dimension ran down the slope. The plywood walls were supported by #5 steel reinforcing bar shafts driven into the hard clay soil. Because of the compacted ground surface, there was no need for a plywood floor.

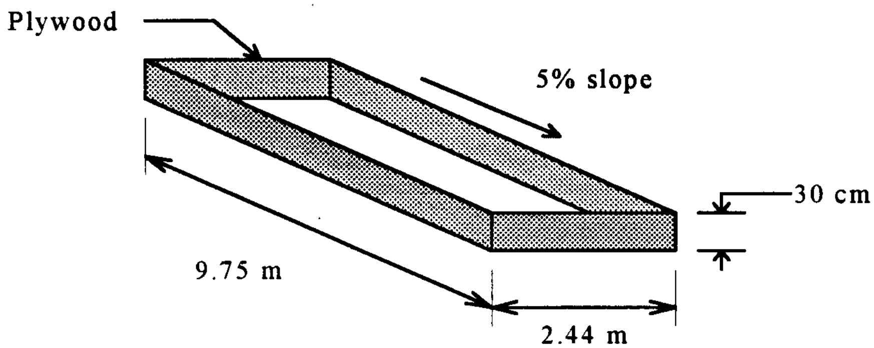

Figure 3-3: Schematic of plot design

A 6-mil reinforced polyethylene liner was laid into the form to act as a seepage barrier and to define the control volume. The liner extended throughout the floor of the plot and upwards at each wall to the ground surface. Each liner consisted of a single piece of polyethylene except the liners in Plots 3 and 4. These liners were constructed from 4-meter (12-foot) wide strips placed across the plot forms. To prevent seepage between the strips, the upslope strips overlapped their adjacent downslope strips by 1 meter, and these lap seams were sealed with silicon caulk. The caulk in conjunction with the weight of the overlying soil on the wide overlapped seam and the low permeability of the underlying ground surface provides a sufficient barrier against leakage through the liner.

The subsurface PVC pipe drain was installed at the bottom edge of the plot after the liner was in place. (See Figure 3-5 for a detail of the collection systems.) Soil was placed on the liner using a small front-end loader and spread using rakes and shovels. Mixing was performed on a loose volume basis; for example, to make a 2:1 loose volume mix, two buckets of loose till were added for each bucket of loose compost. The amended soils were mixed with the tractor bucket on an asphalt surface prior to placement. Later soil sampling verified the effectiveness of the mixing in producing relatively homogeneous amended soils. Compaction was performed manually at 10-cm lifts with a small drum roller. This action was performed to reduce eventual settlement rather than to achieve a target bulk density. Finally, the surfaces of the plots were screeded to a flat, sloping plane after the soil had been placed.

The first two plots were constructed as pilot plots to examine how well the design functioned before constructing the remainder of the plots. A sprinkler test was conducted on September 1, 1994, revealing a significant problem involving the surface topography of the plots. Although the surfaces of the first two plots were screeded in an attempt to produce 2-D surface sheet flow, the soil along the edges of the plots settled more than the soil in the middle, producing a crowned cross-section and causing pooling along the edges of the plots. This effect is undesirable because water which flowed to the side of a plot could be moved quickly along the soil-liner interface. Uneven settling was most likely caused by nonuniform compaction since the drum roller is not as effective along the edges, where the slightly protruding plywood form restricted use of the roller. To remedy the situation, more till was used to fill in the subsided areas along the edges. The till was hand tamped and overlaid by 15 cm wide strips of sod (sections of grass grown in a 2 cm layer of clay and purchased as a roll). Future observations revealed that this procedure effectively shifted the areas of ponding from the plot edge to the edge of the newly installed sod, but seepage may still occur at the soil-sod interface. The remaining five plots were graded with a 3 cm deep swale down the centerline of the plot to encourage surface water to drain away from the edges of the plots.

Seven plots were constructed between July and the end of September, 1995. A shipment of sixty cubic yards of till was delivered from an office building construction site in Redmond, Washington, at NE 31st St. and 156th Ave NE. Because each plot required approximately ten cubic yards of till, and accounting for the compaction and losses of soil around the site, a second shipment was required after completion of Plot 4. This second shipment was delivered on September 19, 1994 from the area of 148th Ave NE and NE 60th St. The composition of the plots and the origins of the till are shown in the Table 3-1. For the remainder of this document, the plots will generally be referred to by their number rather than their constituents.

Table 3-1: Compost mixes selected for the plots

Plot	Till Batch	Mix
1	1	Control (no compost)
2	1	2 till : 1 Cedar Grove fine
3	1	2 till : 1 Cedar Grove coarse
4	1	4 till : 1 Cedar Grove fine
5	2	Control (no compost)
6	2	2 till : 1 GroCo
7	2	3 till : 1 Cedar Grove fine

Site completion involved installing a 4.88 meter by 4.88 meter (16 foot by 16 foot) fenced enclosure for storage of materials and security for the weather station. The fence was painted in subdued earth tones to be unobtrusive.

3.4 Instrumentation plan

3.4.1 Weather station

A Campbell Scientific weather station was installed inside the fenced enclosure in October, 1994 to collect climatic data and provide a datalogger for plot runoff data storage. The station consisted of a 3 meter steel pole secured by concrete and cables. A horizontal mast was mounted at the top and oriented north-south. A sealed instrument enclosure for the datalogger was mounted on the pole where it was easily accessible.

Table 3-2 lists the sensors and instruments which were incorporated into the weather station. All components were purchased from Campbell Scientific, Inc., Logan, Utah. When components were supplied to Campbell Scientific by separate manufacturers the supplier is given in Table 3-2.

Table 3-2: Weather station sensors and components

Sensors:
- LI200S Silicon Pyranometer
- HMP35C Temperature and RH Probe
- 03001-5 Wind Sentry Anemometer/Wind Vane (R.M. Young Co.; Traverse City, MI)
- TE525 Tipping Bucket Rain Gage (Texas Electronics; Dallas, TX)

Data collection and storage components:
- CR10 Datalogger
- PS12LA 12V Power Supply with rechargeable battery
- MSX10 Solar Panel
- (2) SDM-SW8A Switch Closure Module (pulse counters with 8 input channels each)

The rain gauge had a sharp-edged mouth with a diameter of 152 mm (six inches) and 0.25 mm (0.01 inch) rain depth resolution. A debris mesh was placed 5 cm (two inches) below the mouth. Due to the security concerns, the rain gauge was installed the fenced enclosure by mounting the gauge to a vertical pipe so the mouth of the gauge was 0.81 meters (32 inches) above ground level. The surrounding fence was 2.2 meter high chain link fence with a single strand of barbed wire at the top. The presence of the fence raised concerns about its influence on the accuracy of the rain gauge catch.

In response to these concerns several additional rain gauges were used in different locations inside and outside the fenced enclosure to check the rainfall amount recorded by the weather station gauge (the reference gauge). These additional gauges were volumetric and after a period of rainfall the collected volumes were measured in graduated cylinders. The volumes were converted to a depth of rainfall based on measurements of the gauge mouth diameters. Gauge One was a metal gauge with a height of 0.28 meters (11 inches) and mouth diameter of approximately 0.20 meters (8 inches). The edge around the mouth was not sharp and the gauge was elevated so the rim was even with the rim of the reference gauge. The depth of the throat (funnel to mouth edge) was 0.13 meters (5 inches), and no debris mesh was used. Gauge Two was a standard U.S. Weather Service 8-inch weighing rain gauge, with sloping shoulders 0.13 meters (5 inches) below the mouth which was 0.89 meters (35 inches) above the ground. The throat was much deeper, and the mouth edge was sharper. Schematic diagrams of the rain gauges are provided in Figure 3-4.

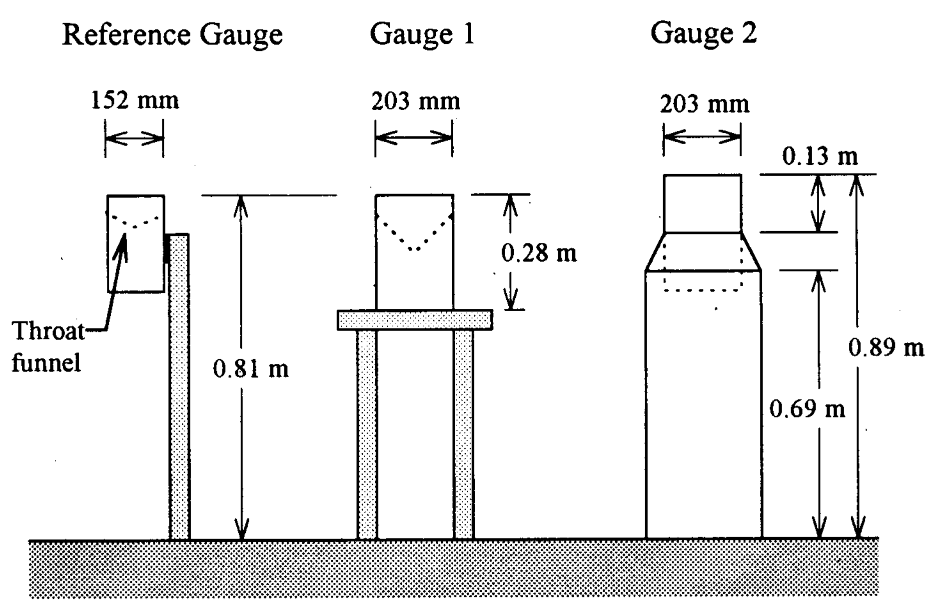

Figure 3-4: Schematic side-view diagrams of the rain gauges

In addition to these rain gauges, buckets were occasionally leveled and left out to catch rainfall. These plastic 5-gallon buckets were 36.8 cm (14.5 inches) tall and had an average mouth diameter of approximately 30 cm (12 inches), but the rim was flat and broad. Though the buckets were not designed to be rain gauges, their large diameters reduced the effects of the undesirable rim geometry and allowed the catch volumes to provide additional indications (though only approximate) of the accuracy of the reference gauge. Physical characteristics of the receptacles used for rain depth measurement are shown in Table 3-3.

Food cans obtained for use as inexpensive rainfall collectors during storm simulations were also used to record rain depths from natural storms. The characteristics of these food cans are given in Table 3-3.

Table 3-3: Descriptions of rain gauges at the site

Gauge	Nominal Diameter, mm(in)	Rim	Mouth Height, m (in)	Debris mesh?
Reference	152 (6)	Sharp	0.81 (32)	Y
Gauge 1	203 (8)	Dull	0.81 (32)	N
Gauge 2	203 (8)	Sharp	0.89 (35)	N
Buckets	~305 (~12)	Flat, broad	0.37 (15)	N
Food cans	152 (6)	Sharp	0.18 (7)	N

The results of the various measurements of rain depth are discussed in Chapter 4.

3.4.2 Runoff collection systems

Surface and subsurface runoff were captured and conveyed to continuously-monitored instruments by separate systems. The subsurface collection system was installed prior to placing the soil in the plots. The surface water collection system was installed after the grass roots had penetrated about 5-7 cm. The collection system is shown schematically in Figure 3-5.

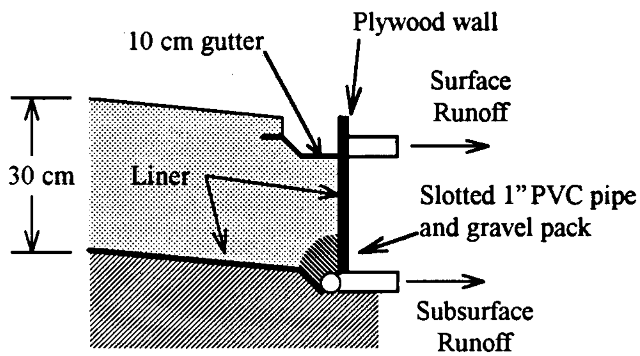

Figure 3-5: Longitudinal section schematic of runoff collection systems

Subsurface flow is intercepted by a perforated pipe. Located along the bottom edge of each plot, the 2.43 meter long, 2.54 cm (8 feet by 1 inch) slotted PVC pipe collects water as it percolates to the lowest point of the soil mass. The pipe is slotted by saw cuts every 2.5 to 5 cm (one to two inches) along its length and overlaid by coarse gravel (about 10 cm cover) which is wrapped in filter fabric. The pipe was laid as two sections sloped towards a sunken outlet in the middle to ensure drainage. The outlet is typically located about 5 cm below the bottom of the plot.

Water traveling along the surface and the shallow root zone (less than 2 cm deep) falls into a 10 cm-wide metal gutter at the bottom of each plot. The gutter has a lip which protrudes about 3 cm into the soil to ensure that surface water flows by gravity into the gutter rather than pooling in front of it. (Installing the gutter required cutting the grass roots with a pruning saw to insert the gutter lip into the soil.) The gutter was installed with the ends slightly higher than the middle to ensure drainage to a low point towards the middle of the gutter, where an outlet was installed. Petroleum-based roof sealant was used to seal around the outlet, at seams, and at the end of the gutter.

Runoff collected by the gutters and slotted pipes was directed by PVC pipes into instrument vaults. Each plot had a single instrument vault about 0.6 meters wide, 1 meter long, and from 0.6 to 1.3 meters deep (two feet wide, three feet long, and from two to four feet deep) located about 0.3 meters away from the down-slope wall of the plot. The vaults were buried to allow gravity drainage into the vaults from the plots. The vaults for Plots 1 and 2 were constructed from plywood and padlocked shut; the remaining five vaults were pre-fabricated, commercially-available electrical/telephone boxes made of heavy plastic. A 7.62 cm-diameter (3 inch) PVC drain pipe which slopes down to a nearby swale was installed prior to the construction of the plots. At each vault the exposed drain pipe was cut open or an open-ended stub-out was added to allow water pooling in the vault to enter the drain pipe. This outlet was covered with a steel mesh and the entire vault floor (including the drainage outlet) was covered with at least 5 cm of coarse gravel.

A critical aspect in analyzing the subsurface and surface runoff measurements individually is determining that no leakage occurs from the surface to the subsurface gutter. That is, water traveling along the surface to the bottom of the slope must not be allowed to "short-circuit" downwards directly to the subsurface collector before reaching the surface-water collection gutter. Field observations and hydrograph inspection would provide evidence about any such errors in operation (for example, large spikes in the subsurface response rather than a subdued response may indicate direct leakage from surface ponding).

3.4.3 Tipping bucket design and calibration

Measurement of the collected runoff was performed by tipping buckets located inside the instrument vaults. These tipping buckets were custom manufactured from rigid plastic, stainless steel sheet metal, and assorted hardware. Figure 3-6 provides a side view schematic of the tipping buckets, and Figure 3-7 provides a photograph of tipping bucket assemblies installed in an instrument vault at the front of one of the plots. A non-contact magnetic switch was installed so that it closed momentarily each time the bucket tipped. This momentary closure was logged by the datalogger.

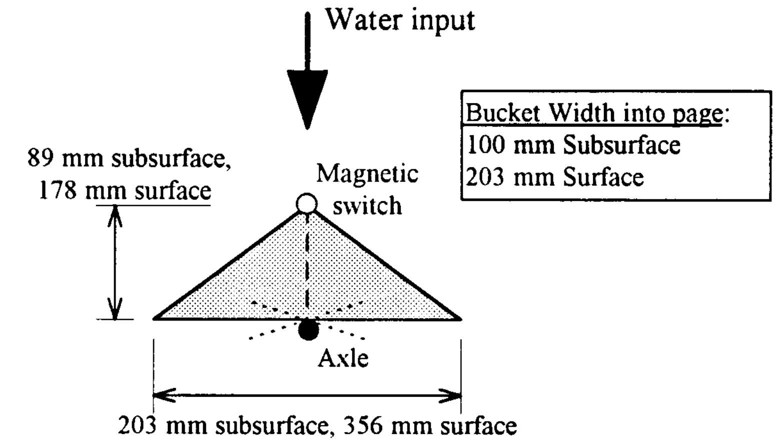

Figure 3-6: Side view schematic of tipping bucket flow meters for measurement of surface and subsurface runoff

Figure 3-7: Photograph of tipping buckets installed in an instrument vault

Determining the size of the tipping buckets involved balancing two opposing factors: small buckets provide more precision (particularly at low flows), while larger buckets provide greater flow rate capacity. Attempting to optimize the tipping bucket sizes given the expected difference in flow rates produced by the two types of runoff, two sizes of tipping buckets were used: small (about 0.13 liters per tip) for the subsurface flow, and large (about 1.35 liters per tip) for surface flow. Inside each vault, flexible plastic tubing directed the water from each PVC inlet into its respective tipping bucket. On March 17, 1995, the tipping buckets for Plots 1, 2, 3, 5, and 6 were mounted to patio stones to allow water quality samples from an associated study to be taken from below the tipping buckets.

To convert tip counts to flow rates each bucket was calibrated to determine the volume of water dispensed with each tip. Because many of the tipping buckets were mounted on patio stones on March 17, 1995 the period of record is divided into two calibration periods: pre-March 17 and post-March 17.

The pre-March 17 calibrations were performed on February 23 and 24, 1995, with a large bucket with a drain plug. A known volume of water draining from the bucket was directed by hose into the tipping bucket in question, and the rate of flow was adjusted to approximate the flows observed during natural rainfall events. Tips were counted manually when possible and verified from datalogger tip.

The post-March 17 calibration values were obtained by estimating calibration values at a number of flow rates for each tipping bucket. The bucket with the drain plug was kept full with a hose to create a constant head and therefore a constant flow rate through the outlet tube. The water was first directed into the tipping bucket, where the number of tips and the time during which those tips occurred were recorded. Then the water was directed into a beaker for a timed duration, providing the flow rate. By plotting the tip rates (tips/minute) versus the flow rate (liters/minute) and performing linear regression through the origin, a line is obtained where the slope provides the calibration value of liters per tip. The number of data points varied for each bucket from three to seven points, and the data showed little scatter along the best-fit line.

3.4.4 Data storage and retrieval

A Campbell Scientific CR10 Datalogger was installed in a sealed enclosure mounted to the weather station mast and used for all automated data collection and storage. Climate sensors on the weather station were wired directly to the CR10 datalogger. To connect the flow-measuring tipping buckets to the datalogger, 2.5 cm diameter PVC conduit was buried which connected the seven instrument vaults to each other and to the weather station datalogger enclosure. Wires from the magnetic switches on the tipping buckets were then run through the conduit and connected to the pulse counting modules in the instrument shelter of the weather station. At the programmed time intervals the CR10 datalogger retrieved the pulse counts for the time period from the counter modules and stored the values for downloading at a later time.

The datalogger was programmed to store data over three time intervals: every fifteen minutes, hourly, and daily. Fifteen-minute data included year, day of year, time (Pacific Standard Time only), rainfall depth, and number of tips for each of the fourteen runoff-measuring tipping buckets. On the hour the same values were stored (though the totals were over the past hour) plus environmental data averaged over the past hour: temperature, relative humidity, wind speed and direction, and short-wave radiation. These environmental data provided the basis for estimating evapotranspiration. At midnight all of the data were averaged (or totaled, as appropriate) over the past 24 hours, in particular to provide daily rainfall and runoff volumes.

Because the storage module had a limited capacity, data were downloaded periodically using a portable personal computer. Typical intervals between downloading were seven days, or shorter if information was desired sooner.

3.4.5 Piezometer design and installation

Although the primary instrumentation was the continuous monitoring of fluxes into and out of the plots, supplemental information on the state of the plot water storage was provided by piezometers. Each piezometer was manufactured from PVC to be 38 cm long and 2 to 2.5 cm in diameter (15 inches long and 3/4 to 1 inch diameter) which was slotted in the bottom one inch, covered with a filter fabric, and inserted into a 7.6 cm (3 inch) diameter hole in the soil.

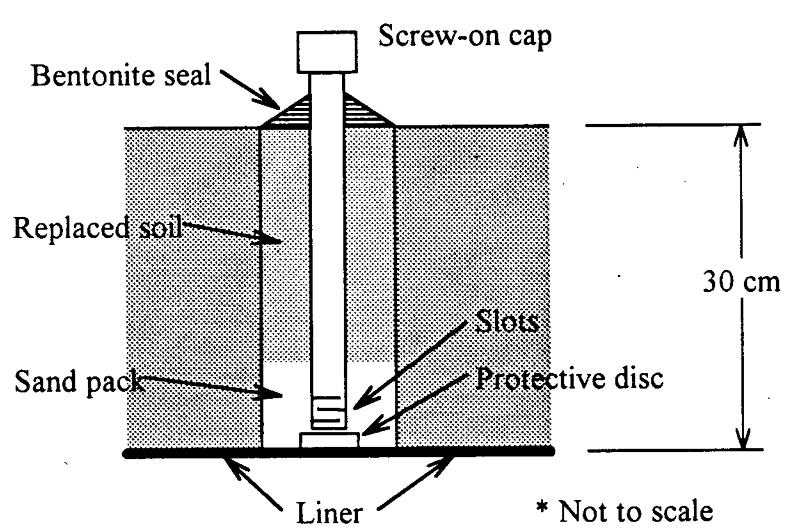

Figure 3-8: Schematic of piezometers

To install a piezometer, a short length of 7.6 cm PVC with a jagged end was used to core down close to the liner (care was taken to avoid cutting the liner). The plug of soil was removed while lodged inside the PVC. A hand shovel completed the excavation, leaving a 7.6 cm diameter hole through the soil column to the liner. (If the shear strength of the soil seemed too low for this open-hole method, the installation was not attempted.) A 0.6 cm-thick disc was placed on the liner to prevent the piezometer from puncturing the liner if pushed upon. The piezometer was held in place in the hole and sand was poured around it to a depth of about 12.7 cm (5 inches). The original soil was replaced around the upper seven inches. A bentonite seal was mounded about the stem where it protruded from the ground and a threaded top was added to allow the piezometer to be capped. All piezometers were located along the centerlines of the plots. The number of piezometers in each plot varied as well as the time of installation; the lack of strength of some of the soils precluded installation in some plots for several months. Table 3-4 details the locations of the piezometers, with the distances measured to the piezometer from the downslope end of the plot (where the surface water collection gutter was located).

Table 3-4: Piezometer locations and installation dates

Plot	Location (meters from gutter)	Date installed
1	0.6, 1.5, 2.7, 4.9, 7.3	8/31/94
2	0.6, 1.5, 4.9	8/31/94
3	1.5, 4.9	2/11/95
4	1.5, 4.9	2/11/95
5	1.5, 4.9	5/10/95
6	1.5, 4.9	3/2/95
7	none	n/a

Piezometer levels were measured manually with a clear plastic 1.3 cm (1/2 inch) diameter dipstick which was placed in the piezometer. By covering the top with a thumb, one could withdraw the tube and directly measure the height of the water column using centimeter gradations. To obtain absolute water depth, corrections were made for the disc at the base of the piezometer and the displacement of the plastic tube to estimate the actual water level.

While natural storms were in progress efforts were made periodically to visit the site and record levels in the piezometers. During simulated events the piezometers were monitored before, during, and after the sprinkling on a regular basis.

3.5 Soil and turf investigations

3.5.1 Soil sampling program

Dr. Robert Harrison of the University of Washington College of Forest Resources performed a series of laboratory tests on the material stockpiles and completed plots to indicate the changes in soil properties when the different amendments were introduced to the till. The first testing was performed on August 31, 1994 with the sampling of the compost and till stockpiles as they were delivered to the research site. Percent carbon and percent nitrogen were determined by weight. The results are given in Table 3-5.

Table 3-5: Laboratory analysis of compost and till as delivered to the site (Values averaged from three samples per source)

Source	Total C (%)	Total N (%)	Water Holding Capacity(%)
C.G. 7/16" Compost	21	1.4	160
C.G. 3/4" Compost	22	1.5	150
Groco Compost	39	1.3	390
Till (First batch)	0.27	0.14	24

Sampling of the soils in the completed plots was also performed for comparison of soil properties between the plots. Percent carbon, percent nitrogen, and particle size distribution values were determined by weight. Plots 1 and 2 only were sampled on

August 31, 1994. All seven plots were sampled on December 13, 1994. Sampling and laboratory testing were impeded by the slurry-like consistency of Plots 4, 5, and 7, and the generally wet condition of all plots. Soil structure was classified as "single grain/weak granular" for every sample, indicating that soil structure had not developed. As a result, the data should be used with caution. The data for these samples are shown in Appendix D.

Sampling from all seven plots was performed again on July 23, 1995, by which time the plots had developed structure (as indicated by well-established turf and soil strength) and were at a suitable moisture content. Three samples were taken from each plot 1.22 m (4 feet) from the upslope end: one at the centerline, and the other two from 8 cm away from the sides. Table 3-6 provides the average values for each plot.

Table 3-6: Laboratory analysis of soils in completed plots (July 23, 1995)

Plot		Total C (%)	Total N (%)	Bulk Density g/cm3	Particle Size Distribution (% in category) Clay <0.002 mm	Silt 0.002-0.05	Sand 0.05-2	Gravel >2 mm
1	Control	0.46	0.05	1.73	5	17	45	33
2	2:1 fine	3.00	0.23	1.37	4	15	41	40
3	2:1 coarse	2.86	0.24	1.36	6	17	48	29
4	4:1 fine	2.61	0.24	1.50	4	15	46	35
5	Control	0.20	0.04	1.84	4	22	50	24
6	2:1 Groco	1.51	0.15	1.40	4	21	47	28
7	3:1 fine	1.72	0.14	1.58	3	22	39	36

The second batch of till (Plot 5) contained more silt and sand than the first till (Plot 1), as shown in Figures 3-8 and 3-9; both tills had extremely low organic contents. This lack of nutrients necessitated application of fertilizer for the establishment of turf. All plots were therefore fertilized uniformly, though the amended soils did not require it. The higher bulk density values for the till plots indicate that the till particles made a denser soil mass when compacted, or that the compost particles were significantly less dense and resulted in a lower overall density when mixed with till particles.

Although Plot 3 (amended with the coarse compost) contained a substantial amount of visible wood fragments larger than 2 mm, the density of the particles was lower than that of the mineral and organic particles in Plots 1, 2, and 4. Thus when the particle size distribution was determined by weight the proportion of particles greater than 2 mm was lower for Plot 3 than for Plots 1, 2, and 4.

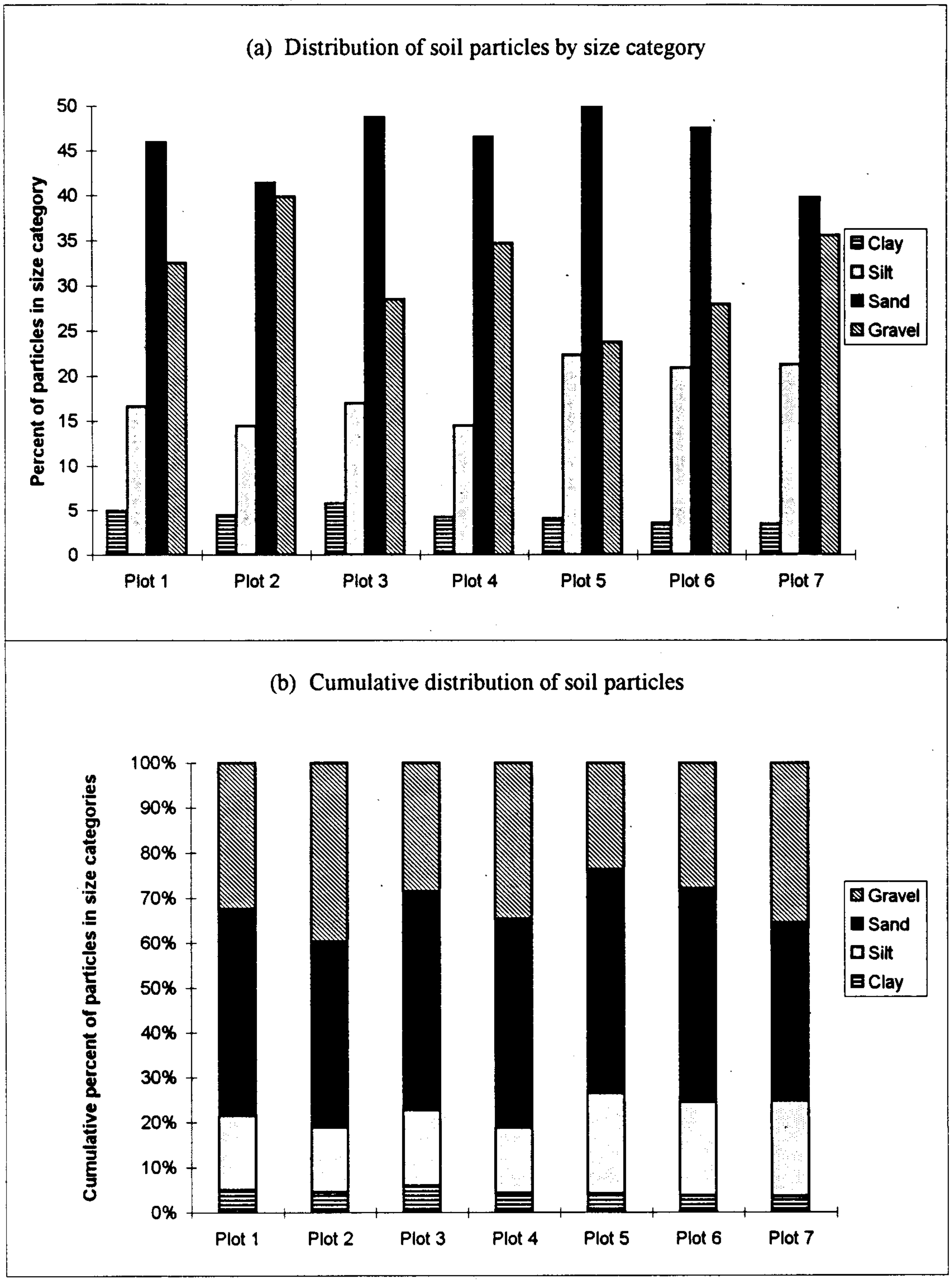

Figure 3-9: Particle size distributions by category

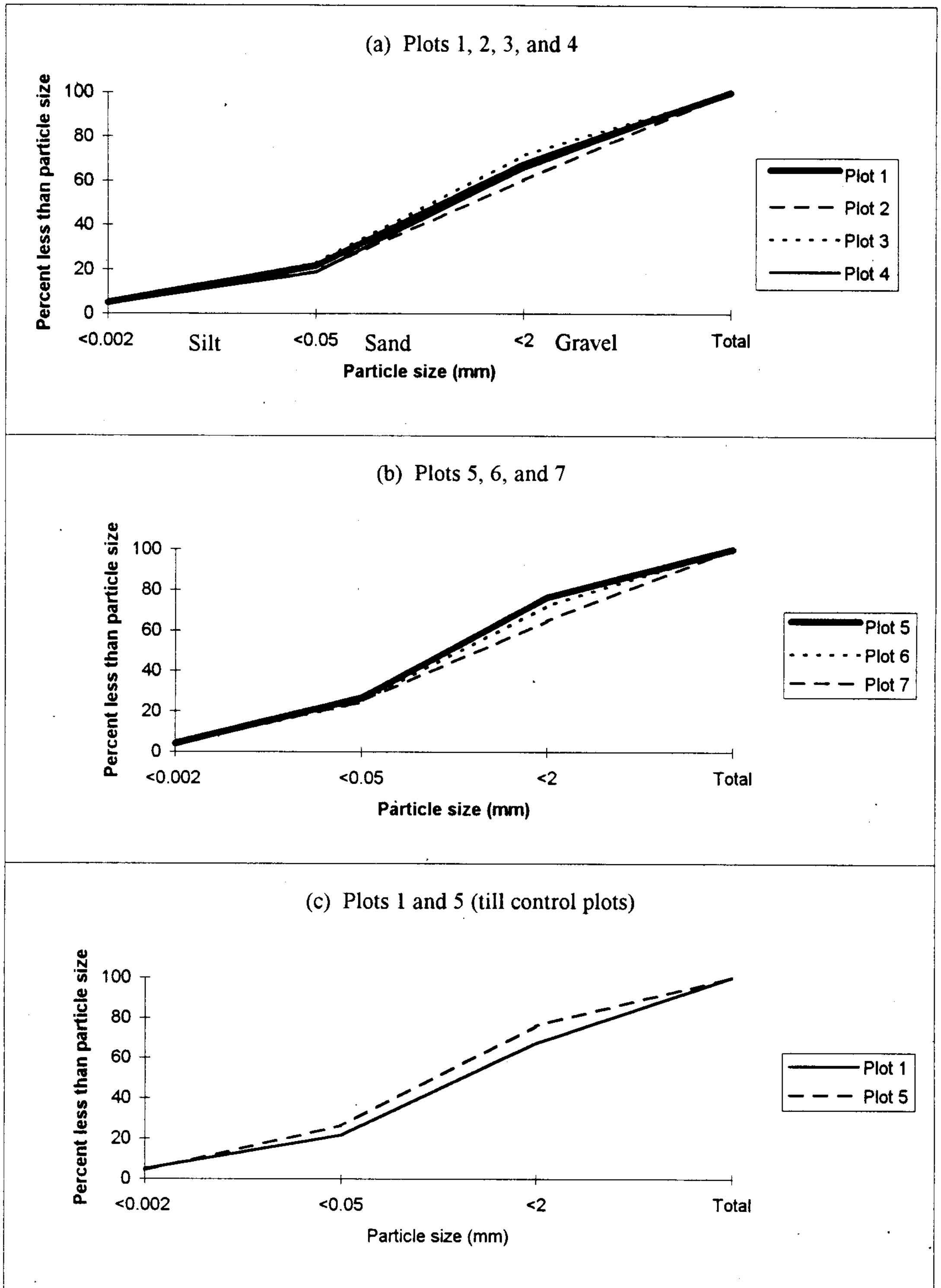

Figure 3-10: Cumulative particle size distributions

3.5.2 Turf root examination

A single grab sample was taken from each of the plots on July 24, 1995 to observe qualitative features of root structure and development. The samples were taken at the centerline of each plot, 1.22 meters (4 feet) from the upslope end of the plot. Each extracted grass/root sample included approximately 36 cm^2 of surface area from the plot with grass blades and thatch, and up to 15 cm of the downward-extending root system. The samples were washed thoroughly to expose the roots. Photographs of the root samples from Plots 1-4 and Plots 5-7 are shown in Figure 3-11 and Figure 3-12, respectively. The numbered labels indicate the plots from which the samples were taken, and the scale is in centimeters.

The root systems from Plots 2, 4, and 6 were more extensive through the depth of the samples. The control plot samples (Plots 1 and 5) show a thin layer of thatch and lateral roots about 1-2 cm thick; below this layer the density of the roots decreases significantly. The length and density of the grass blades are also greater in Plots 2, 4, and 6 then the other plots.

Within the holes resulting from this excavation, additional samples were taken with a soil core sampler to examine the density of roots deeper in the soil column. After noting the root characteristics the core sample was placed back in the plot. Table 3-7 provides qualitative observations of the root densities both from the shallow samples and the deeper samples near the liner as observed on July 24, 1995 by sampling. A network was noted if intertwined systems of coarse and fine roots were observed, rather than single strands.

Figure 3-11: Photograph of root/grass samples from Plots 1, 2, 3, and 4

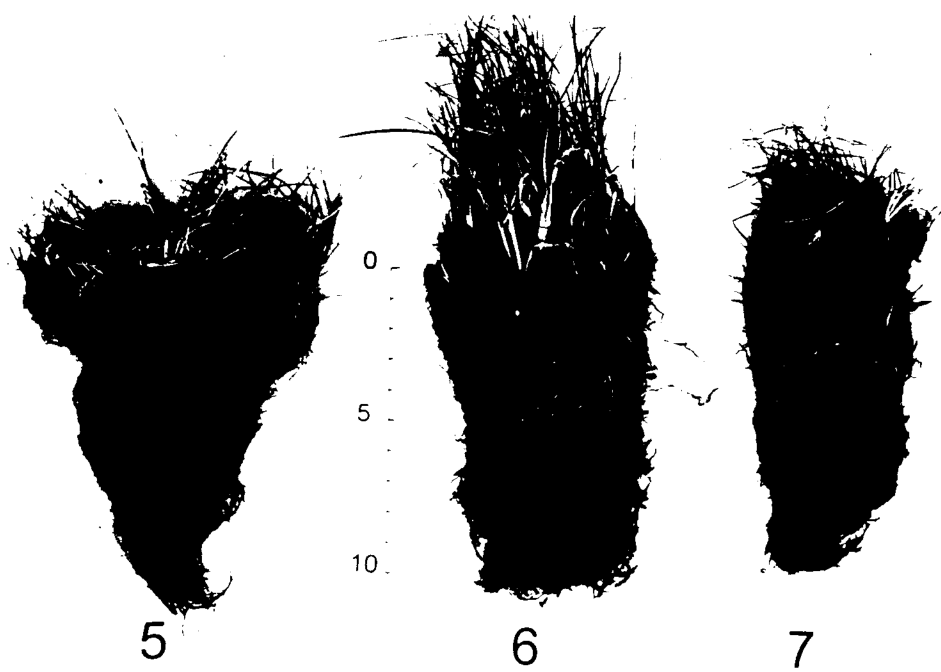

Figure 3-12: Photograph of root/grass samples from Plots 5, 6, and 7

Table 3-7: Qualitative description of observed root densities

Plot	Shallow root density (0-5 cm)	Max. sample depth (cm)	Root density observed at max. sample depth
1	Many	22	Sparse single roots
2	Abundant	28	Moderate network
3	Abundant	23	Light network
4	Abundant	25	Moderate single roots
5	Common	23	Sparse single roots
6	Abundant	23	Light network
7	Many	20	Sparse single roots

The grass established on amended soils developed root systems which were generally denser than the roots of till plots both near the ground surface and towards the bottom of the 30 cm soil column. The root systems in the amended soils could draw water and nutrients from most of the plot depth. The root systems in the unamended soils had access to less of the soil column. This was evident in the appearance of the lawns during extended dry periods. The lawns on amended soils remained greener longer and required less frequent supplemental irrigation then those on till.

Chapter 4 - Rainfall, evapotranspiration, and hydrograph analyses

4.1 Summary of observed natural storms

4.1.1 Climatological setting of Puget Sound

The winter climate of the Puget Sound region is dominated by upper-air patterns which bring air masses from different sources. When upper-level winds are from the north, dry, cold, stable air masses from Northern Canada bring sunny, cool days to Puget Sound. More commonly, however, the Aleutian Low (a subpolar low-pressure system off Alaska) with its counter-clockwise rotation carries dry, frigid polar air masses from Asia across the Pacific towards the west coast of America [*Ahrens*, 1992]. While en route the air masses gain warmth and moisture, becoming a maritime polar air mass. Upon reaching the Washington coast an incoming storm system often splits around the Olympic Mountains and rejoins at the other side. The location where the two portions of the system rejoin is the convergence zone, which resides over Puget Sound. The system then continues its push east where the Cascade Mountain range forces the moist air upward. Because the air is unstable, meaning that air nudged upward continues to rise until its moisture condenses, the convergence zone and the orographic lifting by the Cascade Mountains create locations where rain can be expected to occur for days until the incoming storm system subsides or moves elsewhere. Despite the dominance of frontal rainfall in the region, the complicated dynamics of these atmospheric processes result in locally erratic rainfall.

As summer approaches, the Pacific High moves northward off the coast of California. This semi-permanent high-pressure region not only brings its own dry air to the Pacific Northwest but also shelters the area from the storm systems from the Aleutian Low. Thus the late spring and summer months tend to be much drier, and storms that occur are more likely of short duration (though patterns more typical of winter can occasionally arise).

Rainfall depth frequencies for the Seattle area are given in Table 4-1. (Values for storms smaller than a return period of 2 years were excerpted from the Puget Sound Basin Stormwater Management Manual and are based on rainfall measurements at the Seattle-Tacoma International Airport weather station from 1950 to 1977; the values for the larger storms were estimated from isohyets in *Miller* [1973].)

Table 4-1: Rainfall depth frequencies for the Seattle area, mm (inches)

	Duration		Proportion of
Return period	6-hour	24-hour	rain at or below
1-month	-	17 (0.65)	62%
6-month	-	34 (1.35)	91%
1-year	-	41(1.60)	95% *
2	25 (1.0)	51 (2.00)	98%
5	30 (1.2)	61 (2.4)	-
10	36 (1.4)	69 (2.7)	-
25	41 (1.6)	84 (3.3)	-
50	46 (1.8)	89 (3.5)	-
100	51 (2.0)	99 (3.9)	-

*95% of the 30-year rainfall total was produced by storms of depth less than 41 mm in 24 hours.

4.1.2 Rainfall frequency analysis of rainfall recorded at the study site

The rainfall from natural storms was monitored at the study site from October 25, 1994 through the summer of 1995. Seattle-Tacoma International Airport with its long rainfall record is located 21 km (13 miles) to the south and provides an opportunity to place the 1994-1995 rainy season into perspective. Rainfall records at the airport indicate a calendar year-to-date rainfall amount at the end of May 1995 of 416 mm (16.38 inches), slightly less than the average of 430 mm (16.94 inches) from the previous 30 years. The study site rain gauge logged 417 mm (16.41 inches) during the same period. Table 4-2 shows the distribution of monthly rainfall from November, 1994 to May, 1995.

Table 4-2: Monthly rainfall totals during the study

Location	Nov '94	Dec	Jan '95	Feb	Mar	Apr	May
Millimeters							
Research Site	135	177	121	81	112	71	32
SeaTac	147	207	113	126	103	52	21
SeaTac 30-yr. mean	148	150	137	101	90	59	43
Inches							
Research Site	5.32	6.97	4.77	3.18	4.40	2.80	1.26
SeaTac	5.79	8.15	4.44	4.97	4.05	2.05	0.81
SeaTac 30-yr. mean	5.83	5.91	5.38	3.99	3.54	2.33	1.70

Rain events were grouped into distinguishable storm systems consisting of a series of individual events lasting from a day to two weeks with each event caused by the same invading air mass. The storm systems were identified using the daily rainfall record and the record of sky conditions at SeaTac. The Seattle climate record from December 19, 1994 (when runoff measurement systems were generally operational) to July 1995 was divided into ten storm systems, shown in Table 4-3:

Table 4-3: Division of rainfall record into storm systems

Dates	Rain depth, mm (inches)	Duration (days)
Dec 24 - 27	58 (2.29)	4
Jan 7 - 19	58 (2.28)	13
Jan 28 - Feb 2	68 (2.66)	7
Feb 14 - 20	70 (2.76)	7
Mar 8 - 15	68 (2.66)	7
Mar 17 - 24	41 (1.62)	8
Apr 4 - 14	40 (1.56)	9
Apr 17 - 20	19 (0.75)	4
Apr 29 - May 3	23 (0.92)	4
May 8 - 11	9 (0.37)	4

The maximum 24-hour rain depth recorded at the site was 35 mm (1.38 inches) during the storms on December 20, 1994, resulting in a 6-month return period for the event. Ten other storms had 24-hour rainfall depths of between 17 and 34 mm (0.65 and 1.35 inches) for return periods between 1 month and 6 months (see Appendix B for the ranked list).

4.1.3 Evapotranspiration estimates

The rate of evapotranspiration (ET) from the plots affects analyses which include mass balance computations, such as estimating the changes in storage of the plots or verifying the validity of long-term runoff measurements. In addition, estimating the evapotranspiration rates provides insight into the significance of this mechanism in the hydrology of the test plots. For these reasons estimation of the daily potential evapotranspiration rates was performed using the Penman-Monteith combination equation [*ASCE Manual No. 70* , 1990, pp. 92-97]. A brief explanation of its application follows; computational procedures used to generate the evapotranspiration rate estimates are detailed in Appendix E.

The Penman-Monteith equation provides an estimate of the potential evapotranspiration rate given site characteristics and current conditions. Table 4-4 lists the relevant parameters required by the Penman-Monteith equation.

Table 4-4: Input parameters for the Penman-Monteith equation

Site characteristics	Current conditions
Latitude	Air temperature
Longitude	Relative humidity
Elevation	Incident short-wave solar radiation
Canopy resistance	Wind speed at 3 meters
Absorptivity	Date
	Time

The site location and elevation were obtained from topographic maps. Typical values for short grasses were used to estimate the canopy resistance as 70 sec/meter and the absorptivity as 0.77. These values were assumed to be the same for each of the seven plots though turf conditions varied across the plots. The required current conditions were sampled and stored hourly by the weather station. A computer code was written to compute the hourly evapotranspiration depth using these parameters and output the daily totals for the period of analysis.

The daily potential evapotranspiration estimates and the daily rainfall amounts are shown in Figure 4-1a. The graph demonstrates the low potential evapotranspiration during the winter months relative to the summer months and the drop in evapotranspiration during storms. The expected rise in average daily evapotranspiration as the months progress from winter to summer is evident in Table 4-5.

Table 4-5: Estimated average daily potential evapotranspiration by month from December 19, 1994 to June 4, 1995.

Average potential ET	Dec	Jan	Feb	Mar	Apr	May
mm	0.33	0.46	0.71	1.22	1.78	2.49
inches	0.013	0.018	0.028	0.048	0.070	0.098

To examine the significance of evapotranspiration during storms, the daily rainfall and evapotranspiration rates were plotted to the same axis (Figure 4-1b). The graph shows that the rainfall input dominated during days with more than 8 mm (0.30 inches) of rainfall through early March. Figure 4-1c shows the significance of rainfall during days with more than 2.5 mm (0.10 inches) of rain. The rate of actual evapotranspiration was generally less than 5% of the rain rate through mid-March, at which point the rate of evapotranspiration increases greatly relative to the rainfall rates.

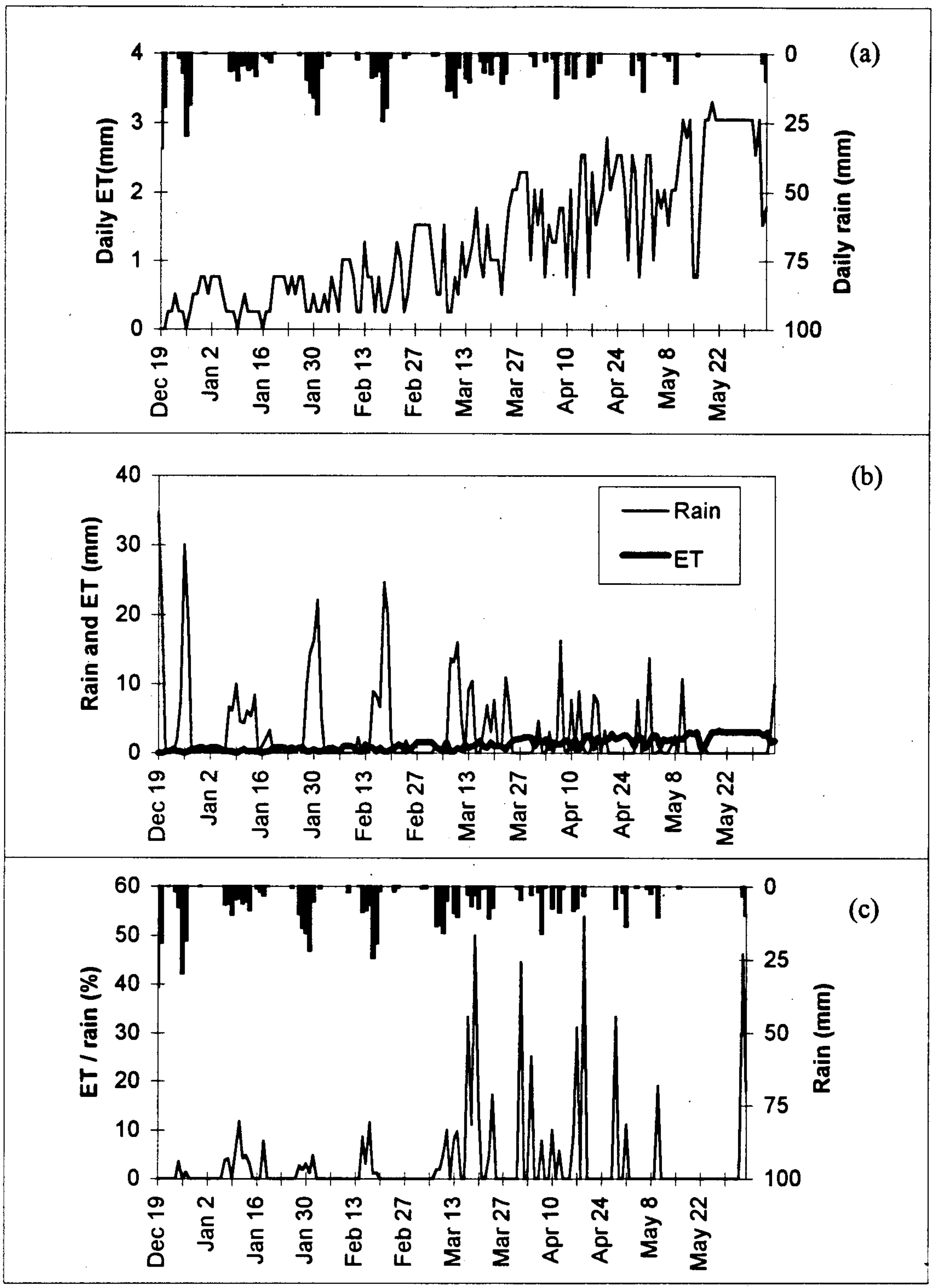

Figure 4-1: Predicted daily potential ET depths, 12/19/94 to 6/5/95
(a) Rainfall hyetograph and daily ET, (b) Rain and ET to same scale,
(c) daily ET/Rain depth for days with rainfall greater than 3 mm

The amount of evapotranspiration that occurred during storms was examined by dividing the daily record into days with rain (during storms) and days without rain (between storms). The accumulated estimated evapotranspiration amounts and the ratios to the total amount are shown in Table 4-6.

Table 4-6: Potential evapotranspiration during and between storms

	Estimated ET(mm)	Number of days	Mean ET (mm/day)
During days with rain	61 (28%)	77 (46%)	0.79
During days with no rain	154 (72%)	91 (54%)	1.69
All days	215	168	1.28

From the Penman-Monteith routine, an estimated 72% of the evapotranspiration occurred during the days between storms, which made up about half of the total days. The estimated evapotranspiration rate during storms was about half the rate expected between storms.

4.1.4 Summary of the observed climate

The rainfall data and evapotranspiration estimates reflect the typical changing nature of the Puget Sound climate from December into the following summer. The seven observed storms with 24-hour depths over 17 mm (24-hour per-month average recurrence frequency) occurred between December and mid-March, while six of the seven highest hourly rainfall depths occurred after March 23. The estimated evapotranspiration rates rose faster after February, indicating the change from short, cloudy days to longer days with more variable sky cover. In short, the observed winter storms were produced by lingering frontal systems while spring and early summer storms were shorter and more dynamic.

The monitoring of the plots from December, 1994 to early June, 1995 did not capture any events greater than the approximate 6-month, 24-hour magnitude. Though the data lack storms of larger magnitude, they contain a number of storms the size of which typically produce about 90% of the area's yearly rainfall depth.

4.2 Recording of rain depth

The accuracy of the data from the site's monitored rain gauge, referred to here as the reference gauge, was critical to mass balance calculations. A series of investigations were performed to confirm that the primary rain gauge recorded accurately the actual rainfall which fell on the plots.

4.2.1 Calibration

The reference gauge calibration was checked four times to determine the accuracy of the tipping mechanism. As instructed by the manufacturer, sixteen ounces of water were poured into a plastic cup sitting on the debris mesh in the gauge. A tiny hole in the bottom allowed the water to drip into the gauge, with the test being valid if the total time to drain was greater than 45 minutes. A properly calibrated gauge would register 100 ± 3 tips. The results of the calibration checks are shown in Table 4-7.

Table 4-7: Rain gauge calibration tests

Test	Date	Tips recorded
1	2/28/95	92
2	3/2/95	92
3	4/25/95	93
4	4/25/95	92

Rather than attempting to adjust the gauge, which would preclude comparing rainfall amounts before and after the modification, we used an adjustment factor of 1/0.92 = 1.087 to all past and future rainfall amounts registered by the reference gauge. In this document, all rainfall depths recorded by the weather station's tipping bucket rain gauge have been multiplied by this factor.

4.2.2 Location and accuracy

Placing the gauge inside the fenced area (Figure 3-2) raised concerns over the catch of the gauge. A series of tests were performed using additional gauges which were emptied following rainfall. The volume of water in each gauge was measured periodically and converted to a depth which was compared to the depth recorded by the reference gauge. The characteristics of the gauges are repeated here in Table 4-8.

Table 4-8: Descriptions of rain gauges at the site

Gauge	Nominal Diameter, mm(in)	Rim	Mouth Height, m (in)	Debris mesh?
Reference	152 (6)	Sharp	0.81 (32)	Y
Gauge 1	203 (8)	Dull	0.81 (32)	N
Gauge 2	203 (8)	Sharp	0.89 (35)	N
Buckets	~305 (~12)	Flat, broad	0.37 (15)	N
Food cans	152 (6)	Sharp	0.18 (7)	N

Gauges 1 and 2 were placed about one meter and one-half meter respectively from the reference gauge inside the fenced area. Gauge 1, the shorter 8-inch gauge, was placed upon a support so its mouth was at the same height as the mouth of the reference gauge. Also, two 5-gallon plastic buckets and food cans distributed about Plots 1 and 2 were used as additional measures for comparison. Precise measuring cylinders were used to measure the collected water volumes.

Rainfall catch measurements for all gauges are provided in Table 4-9.

Table 4-9: Rainfall depth measurements for the comparison gauges (Gauge depths in mm)

Time gauges emptied	Time volumes measured	Reference Gauge	Gauge 1	Gauge 2	Bucket 1	Bucket 2	Food Cans
April 5, 10:00	April 9, 10:45	17	-	16	15	-	-
April 9, 10:45	April 13, 09:45	17	18	16	16	-	-
April 13, 09:45	April 14	13	13	13	13	13	-
April 14	April 20, 12:45	20	21	19	18	18	-
April 20, 12:45	April 30, 09:30	8	8	8	-	-	-
April 30, 09:30	May 4, 09:30	16	17	15	14	14	-
May 9, 09:00	May 11, 09:20	4	5	4	-	-	-
May 11, 09:20	May 12, 08:00	9	11	9	-	-	9
May 12, 08:00	June 6, 09:15	15	14	13	-	-	-
June 6, 09:15	June 15, 08:40	16	17	14	-	-	-

Eight food cans were distributed about Plots 1 and 2 during the night of May 11-12, 1995. A rainfall simulation had been set up the morning of May 11, but high winds forced the abandonment of the simulation after five minutes of sprinkling and these eight cans were left in place with negligible amounts of water in them. That night it rained, and the next morning the volumes of water in the cans were measured. The average depth of water in the 152 mm-diameter cans was 9 mm (0.36 inches), with catch volumes ranging from 163 ml to 174 ml. The reference gauge recorded 9 mm (0.37 inches), as did Gauge 2. Gauge 1 collected 13% more than all other gauges, a difference significantly above the expected difference of about 5%. No explanation for this anomaly could be found. Winds at 3-meter elevation during the eight hours of rain averaged 3.9 km per hour (2.4 mph) and were generally from the north. Excluding Gauge 1, all gauges collected depths of rainfall which were approximately equal, indicating that the catch of the reference gauge in the fenced enclosure accurately represents the rain which fell on the plots.

For the period during which the comparison gauges were monitored, the accumulated rainfall depths recorded by the comparison gauges were compared to the accumulated depths recorded by the reference gauge. Table 4-10 summarizes the volumes and the ratio of the comparison gauge catch to the reference gauge catch. Gauge 1 collected 6% more rain than the reference gauge, and Gauge 2 collected 4% less than the reference gauge. Accumulated over a combined eight sample periods (some duplicated between the two buckets), the 5-gallon buckets collected about 8% less than the reference gauge.

Table 4-10: Difference in catch between reference gauge and comparison gauges

	Sample Periods	Gauge catch, mm (in)	Reference gauge catch, mm (in)	Relative to reference gauge
Gauge 1	9	124 (4.88)	117 (4.61)	1.06
Gauge 2	10	128 (5.05)	134 (5.27)	0.96
Bucket 3	5	77 (3.05)	83 (3.27)	0.93
Bucket 4	3	46 (1.79)	50 (1.95)	0.92

Although Gauges 1 and 2 agree within reasonable limits with the reference gauge, the accumulated bucket measurements are not within acceptable bounds. The significant difference in rainfall catch between the reference gauge and the buckets is likely to have resulted from evaporation. Measurements after longer sample periods result in lower bucket catches relative to the reference gauge. Back-calculation from the period with the lowest catches, from April 14 to 20, results in a potential mean potential evaporation estimate of 0.43 mm/day (0.017 inches/day). The Penman-Monteith routine estimated a higher mean rate of 1.9 mm/day (0.076 inches/day). Thus the hypothesis of evaporative loss does not require unreasonable evaporation rates.

Conversely, the April 14 measurements, after a one-day sample period during which evaporation would be negligible compared to the rainfall, showed a catch in both buckets nearly equal to that of the reference gauge. Gauge 1 and Gauge 2 would not be affected by evaporation because they are isolated from wind fields by the funnels, whereas the entire water surface in each bucket was exposed to the atmosphere.

4.3 Performance and operation of the tipping buckets

The fourteen tipping buckets for measuring runoff from the plots generally performed adequately upon installation. However, stoppages did occur, and bucket failures were usually not identified until after data had been lost during a storm. Most stoppages were due to grit in the simple sleeve bearings. In one case the grit deposition was caused by water which pooled around the instrument vault, entered the vault where the PVC drain pipes penetrated the wall, and splashed onto the bucket axle. Other stoppages appeared to be caused by swelling of the plastic frame around the axle; they were rectified by loosening the bearings.

Subsurface buckets were generally in operation from December 2, 1994, when the program for counting the tips was loaded into the monitoring equipment. Surface buckets were generally in operation by December 20, 1994. Installation of the surface-runoff collection gutter in Plot 5 was delayed until February 11, 1995, after the soil and root structures had developed to the point where excavation into the soil was possible. The periods of operation of the tipping buckets are described in detail in Appendix C.

4.4 Hydrograph analysis - Plots 1 and 2

4.4.1 Introduction

The main focus of this work was to examine the hydrologic response of the test plots to rainfall. This examination was principally done from hydrograph analysis: comparing the patterns and magnitudes of runoff observed from the till plots to the runoff observed from the amended plots. Also, mechanisms of runoff generation and hydraulic characteristics of the soils and vegetation were inferred by relating the observed runoff to the rainfall which produced it. Much of the discussion which follows is qualitative as important features of the graphs are pointed out, described, and explained. The supporting information (laboratory soil tests, root examination, and piezometer monitoring) provides additional information about the internal mechanisms which produce the observed runoff measurements. Many aspects of each hydrograph's magnitude and shape were considered, including the following features:

1. peak runoff rates
2. lag times (time from first rainfall to a significant runoff response)
3. recession flows (runoff rates after rain ends)
4. addition to storage (difference between rainfall and runoff for each hour)

The following sections deal with principal features of the runoff hydrographs for Plots 1 and 2. Each of the hydrograph plots includes four time series. At the top of the plot is the rainfall hyetograph in units of mm per hour (right vertical axis); along the bottom are the rainfall input rate, total runoff from Plot 1, and total runoff from Plot 2, all plotted in units of liters per hour (left vertical axis). The rainfall input rate is the rain depth per unit time (one hour here) multiplied by the plan view area of the plot. It corresponds to the rate at which the rain water would run off from the plot if the plot had an impermeable surface and equilibrium had been established. Thus, comparison between the rainfall input rate curve and the plot runoff curves shows the degree to which the plots behave like an impervious surface. From mass conservation for a given time increment, the difference between the rainfall input rate and runoff is equal to the water added or removed from storage. (Evapotranspiration is ignored during storms because the rates of evapotranspiration are negligible compared to rainfall and runoff rates during the winter storms.) When appropriate, the rainfall depths of distinguishable storm events within the storm system are shown on the charts.

One measure of hydrologic effectiveness of an amended till is the frequency of channel-altering flow rates generated from it relative to the frequency from unamended till for the same rainfall patterns. No specific investigations have been conducted in Puget Sound Lowland streams to determine channel-altering flow rates. Based on professional experience and judgment, Dr. Derek Booth, King County, Washington Department of Public Works Basin Planning Division, developed a criterion that channel alteration occurs at a flow rate of approximately 0.5 times the 2-year peak flow rate. He estimated that the specific discharge (flow rate per unit catchment area) for the 2-year peak flow rate for the Puget Sound Lowlands ranges from 0.5 L/hr/m^2 to 2.5 L/hr/m^2 (0.02 to 0.1 ft^3/sec/acre). These estimates were based on measurements from small catchments in other regions reported by *Andrews* [1984], *Carling* [1988], *Leopold* [1988], *Pickup and Warner* [1976], and *Sidle* [1988]. Using the 0.5 times the 2-year flood magnitude estimate, channel-altering flow rates from each test plot (plan area 23.78 m^2) would range from 12 to 60 L/hr. Flow rates reported in this report for our plots in excess of this range would likely lead to alteration of the geometry and sediment movement in a receiving channel.

The discussion focuses initially on the first two of the seven plots. Plot 1 was a control plot with grass growing in till. Plot 2 had grass growing in till amended with fine compost. The responses of this pair of plots will be compared for several significant storm systems during the period of record to examine general differences in behavior between lawns grown in till soils and amended soils. Once the general effects of the amendment are identified, one of these storms will be used in the next section to illustrate the degree of these effects in each of the other five plots.

4.4.2 December 24 - 27

This storm demonstrated many of the features that became evident in succeeding storms. It produced approximately 58 mm (2.29 inches) of rainfall in two distinctive events separated by about six hours. The second event was the largest single event monitored during the December-May period, producing 34 mm (1.33 inches) of rain during the 24 hours from 10:00 am, December 26, to 10:00 am the next morning. This depth qualified the storm as approximately a 6-month, 24-hour recurrence interval event. In the preceding ten days 103 mm (4.05 inches) of rain fell and the plots were generally wet, as evidenced by the baseflow present from Plot 1 as the rain began on December 24. The monitoring systems on both plots were operational during these storms. The hydrographs are shown in Figure 4-2.

As the first significant rainfall began during the afternoon of December 25, most of the rain was stored on and in the plots. By midnight, however, the discharge of Plot 1 was increasing noticeably while the discharge from Plot 2 increased at a slower rate. Both hydrographs peaked at 03:00 on December 26, with Plot 1 peaking at 78 L/hr and Plot 2 peaking at 62 L/hr. After the rain ended the flow rates from the two plots were similar.

As the second rainfall event began during the afternoon of December 26, both plots were unable to store as much of the rain water as they had during the previous event. The hydrographs rose faster than they did at the beginning of the first event, though Plot 1 runoff again increased faster than the Plot 2 runoff. By midnight, after 30 mm (1.18

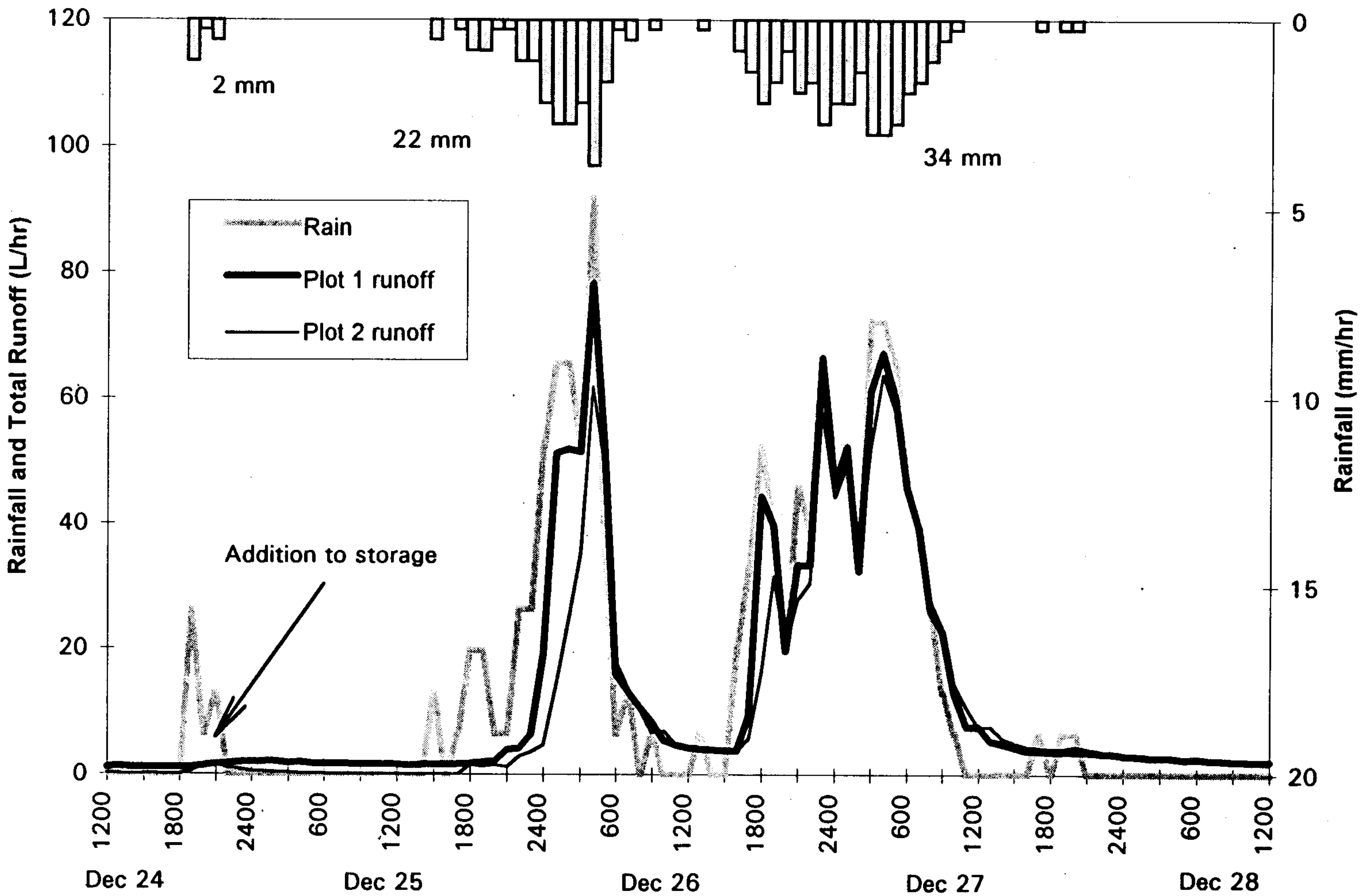

Figure 4-2: Rainfall and runoff for Plots 1 and 2 for the storm system of December 24-28, 1994

inches) of rainfall in the past 36 hours, Plot 1 appeared to have little capacity for additional storage and the runoff rate equaled the rainfall rate. From this time Plot 2 peaks continued to be lower than those of Plot 1.

4.4.3 January 28 - February 2

This storm system delivered about 68 mm (2.68 inches) of rain from four distinguishable events over five days. The dry periods between the consecutive rain events were 12, 12, and 11 hours long. The first event produced the 4th-largest 24-hour depth of the study (0.91 inches) and the third event produced the 3rd-highest 24-hour depth of 23 mm (0.93 inches). The second event generated 4 mm (0.17 inches) from 7:00 to 8:00 am, January 30, the fifth-highest recorded hourly rainfall rate.

The preceding eight days were dry with a few sunny to partly sunny days, so the plots were likely near field capacity at the onset of rainfall. The absence of flow from the plots at the start of the storm supports this estimate of moisture conditions.

Several features of the hydrographs are evident. First, the recession flow rates of Plot 2 were consistently higher than those of Plot 1 between all four events. Second, Plot 1 storage was nearly full when the heaviest rain occurred at 9:00 a.m. on January 30, while Plot 2 continued to hold and retain rain water until the morning of January 31 (during the third storm event). Third, during the first event Plot 2 was significantly more effective at storing rain water than Plot 1, which appeared to be approaching saturation by the time the rainfall began to decrease.

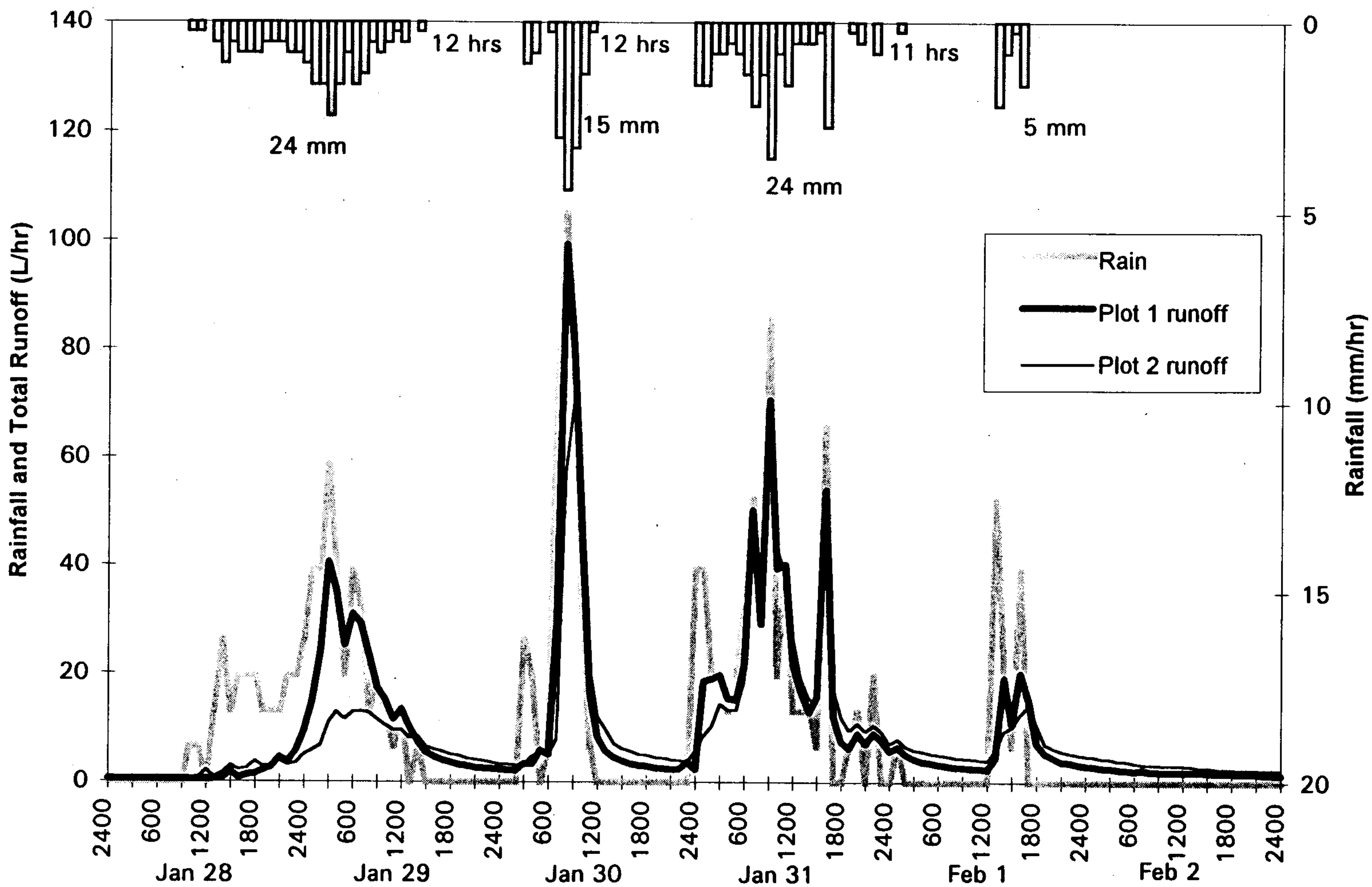

Figure 4-3: Rainfall and runoff for Plots 1 and 2 for the storms of January 28-February 2, 1995

4.4.4 February 14 - 20

This long-duration storm system produced 70 mm (2.76 inches) of rain over six days. Figure 4-4 shows the recorded rainfall and runoff from the storms. The rain pattern can be grouped into four erratically-spaced, varying-magnitude events; the rain depth for each event is shown in Figure 4-4.

For comparison to the historical rainfall magnitudes in the Seattle area, the study site rainfall depth in the past 24 hours was calculated for each hour of the February 14 - February 20 period. The third event, which began on the morning of February 18, produced a peak 24-hour depth of 25 mm (0.97 inches), the second-highest 24-hour depth recorded during the study. The return period for this event was approximately 4 months. The last event, which began on the morning of the following day (the 19th), produced a 24-hour depth of 19 mm (0.76 inches), a 1- to 2-month event which was the sixth-highest recorded depth of the study.

Except for 2 mm (0.09 inches) of precipitation on February 11 (snow fell throughout the area, though none was observed on the site), no rainfall was recorded for the ten days prior to this storm system. The negligible baseflows recorded on February 14 further indicate the dry antecedent condition of the plots, which were likely somewhat below field capacity.

Both plots effectively attenuated and delayed the first peak, accepting most of the 9 mm (0.36 inches) into storage. The response lag time of several hours reflect the initial dry conditions. The recession rates were nearly equal.

During the second rainfall event (February 16 to 17) both plots showed a slightly shorter lag time, but upon responding Plot 1 responded much more dramatically. Plot 1 ceased to accept rainfall to storage by 5:00 a.m., February 17, while Plot 2 continued to attenuate peaks throughout this period of rainfall. Plot 2 recession flows exceeded those of Plot 1.

When rain resumed on February 18, Plot 2 had released more water than Plot 1 since the last storm, making available much of the soil's water storage capability. This regained capacity resulted in a substantial difference in the peak flows of the plots during the rainfall burst of 0.14 inches between 10:00 a.m. and 11:00 a.m., at which point Plot 1 runoff peaked at 65 liters per hour and Plot 2 runoff peaked at only 19 liters per hour. By the next rain burst four hours later, however, both plots began to behave similarly. The discharge from Plot 2 exceeded that of Plot 1 for the remainder of the rainfall. The recession flows of Plot 2 were also substantially higher than those of Plot 1 from this point on.

There were also differences in response to the small rainfall spikes of February 19 at 7:00 a.m. and February 20 at 4:00 p.m. On both occasions the response from Plot 1 was slightly longer, while Plot 2 appeared to attenuate the pulse and smooth the response more than Plot 1.

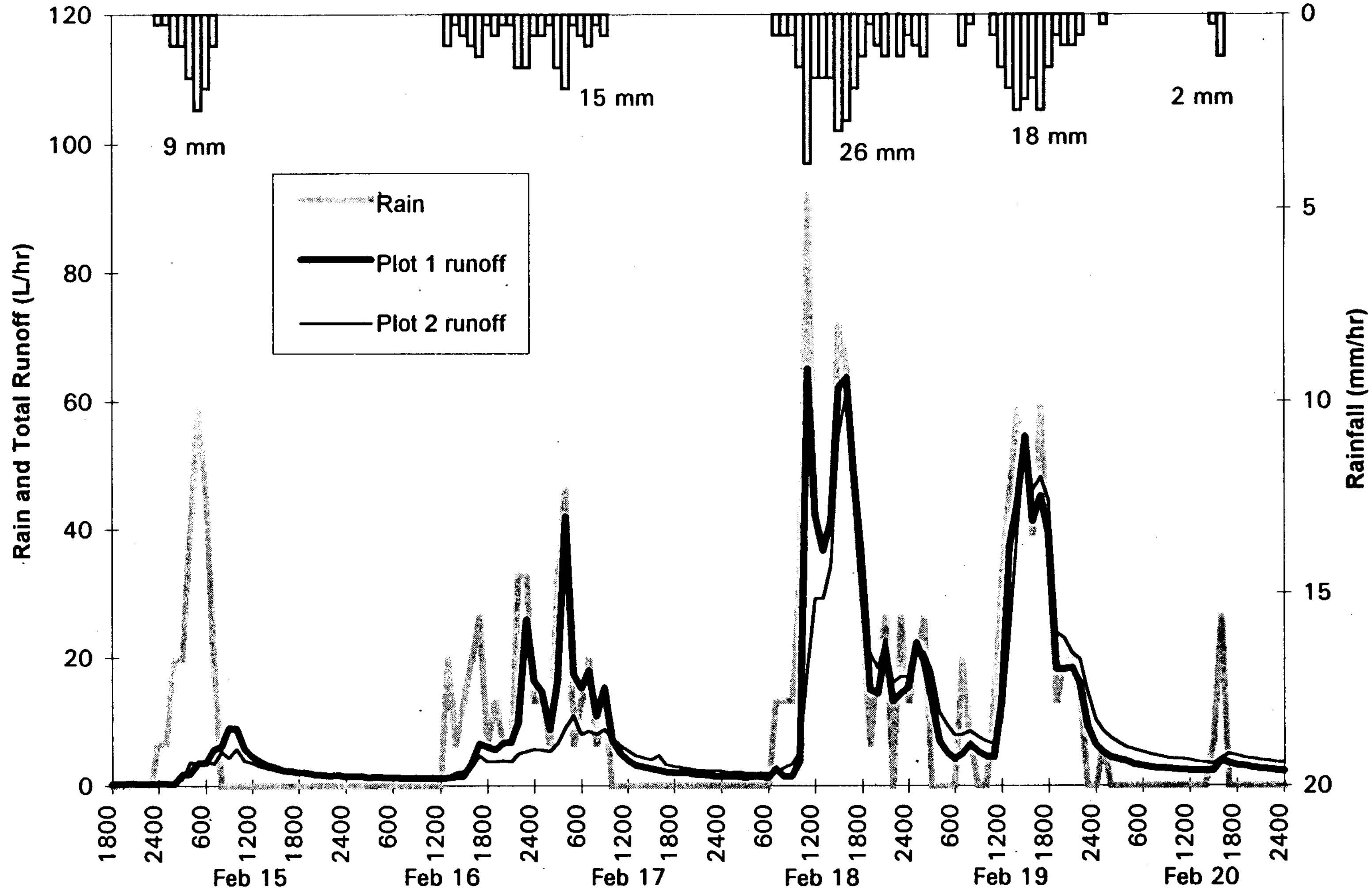

Figure 4-4: Rainfall and runoff for Plots 1 and 2 for the storm system of February 14 - 20, 1995

4.4.5 March 8 - 15

This week-long storm system produced 68 mm (2.66 inches) of rain in temporally variable patterns. The longest dry period was 27 hours from March 12 -13 after the first 48 mm (1.89 inches) had fallen. Conditions were generally dry, with less than 2 mm (0.07 inches) of rainfall measured three to four days before the storm. Other than this two-day, the ten days prior to the storms were dry and often sunny. Baseflow was negligible as the storms began.

Both Plots 1 and 2 showed little response to the first eleven hours of rainfall (7 mm). Then Plot 1 generated significantly higher runoff rates than Plot 2 as rainfall intensities increased. Plot 2 continued to attenuate runoff peaks more effectively than Plot 1 throughout the rest of the events.

Plot 1 ceased to accept water into storage on March 9 at 7:00 a.m. after 22 mm (0.85 inches) of rainfall, 26 hours since the first rain. Table 4-11 provides the piezometer indications about 4 hours after Plot 1 runoff first approached the rain rate. After this point, Plot 1 peak runoff rates were nearly equal to the responsible rainfall rates if the intensities were maintained for more than one hour. For example, three short-duration rainfall peaks occurred between the afternoon of March 9 and 1:00 am of the 10th where Plot 1 stored the incoming water, thereby resulting in reduced peaks. In contrast, in the late evening of March 10 several hours with equivalent intensities of rainfall occurred in succession. The response to these grouped hours of rainfall resulted in significantly higher runoff rates with respect to the incoming rainfall. This storm system demonstrated that the timing pattern of rainfall is as important as magnitude for runoff production. This also emphasizes the need for analytical approaches which involve continuous time series of storm patterns rather than a particular event to explore urban hydrologic design alternatives.

Table 4-11: Water table depths on March 9, 1995 at 11:30 a.m. (cm)

	Distance of piezometer from bottom of slope (m)				
	0.66	1.5	2.75	4.88	7.32
Plot 1	dry	dry	22.0	22.0	27.5
Plot 2	17.5	24.0	-	20.0	-

The peak runoff rates from Plot 2 were consistently lower in magnitude than the peak rates from Plot 1 from the first rain on March 8 until the storm of March 14. This morning storm produced 8 mm (0.31 inches) of rainfall in three hours and both plots were wet due to storms the previous day. By the third of these three hours of intense rainfall, the runoff rate from Plot 2 was rising relative to the rainfall input rate, indicating that the additional amount of rain water stored in or on Plot 2 was dropping as the heavy rain continued and a larger portion of Plot 2 became saturated. Piezometer readings at the time confirmed the general saturation of both Plots 1 and 2, and are shown in Table 4-12.

Table 4-12: Water table depths on March 14, 1995 at 8:15 a.m. (cm)

	Distance of piezometer from bottom of slope (m)				
	0.66	1.5	2.75	4.88	7.32
Plot 1	dry	2.5	23	g.s.*	g.s.*
Plot 2	22	g.s.*	-	g.s.*	-

*g.s. indicates water level was at the ground surface

By comparing the water tables of Table 4-11 and Table 4-12 and the respective Plot 2 runoff rates relative to rainfall, it is apparent that the soil column saturation had a greater effect on the runoff from Plot 2. On the first visit (Table 4-11) none of the piezometers indicated full-depth saturation; on the follow-up visit (Table 4-12), piezometers indicated

Plot 1 was about 60% saturated (lengthwise along the centerline) and Plot 2 was nearly 90% saturated. The runoff from Plot 1 was approximately equal to the rain at the time of both visits. In contrast, while Plot 2 was still attenuating the peak at the first visit, it was beginning to shed nearly all the rainfall at the second visit. These observations indicate that the runoff-generating mechanisms are different in Plot 1 and Plot 2. Plot 1 behavior may be dominated by infiltration-limited runoff generation (Horton overland flow), shedding rainfall while ponded water slowly infiltrates until after an extended period of rainfall the soil column is saturated; Plot 2 may allow rain water to infiltrate until the water table rises to the ground surface in some parts of the plot (which happens faster than for Plot 1) within which saturation-overland flow is generated. These possibilities are discussed in later sections and chapters.

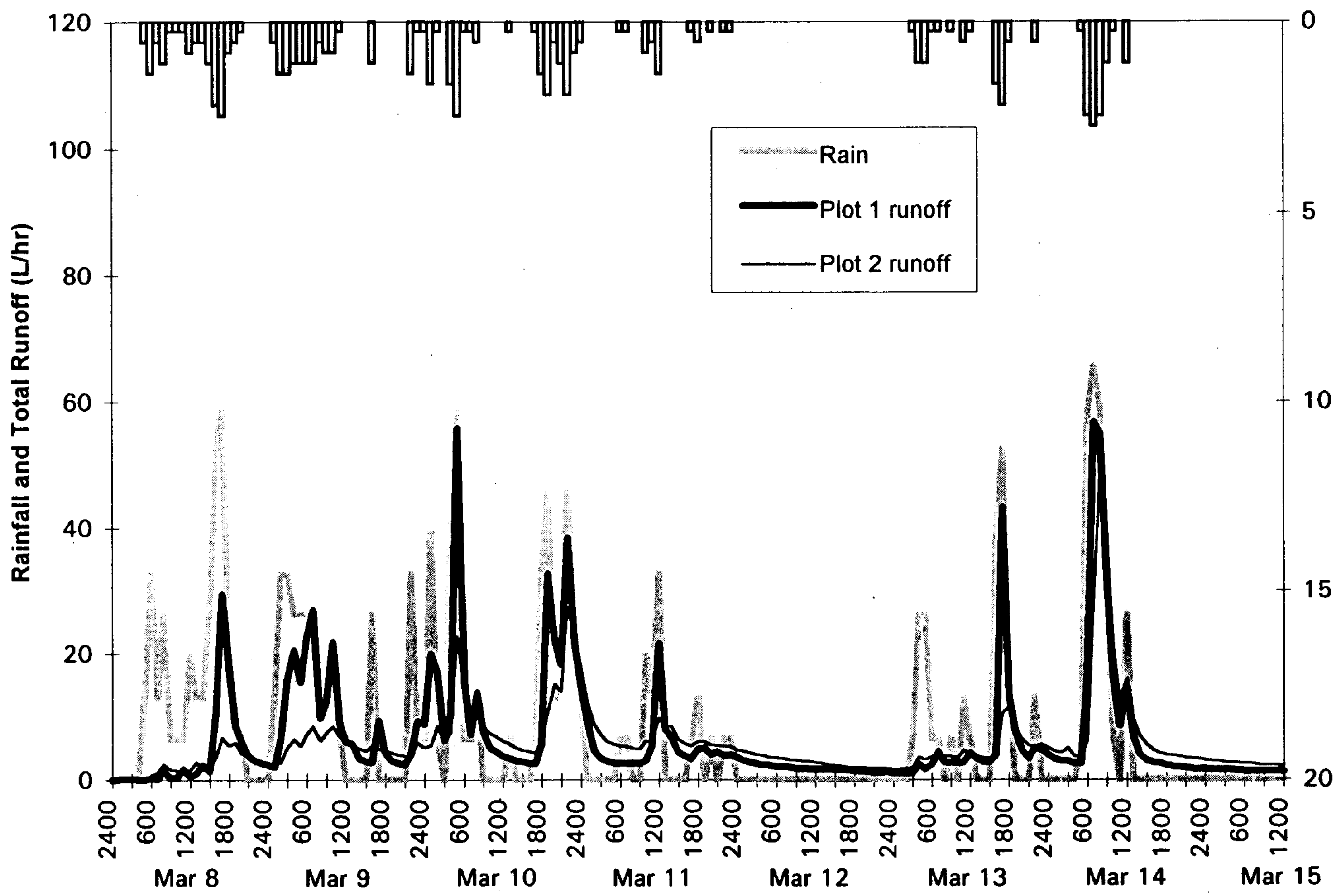

Figure 4-5: Rainfall and runoff for Plots 1 and 2 for the storm system of March 8-15, 1995

4.5 Hydrograph analysis - All plots, February 14 - 20

The previous section focused on Plots 1 and 2 over a series of storm systems. For this section the same type of analysis was performed on all seven plots to compare the responses of the various plots. The storms of February 14 - 20 were selected because they were fairly representative of the winter storms observed at the study site and the monitoring systems were generally operational on all of the plots.

As described in section 4.4.3, the storms of February 14 - 20 produced 70 mm (2.76 inches) of rain over four events. The ten days prior to the onset of rainfall were dry.

4.5.1 Condition of instrumentation

The monitoring systems were generally operational at the time of the storm. Gutters had been completely installed and bentonite had been used to seal any likely leak locations. A few malfunctions were noted, however.

> Plot 3 Subsurface Bucket: Data analysis revealed that prior to the storm the subsurface bucket for Plot 3 was not functioning. On inspection the bucket was found to have stuck in the center position, probably due to grit in the sleeve bearings. The bucket was returned to operation at 3:10 p.m. on February 16, immediately prior to the first storm peak, but the initial flows before the storm were not recorded.

> Plot 7 Subsurface Bucket: The data reveal that the subsurface bucket for Plot 7 stuck at midnight on the night of February 20, probably also due to grit in the bearings. It was cleaned and returned to operation, but too late to catch the full recession of Plot 7 after this storm.

4.5.2 Storm analysis, Plots 1; 3, and 4

Because Plot 2 was discussed in the previous section, only the hydrographs from Plots 3 and 4 will be discussed and compared to their control (Plot 1) here. The relevant hydrographs are shown in Figure 4-6.

Runoff from Plot 3 was not monitored during the first event (February 15). With the exception of a small reduction in the first peak of the second event (afternoon of February 16), the difference in hydrologic behavior between this amendment and the unamended till control (Plot 1) was minimal. The runoff rates of Plot 3 were nearly equal to those of Plot 1 as of the morning of February 17. Runoff peaks from Plot 3 actually exceeded those of Plot 1 on February 18, 15:00, and February 19, 15:00. The recession flow rates of Plot 3 were slightly lower than those of Plot 1, but the difference was negligible.

Plot 4 (fine Cedar Grove, 4:1) showed the most unexpected behavior of all the plots. The runoff rates during the initial peaks of the first two events (February 15, 09:00, and February 16, 18:00) were substantially higher than those of the control plot, with flow produced principally by surface runoff. Thereafter, storm runoff rates were about equal to those of the control plot. Inter-event drainage was slower than that of the control soil, sometimes by a factor of two (e.g. February 15, 15:00, February 17, 12:00, and February 20, 03:00).

Piezometer readings from Plots 1 through 4 at the onset of the second event are shown in Table 4-13. Ponding was observed only on Plot 4, with the lower 75% of the plot exhibiting surface saturation and water ponding on the surface.

Table 4-13: Water table depths before and after the event of Feb. 16-17, 1995 (cm)

	Distance of piezometer from bottom of slope (meters)				
	0.66	1.5	2.75	4.88	7.32
Plot 1	dry (dry)	dry (15.0)	12.5 (22.0)	13.5 (17.5)	18.0 (27.0)
Plot 2	11.5 (17.0)	13.0 (23.0)	-	-	-
Plot 3	-	17.5 (21.5)	-	-	-
Plot 4	-	23.0 (23.5)	-	-	-

February 16, 3:15 p.m. (February 17, 12:00 noon in parenthesis)

Though the runoff volumes from Plots 1 and 4 between the piezometer readings of Table 4-13 were about equal, the piezometers levels in Plot 1 changed significantly during the storm while the piezometer of Plot 4 remained fairly static. From simple mass balance, one would expect water levels to change similarly in the two plots (assuming similar porosity). This discrepancy indicates that water table depths from a few piezometers along the sloping plot may lead to erroneous inferences of the water table profile dynamics.

Water tables were observed at or near the ground surface on all plots on February 19 at 2:45 p.m., at the peak of the last storm event. Plot 4 piezometer readings were typically higher than those of Plots 1, 2, and 3 during storms throughout the study.

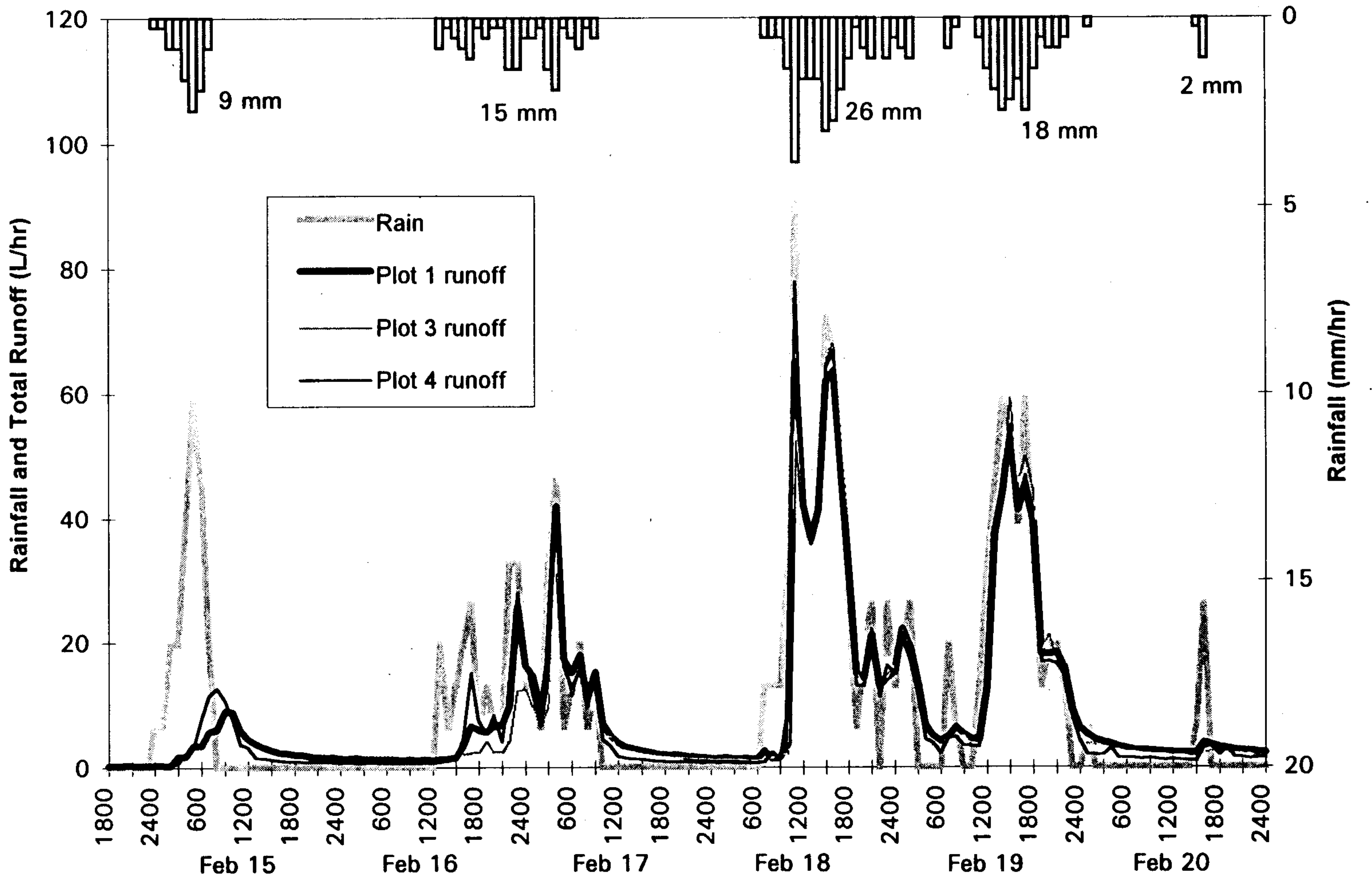

Figure 4-6: Rainfall and runoff for Plots 1, 3, and 4 for the storm system of February 14-20, 1995

4.5.3 Storm analysis, Plots 5-7

Plot 5, the control for the second batch of till, was observed to be non-conductive to the point of impermeability during the winter and early spring of 1995. Plot 5 drained poorly and typically remained near saturation, resulting in surface runoff generation due both to a lack of additional storage for rain water and the low infiltration rates into the tight soil. Therefore runoff from Plot 5 should be an upper bound for the runoff of Plots 6 and 7. These properties of Plot 5 are apparent in Figure 4-7. The runoff measured from Plot 5 through the period of record consisted almost entirely of surface runoff, and subsurface flow volumes were generally negligible in comparison.

The only notable difference between Plot 5 and Plot 7 was at the first storm peak, where the amended soil of Plot 7 reduced the peak runoff by about 25% and delayed the peak by approximately one hour relative to Plot 5. This delay might be caused by differences between Plots 5 and 7 in surface topography and vegetation. For the remainder of the storms the hydrographs of Plots 5 and 7 were nearly identical during periods of rainfall. During dry periods Plot 7 drained at higher rates than Plot 5, but not at rates high enough to make storage available for subsequent rainfall.

Plot 6, the 2:1 Groco mix, demonstrated responses clearly different from those of Plots 5 and 7. All peak runoff rates were reduced, soil water storage capacity was markedly higher, and recession flow rates were higher between storms. The amended soil nearly completely absorbed the first event and still had storage capacity to significantly attenuate the initial rain of the second storm on February 16. Between storms Plot 6 drained at rates approximately twice that of Plot 7.

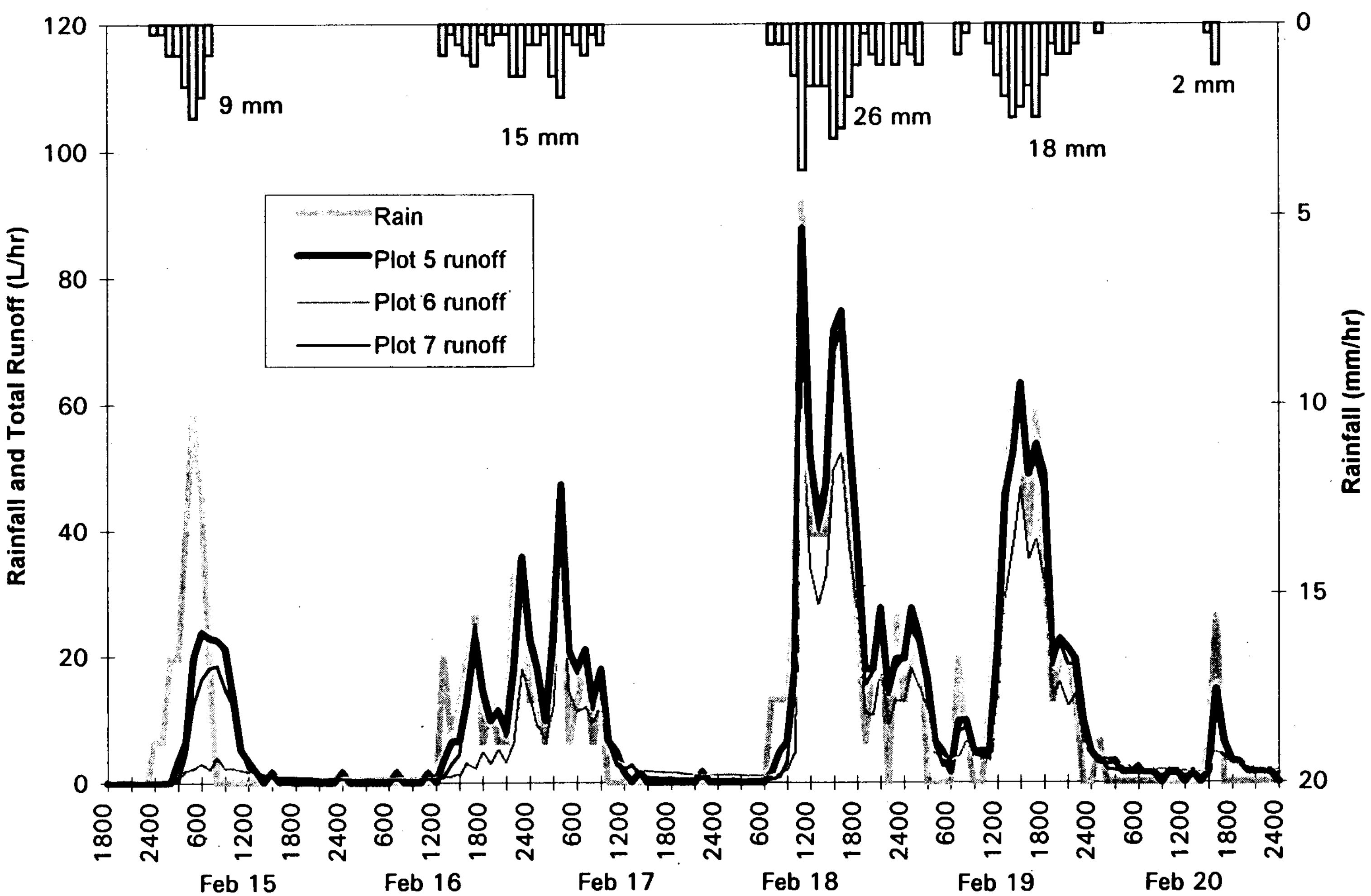

Figure 4-7: Rainfall and runoff for Plots 5, 6, and 7 for the storm system of February 14-20, 1995

Chapter 5 - Statistical summaries of hydrologic behavior of the plots

5.1 Procedures for comparing plot response behavior statistically

5.1.1 Introduction

In addition to analyzing features of the various recorded time series, the hourly runoff data from the seven plots were used to develop summary statistics of runoff behavior. The procedures are suitable for any combination of the seven plots and result in quantitative corroboration of behavior observed from the storm system hydrograph records. The value of this approach lies in its simplicity, flexibility, non-reliance on arbitrary selection of data, and repeatability for future comparisons. The statistical procedures use data from December 19, 1994, when the monitoring systems were generally operational, to April 23, 1995, the day before the first artificial rainfall simulation.

5.1.2 Measures of baseflow and fast flow production

During a period of record, there existed N hours during which plot i (control) and plot j (amended) were operational and logging runoff accurately. With N sufficiently large the two sets of runoff measurements $\{Q_1, Q_2, ..., Q_N\}_i$ and $\{Q_1, Q_2, ..., Q_N\}_j$ can be compared by calculating each plot's mean hourly runoff rate and the total flow volume for the N hours of flow. By plotting the respective cumulative distribution functions any differences in response between an amended plot and its control at high and low runoff rates become evident.

The same procedure can be used with a slight variation to compare the fast flow response of different plots. Quick-response runoff is composed primarily of surface runoff and shallow subsurface flow (through loose topsoil at the surface) and subsides within one to two hours after the end of rain for these particular test plots. Because it was hypothesized that amending till with compost would improve infiltration and reduce and delay runoff peaks, a statistical measure was developed which provides a relative measure of the fast flow response behavior in the plots over the period of record. The procedure described above for obtaining a set of runoff values for each plot was performed, but for the fast response analysis the set of N values was reduced to include only those hours during which rainfall occurred. This sample selection criterion produces sets of flows that occur while a storm is in progress.

To aid interpretation, the baseflow cumulative distribution functions are plotted on a logarithmic scale to clarify the graph at low flow rates. The fast flow response cumulative distribution functions are plotted on a linear scale to emphasize the results in the range of high flow rates.

5.1.3 Runoff volume scatterplots

Each plot with amended soil was compared to its control plot using scatterplots. The ordered pairs of runoff volumes were plotted with the control's runoff on the X-axis and the amended plot's runoff on the Y-axis. Thus, for time t in the period of record the point (x_t, y_t) was plotted on the scatterplot, where x_t and y_t were the runoff volumes for the control plot and the amended plot (respectively) during the time increment t to $t+\Delta t$. If the responses of the plots were identical for every time increment, all points would lie on a line from the origin with a slope equal to 1.0. The spread, density, pattern, and locations of the observed data points can be interpreted to infer the difference in response behavior between the two plots.

To explore the time scales at which differences in behavior were most notable, the scatterplots were drawn for four time increments: $\Delta t = 1, 3, 6,$ and 24 hours.

5.1.4 Effects of rain depth on differences in response

To explore any relationships of rain depth and differences in response between the amended plots and the control plots, ΔR_{ij}, the difference in runoff volume between the plots *i* and *j* during the time increment Δt, was plotted against the depth of rainfall during the same time increment. If the responses from the plots were identical, all points would lie along the line $\Delta R_{ij} = 0$.

These graphs were drawn for four time increments: $\Delta t = 1$, 3, 6, and 24 hours. This procedure was performed only for two pairs of plots: Plots 1 and 2, and Plots 5 and 6.

5.2 Comparisons of Plot 1 and Plot 2

5.2.1 Baseflow and fast flow

The period of runoff measurements from December 19 to April 24 contained 2307 hours where the instruments for Plots 1 and 2 were both logging data. The cumulative distribution functions of both plots are graphed in Figure 5-1a. Approximately 92% of the runoff values for both plots were below 7 liters per hour. Flow rates below 7 liters per hour occurred more often in Plot 2, reflecting the higher recessional flows measured from Plot 2 and indicating that Plot 2 produces sustained baseflow rates higher than Plot 1. The median flow from Plot 2 was about 50% higher than the median flow from Plot 1.

From the same period of record, 349 hours were extracted during which rainfall occurred and the monitoring systems for Plots 1 and 2 were operating. The cumulative distribution functions are shown in Figure 5-1b. Twenty percent of the flows from Plot 1 exceeded 20 L/hour, while only 13% of the flows from Plot 2 exceeded the same mark.

Accumulated flow volumes from the sample sets were used to generate additional statistics. Total runoff during the sampled hours was approximately equal between the two plots, with 6456 liters from Plot 1 and 6272 liters from Plot 2. Ignoring the changes in storage between the beginning and the end of the sampling period, the amounts of water lost from evapotranspiration were nearly equal for Plots 1 and 2. With a total of 11984 liters of precipitation recorded (equivalent to 504 mm, or 19.84 inches), Plots 1 and 2 lost approximately 47% of the rainfall to evapotranspiration during this period of record (December to April) at an average rate of 0.10 mm/hour (0.0041 inches/hour). In a comparison, the Penman-Monteith calculations (Section 4.1.3) produced a mean estimated daily evaporation rate from December to May of 12.7 mm/day (0.050 inches/day), which would require approximately 12.5 hours of evaporation at the mass balance-estimated hourly rate of 0.10 mm/hour. (This simple comparison does not take into account the non-linearity of daily and seasonal evapotranspiration rate fluctuations, or the dates from which the sampled hours were actually extracted for these statistical procedures.)

In terms of accumulated volumes, Plot 2 generated only 74% of the runoff of Plot 1 during these 349 hours of rainfall. Plot 1 released 66% of its total runoff (4245 liters) as fast-response flows, while Plot 2 released only 50% of its total runoff as fast-response flows (3152 liters out of 6272 total liters).

As discussed in Chapter 4, estimates of channel-changing flows range from 12 to 60 L/hr. Using the low end of the range (12 L/hr) as the threshold, Plot 1 generated significant runoff during 176 hours compared to 131 hours for Plot 2. At the upper end of the range, Plot 1 runoff exceeded 60 L/hr 41 times, while Plot 2 runoff exceeded the same mark only 33 times.

5.2.2 Scatterplot analysis

The four scatterplots of the runoff rates of Plots 1 and 2 are given in Figure 5-2. The patterns of all four graphs indicate that flows from Plot 1 typically exceeded flows from Plot 2, especially during time periods with higher runoff volumes. Plot 2 runoff exceeds Plot 1 runoff during periods between storms, when water is being released as baseflow.

The scatter of the plots decreases with larger time increments, with the best correlation between plots seen at the 24-hour time scale: with most storms lasting less than 24 hours, the higher recession flow rates from Plot 2 would compensate for the lower flow rates during the storms and result in comparable 24-hour runoff volumes between Plot 1 and Plot 2. This observation indicates that the beneficial effects of soil amendment on storm flow reduction are more significant (though more erratic) at shorter time periods for the 9.5 meter-long plots used here.

5.2.3 Effects of rain depth on differences in response

The difference in runoff between Plots 1 and 2 as a function of rainfall depth is plotted for the four time intervals in Figure 5-3. The general trends for all four plots show that Plot 2 generated more flow than Plot 1 at lower rainfall rates, while Plot 1 generated more runoff at moderate to high rainfall depths, though the magnitudes of the difference were significantly higher when Plot 1 produced more runoff.

The scatter in the data points increased with higher rainfall depths. This is probably because the responses of the plots to higher rainfall volumes were more dependent on antecedent conditions. Scatter also increased slightly with longer time intervals, but no single time scale proved critical in determining the effects of the amendment.

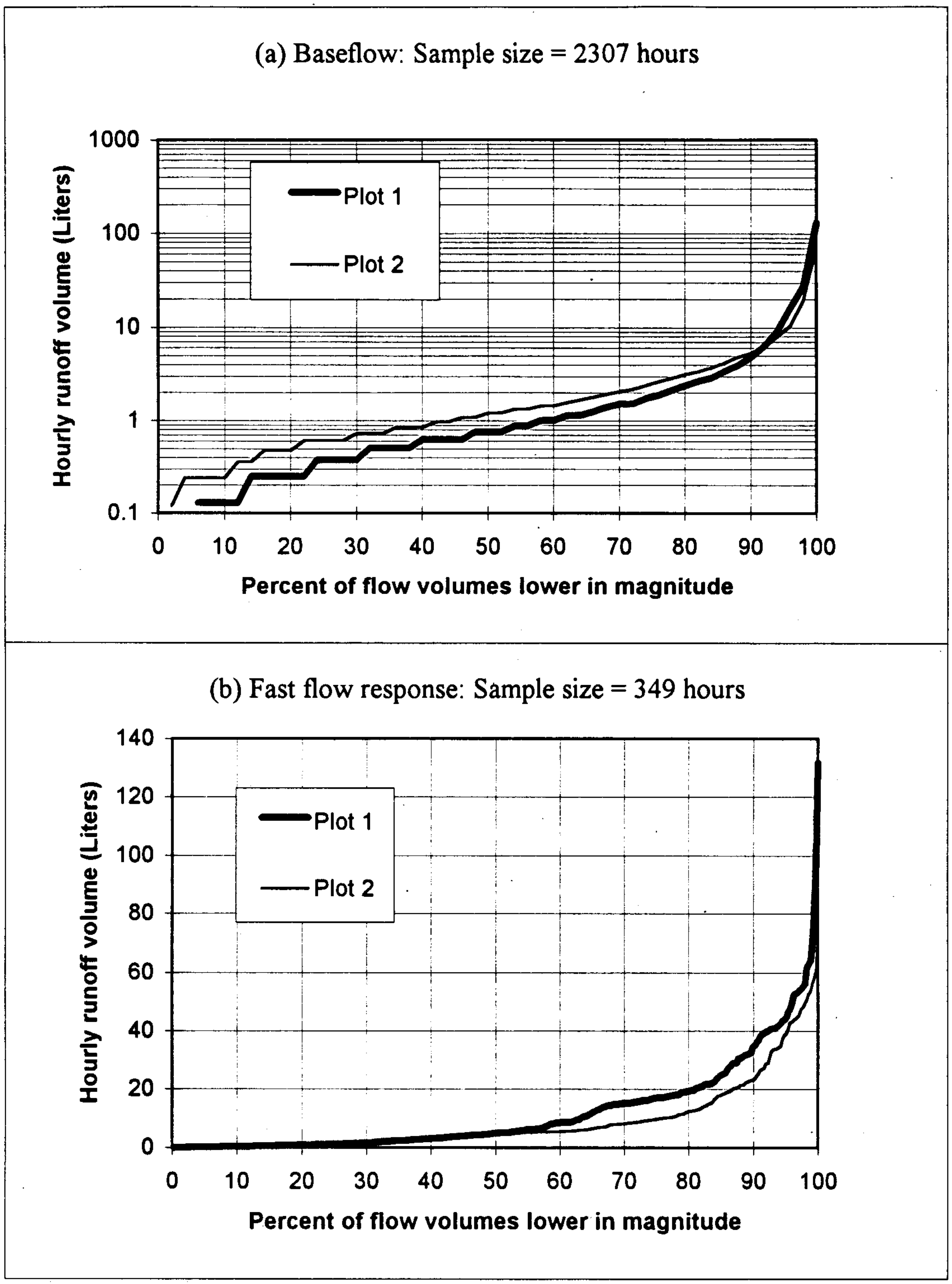

Figure 5-1: Cumulative distribution functions for Plots 1 and 2
(a) During all operational hours; (b) during hours with rainfall

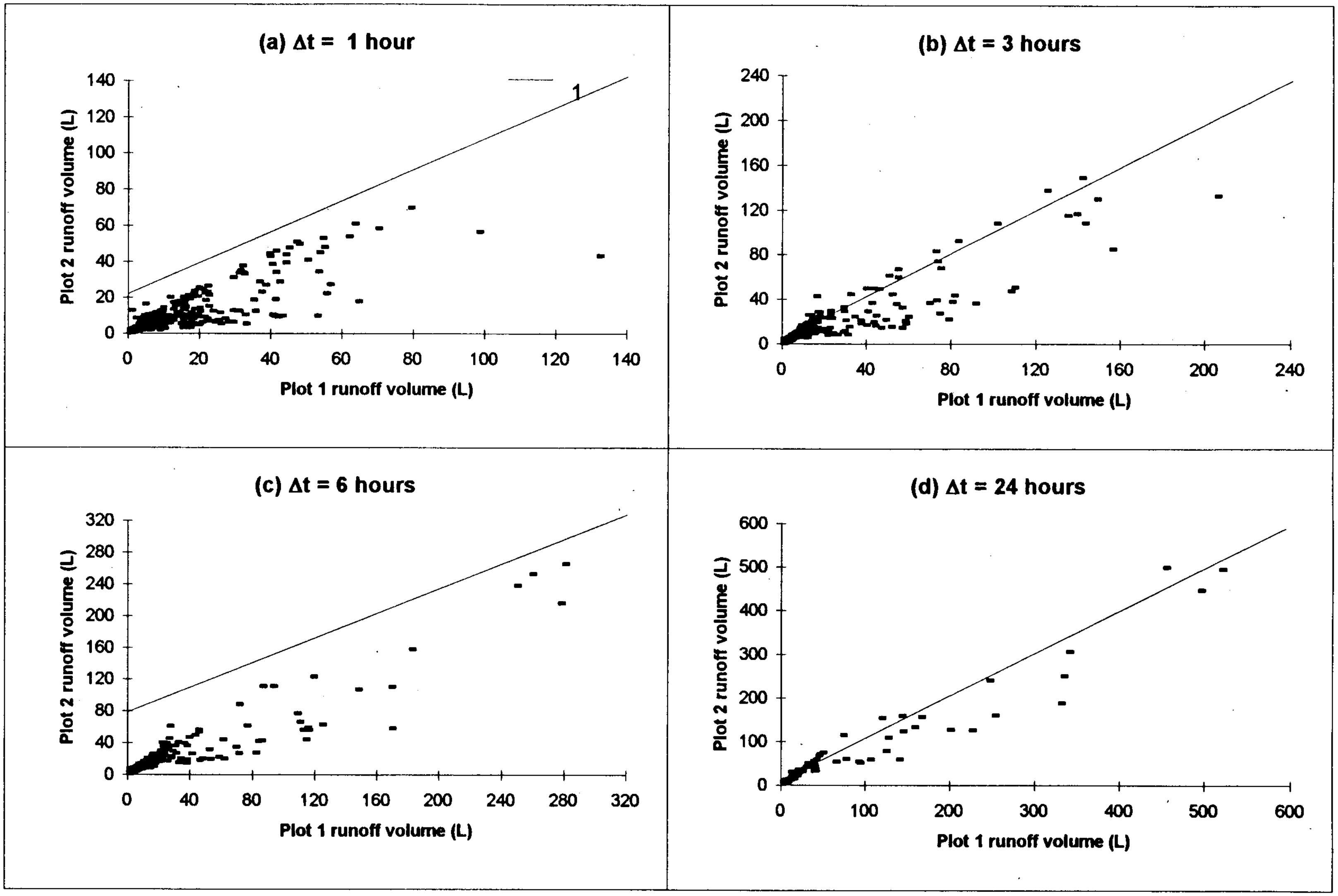

Figure 5-2: Scatterplots of Plot 1 runoff and Plot 2 runoff for four time increments

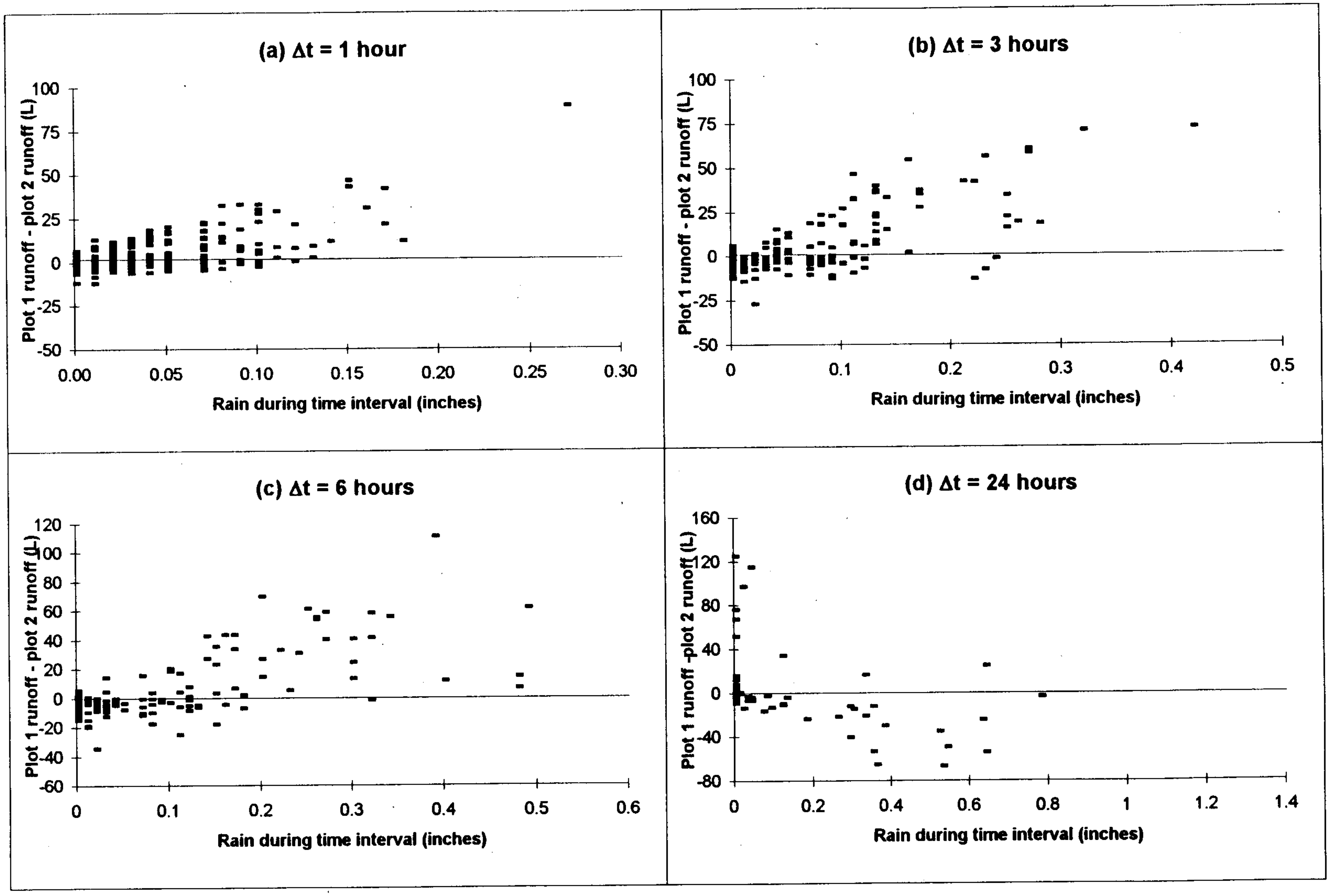

Figure 5-3: Difference between Plot 1 runoff and Plot 2 runoff versus rainfall for four time increments

5.3 Comparisons of Plot 5 and Plot 6

5.3.1 Baseflow and fast flow

Plot 5 and Plot 6 were both operating for 1549 hours. During approximately 60% of these hours, Plot 5 (the till control plot) was generating no runoff. The cumulative distribution function (Figure 5-4a) shows that another 14% of the flows were measured with only one subsurface bucket tip per hour. The highest 22% of the flows are higher by an order of magnitude. Few runoff measurements between these lower and higher flow rates were recorded. Thus runoff from Plot 5 occurred at high rates during storms, but baseflow was rarely observed.

In contrast, flow from Plot 6 occurred often and across a wide range of flow rates. Baseflows were common, with the plot generating at least 0.5 liters per hour during more than 50% of the sampled hours and at least 1 liter per hour 30% of the time. Plot 6 generated measured runoff during more than 98% of the sampled hours, indicating a reliable baseflow like that observed in Plot 2 earlier.

Hourly runoff volumes for the 245 hours with rainfall and functioning instruments are shown in Figure 5-4b. The curves show that Plot 5 generated high runoff volumes for a greater proportion of the time during storms than Plot 6.

Plot 5 generated 39% more runoff than Plot 6 overall (4404 liters for Plot 5 and 3162 liters for Plot 6), and generated 88% more runoff during hours with rain (3747 liters for Plot 5 and 1997 liters for Plot 6). Also, Plot 5 produced 85% of its runoff during the storms, while Plot 6 produced 63% of its runoff during storms. All of these simple statistical measures indicate that Plot 5 shed water quickly and rarely provided baseflow, while Plot 6 absorbed the rainfall, stored it, and released it slowly as baseflow.

Using the estimated magnitudes of channel-changing discharges, Plot 5 generated significant runoff about twice as often as Plot 6. Plot 5 runoff exceeded 12 L/hr during 144 hours, while Plot 6 exceeded the threshold during only 78 hours. Similarly, Plot 5 generated at least 60 L/hr during 25 hours, compared to 12 hours for Plot 6.

5.3.2 Scatterplot analysis

Scatterplots for comparing Plot 5 hourly runoff volumes to Plot 6 runoff volumes are shown in Figure 5-5. It is clear from the scatterplots that Plot 6 volumes were lower than the corresponding Plot 5 volumes in nearly every instance. The trends were similar at each time interval, with no single time scale providing more correlation than the others.

5.3.3 Effects of rain depth on differences in response

Figure 5-6 indicates that the amount of runoff from Plot 5 relative to Plot 6 increased with higher rainfall depths. This trend illustrates how Plot 6 stored rain water from storms of all magnitudes, while Plot 5 shed more water as rain input increased.

The pattern of the data points varied for the different time increments. At $\Delta t = 1$ hour (Figure 5-6a), hourly rainfall of any magnitude resulted in more runoff from Plot 5 during that hour. As time intervals increase Plot 6 is more likely to produce more runoff with low rainfall depths. This difference occurs because the fraction of time without rain increases as the time increment increases, and recession flow from Plot 6 between storms can result in higher accumulated runoff volumes from Plot 6. As was noted from Plots 1 and 2, the effect of amendment on reducing storm flow rates is most pronounced at shorter time increments for these plots.

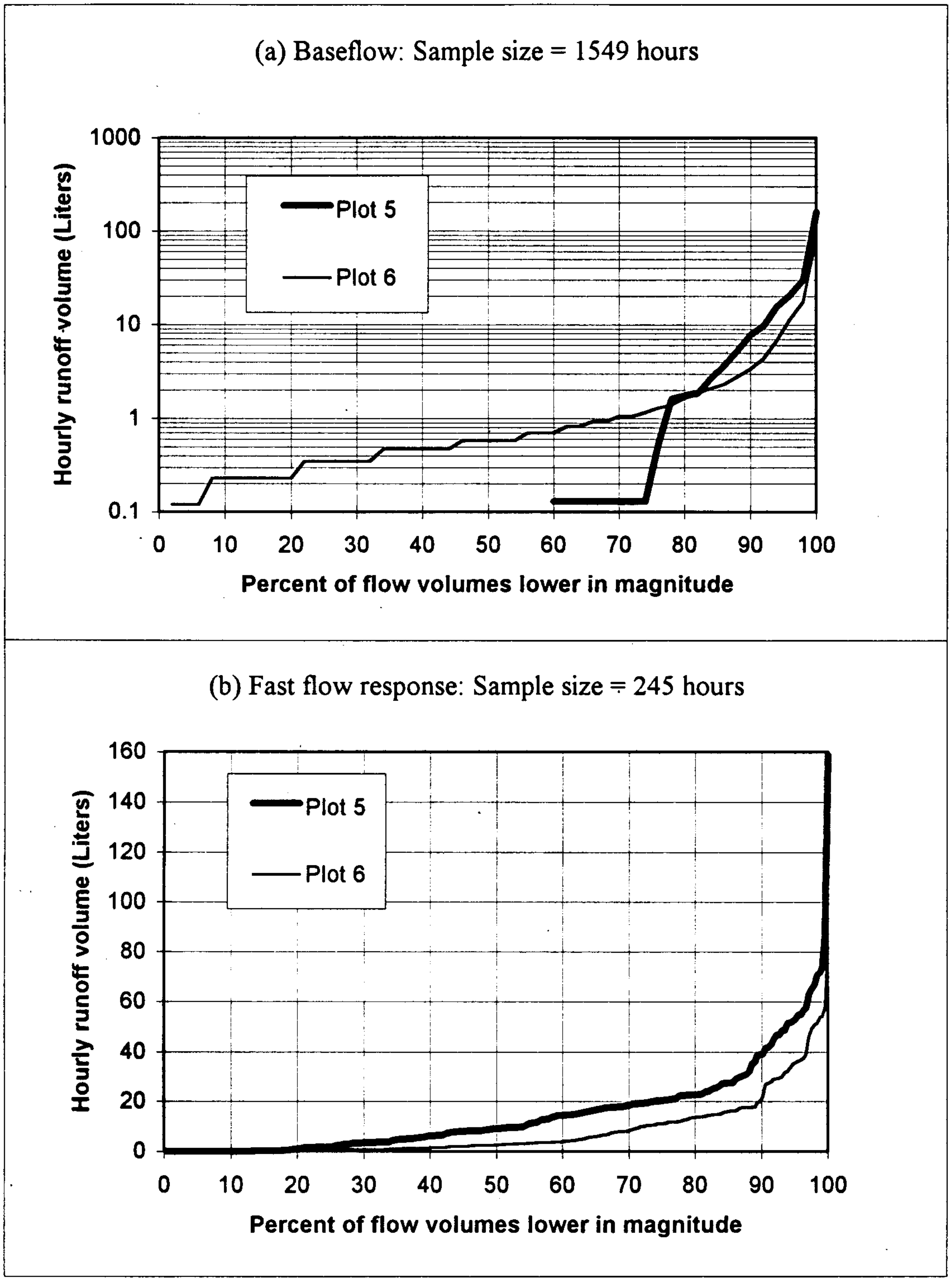

Figure 5-4: Cumulative distribution functions for Plots 5 and 6
(a) During all operational hours; (b) during hours with rainfall

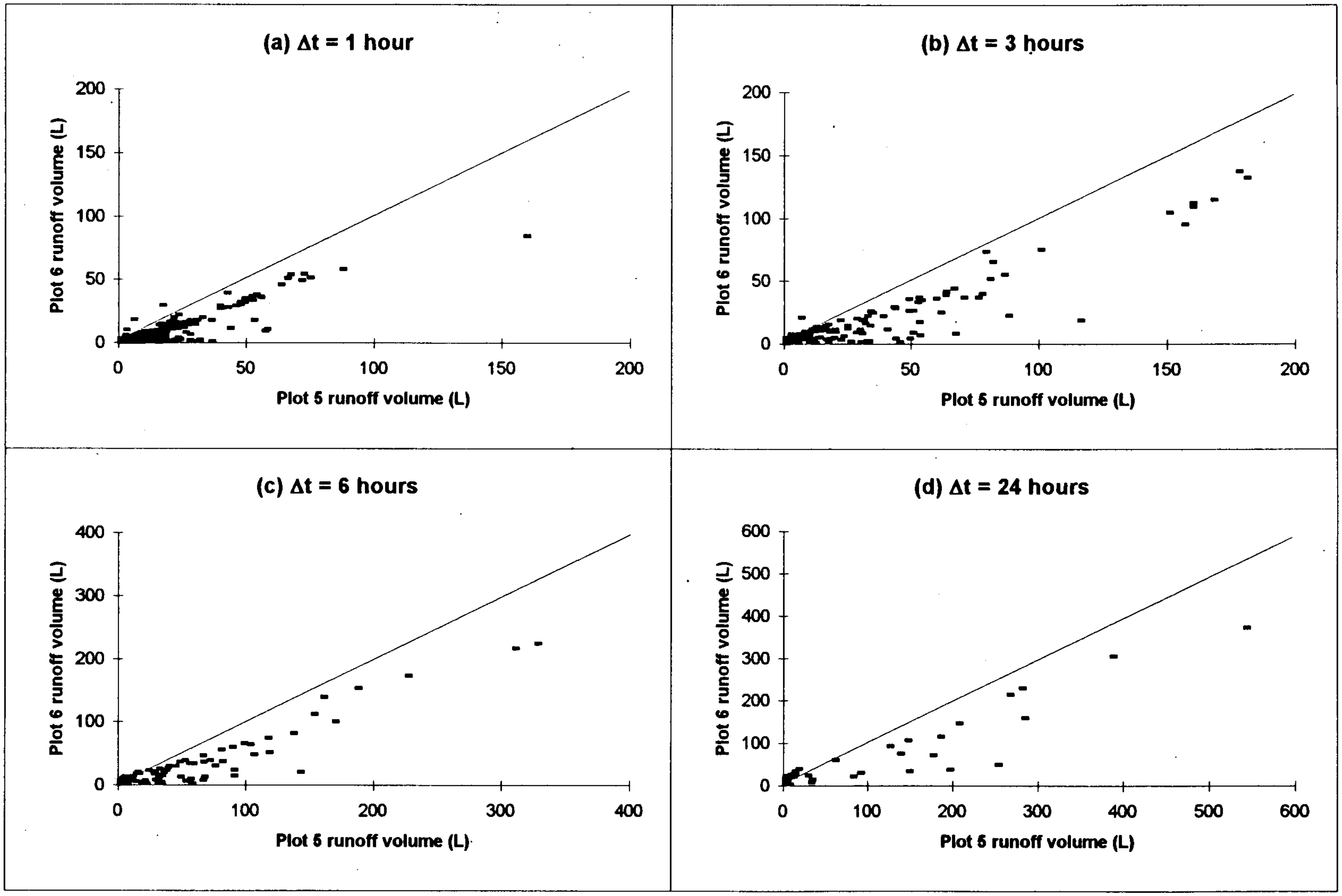

Figure 5-5: Scatterplots of Plot 5 runoff and Plot 6 runoff for four time increments

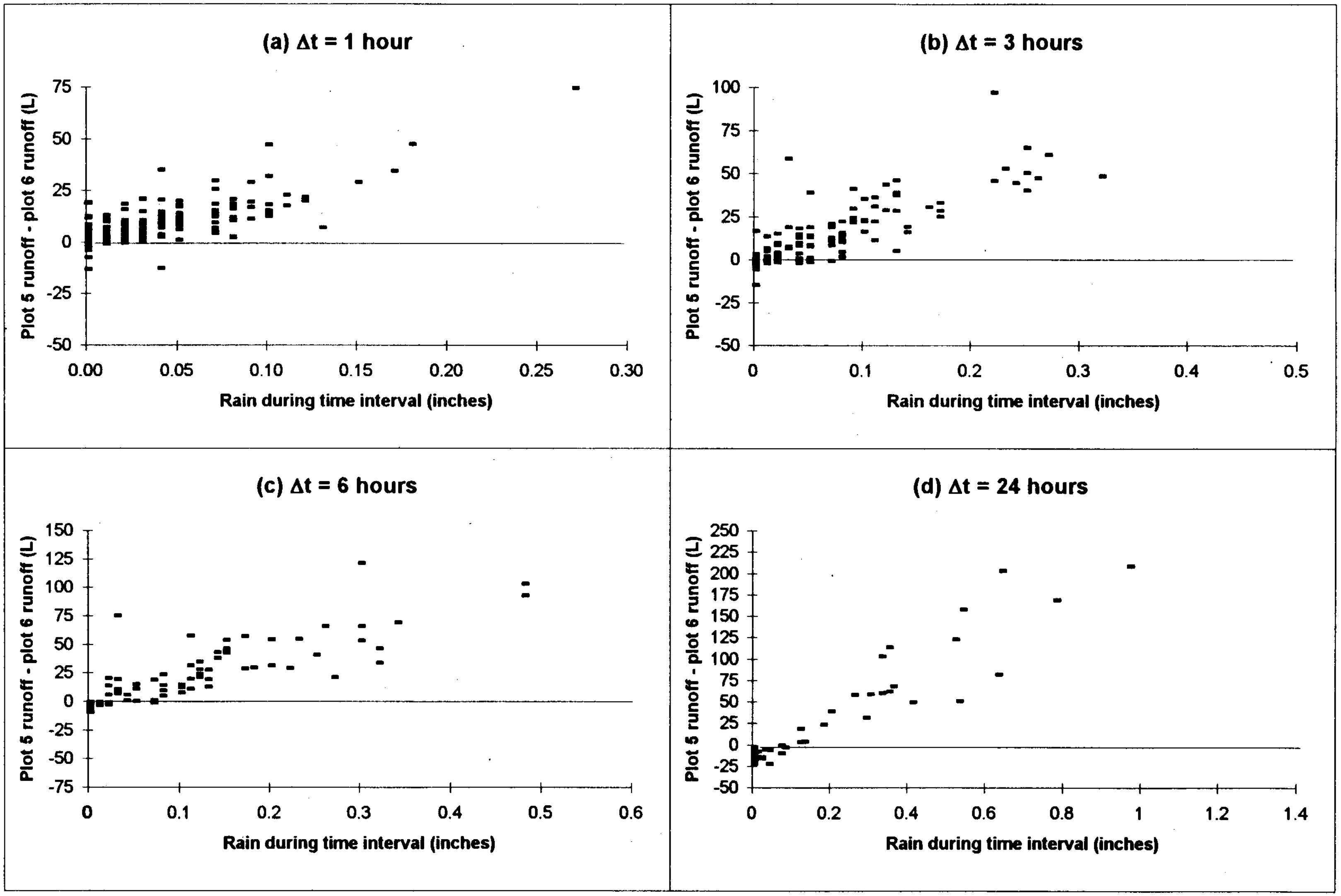

Figure 5-6: Difference between Plot 5 runoff and Plot 6 runoff versus rainfall for four time increments

5.4 Statistical comparison of all plots

5.4.1 Runoff statistics from all seven plots

From December 19, 1994 to April 24, 1995, the data contained 1382 hours during which all seven plots were operational. Most of the hours which satisfied this criterion were between February and April due to the delays in installing some of the collection systems, so the statistics are not as representative of the response behavior of the plots as the statistics in the previous analyses of the pairs of plots.

The accumulated runoff volumes recorded from the plots and statistics derived from these values are listed in Table 5-1.

Table 5-1: Summary runoff statistics for all seven plots

	Plot 1 Control	**Plot 2** 2:1-Fine	**Plot 3** 2:1-Coarse	**Plot 4** 4:1-Fine	**Plot 5** Control	**Plot 6** 2:1-Groco	**Plot 7** 3:1-Fine
During all hours (N=1382)							
1. Total runoff (Liters)	3450	3253	2863	2875	3865	2800	3593
2. Total runoff /control runoff	*n/a*	*94*	*83*	*83*	*n/a*	*72*	*93*
3. Maximum flow rate (L/hr)	132	92	95	116	159	88	151
During hours with rain (N=212)							
4. Total runoff (Liters)	2332	1641	2033	2315	3370	1783	3080
5. Total runoff /control runoff	*n/a*	*70*	*87*	*99*	*n/a*	*53*	*91*
6. Runoff during rain / total runoff	*68*	*50*	*71*	*81*	*87*	*64*	*86*
6a. Values from previous sections	*66*	*50*	-	-	*85*	*63*	-

Note: Fractions are expressed as percentages

In Table 5-1, line 2 (total runoff/control runoff) indicates the effectiveness of each amendment in retaining water over long periods of time, with low runoff ratios in relation to the control indicating that more water was retained and eventually lost to evapotranspiration. The Groco amendment in Plot 6 produced the most significant effect in this respect, while Plots 2 and 7 released nearly as much water as their controls in the long term.

From line 3, plots with higher soil hydraulic conductivity (Plots 2 and 6) produced lower maximum recorded flow rates than the plots with low conductivity (Plots 1, 4, 5, and 7). More conductive soil can sustain higher infiltration rates at the outset of rainfall, and after the storm the soil transports water to the subsurface outlet, thereby providing water storage capacity to accommodate ensuing rain water. Both of these mechanisms resulted in the lower recorded maximum runoff rates.

Line 5 illustrates the effectiveness of the amended soils in reducing the fast response flows (runoff while the storm is still in progress). Plot 2 reduced the fast response runoff most effectively of the first four plots, generating only 70% as much runoff as Plot 1 during hours with rain. Plot 4 behaved poorly in this respect, producing nearly as much runoff as Plot 1 during storms. Plots 3 and 7 were marginally effective. Plot 6 proved most effective at altering the control's behavior by producing about half as much runoff as Plot 5 during storms.

Finally, line 6 provides information about the tendency of plots to produce runoff while the storm is in progress or after the storm ends. (Values from Sections 5.2.1 and 5.3.1, where the samples were larger, are shown on line 6a for comparison.) In this respect Plot 2 was most effective, with only 50% of its runoff occurring during rainfall. Plot 6 produced 64% of its runoff during storms. Significantly, the 4:1 amendment of Plot 4 affected this behavior detrimentally by a significant magnitude: 81% of the runoff from Plot 4 occurred during rainfall, compared to only 68% for its control. The amendment for Plot 7 was ineffective at altering the soil's behavior, while the amendment used in Plot 6 significantly altered the response behavior relative to the unamended till in Plot 5.

Of concern is the indication that Plots 3 and 4 produced nearly equal runoff volumes which were significantly below those of Plots 1 and 2 (lines 1-3). These values are counter-intuitive and seem to contradict the indications from field observation, time series information, and the statistics from lines 4 through 7 of the table. Two possible reasons are (1) leaks in the liners or (2) the influence of friction on the tipping buckets at low flow rates, but neither of these explanations were corroborated by other evidence or observation.

5.4.2 Comparison of Plots 3 and 4 to their control

The cumulative distribution functions for Plots 1, 2, 3, and 4 are shown in Figure 5-7 both for all 1382 hours and for the 212 hours with rain. The fast response behavior of Plots 3 and 4 was similar to the behavior of Plot 1, while Plot 2 produced more low flows during storms. Plots 3 and 4 produced no baseflow 35% and 43% of the time, respectively, a trait which is contradictory to the behavior of Plot 2.

The scatterplots of Plot 3 versus Plot 1 (Figure 5-8) and Plot 4 versus Plot 1 (Figure 5-9) show that both Plots 3 and 4 produce runoff that corresponds closely with the runoff from their control. At shorter time intervals the amended plots often produce runoff volumes greater than those of the control, but at all time intervals the data generally follow the line of 1:1 correspondence.

Plots 3 generally behaved like the control (Plot 1) during rainfall, yet produced little baseflow between storms. Plot 4, with soil properties more like those of the control (see Section 3.5), behaved even more like the control during storms and also produced little baseflow. This behavior is evident from the cumulative distribution functions, the scatterplot comparisons, and the accumulated volume statistics of Table 5-1.

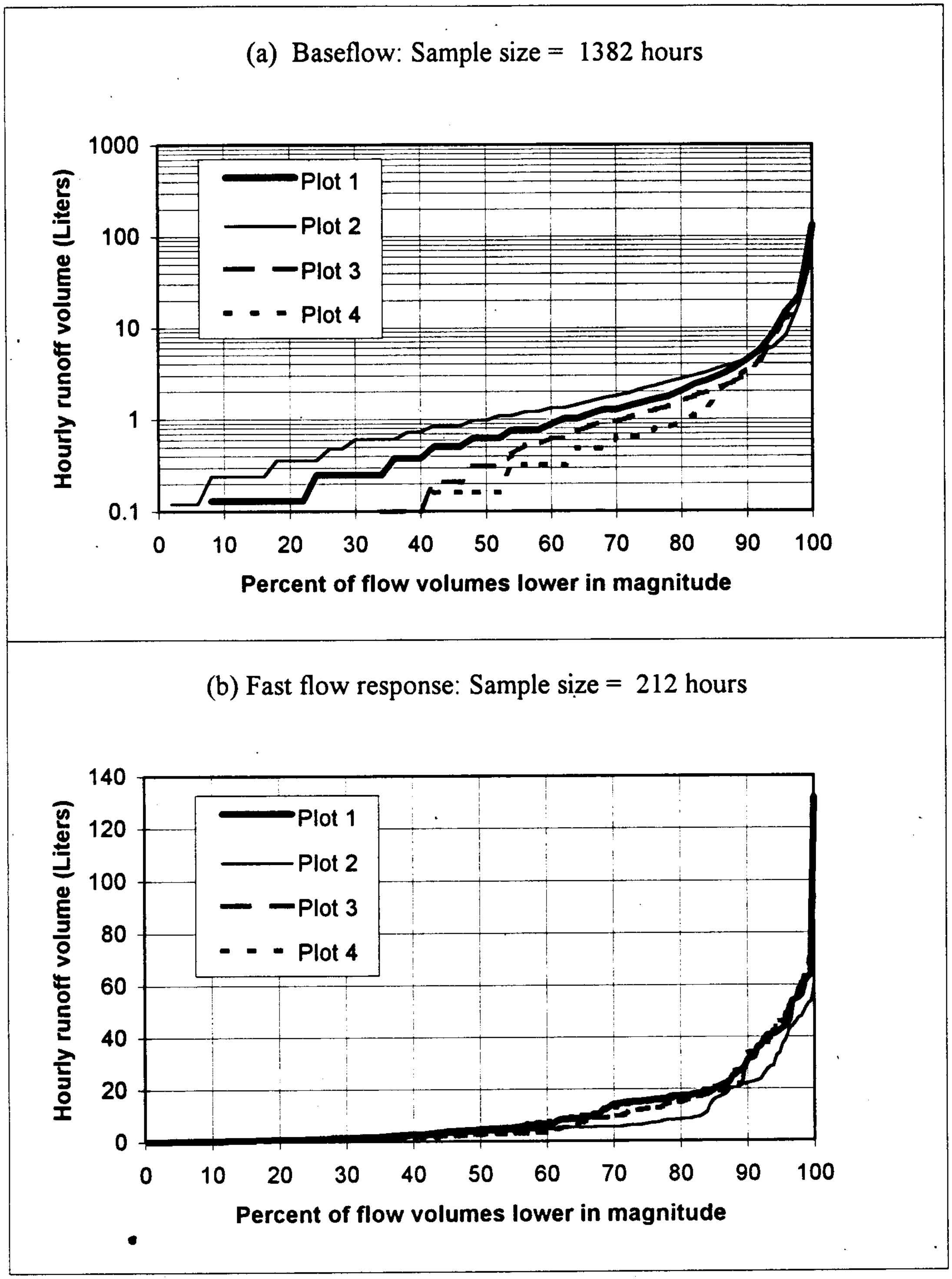

Figure 5-7: Cumulative distribution functions for Plots 1, 2, 3, and 4
(a) During all operational hours; (b) during hours with rainfall

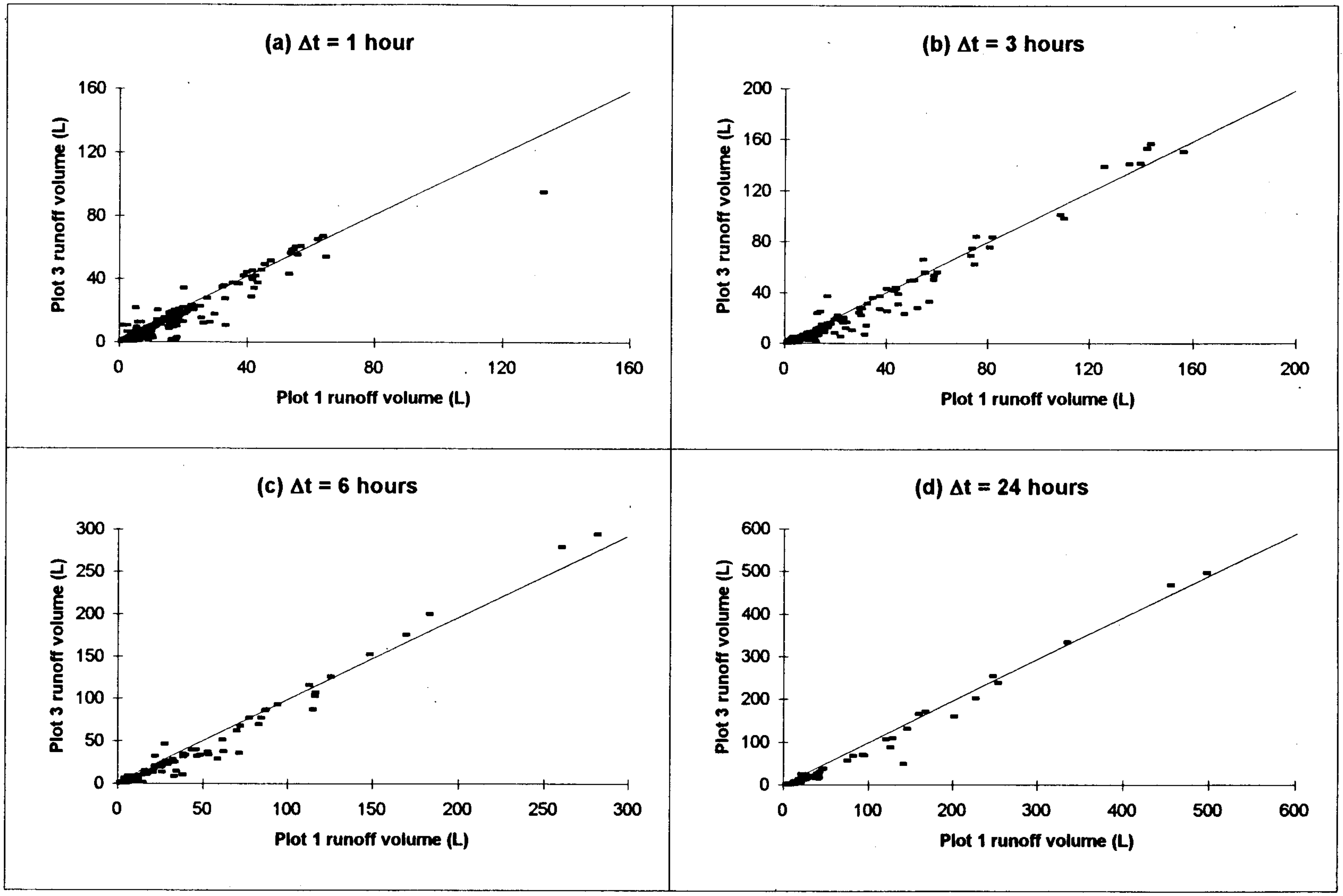

Figure 5-8: Scatterplots of Plot 3 runoff and Plot 1 runoff for four time increments

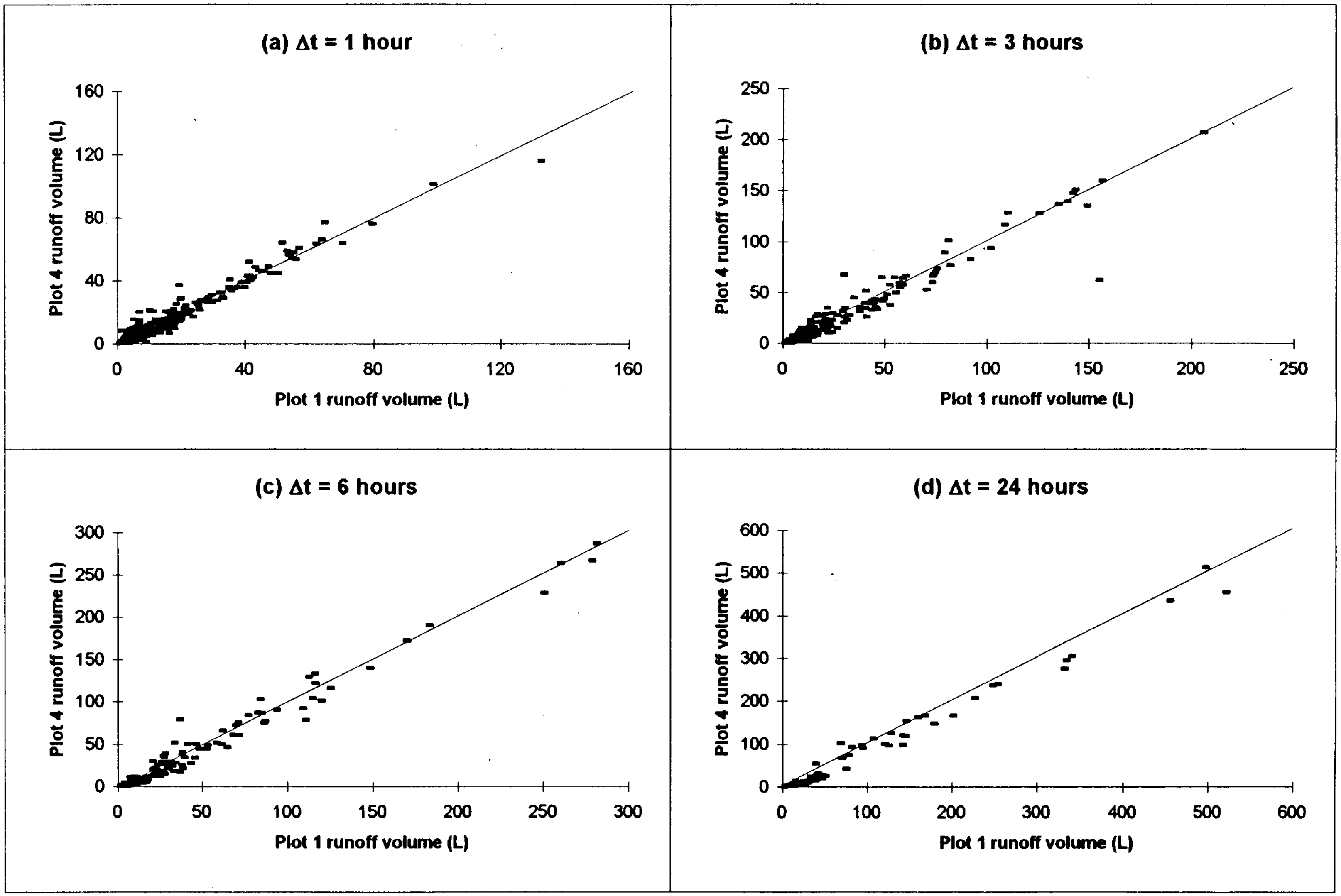

Figure 5-9: Scatterplots of Plot 4 runoff and Plot 1 runoff for four time increments

5.4.3 Comparisons of Plots 6 and 7 to their control

The cumulative distribution functions for Plots 5, 6, and 7 are shown in Figure 5-10. Plot 6 was the only one of these three plots to produce consistent baseflow and lessen the fast flow response. Plot 7 behaved much like the control, particularly during storms.

The scatterplot of Plot 7 runoff versus Plot 5 runoff is shown in Figure 5-11. At $\Delta t = 1$ hour Plot 7 occasionally produced higher flow volumes than the control, but only at lower flow magnitudes (most likely during light rain after large events). For longer time intervals Plot 7 rarely produced as much runoff as the control, but the correlation between the flow volumes was very nearly 1:1 with little scatter compared to the scatterplot analyses of other plots.

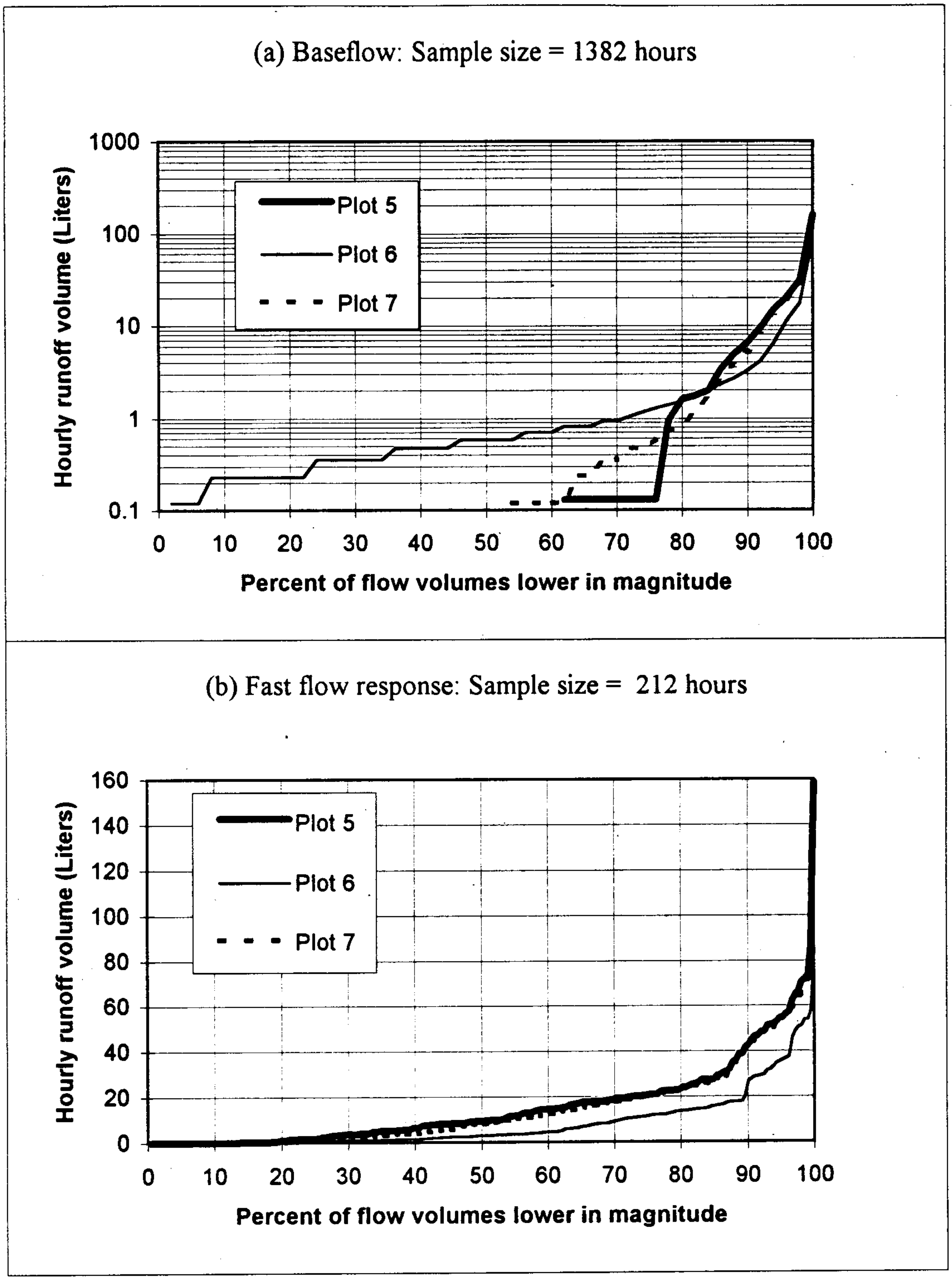

Figure 5-10: Cumulative distribution functions for Plots 5, 6, and 7
(a) During all operational hours; (b) during hours with rainfall

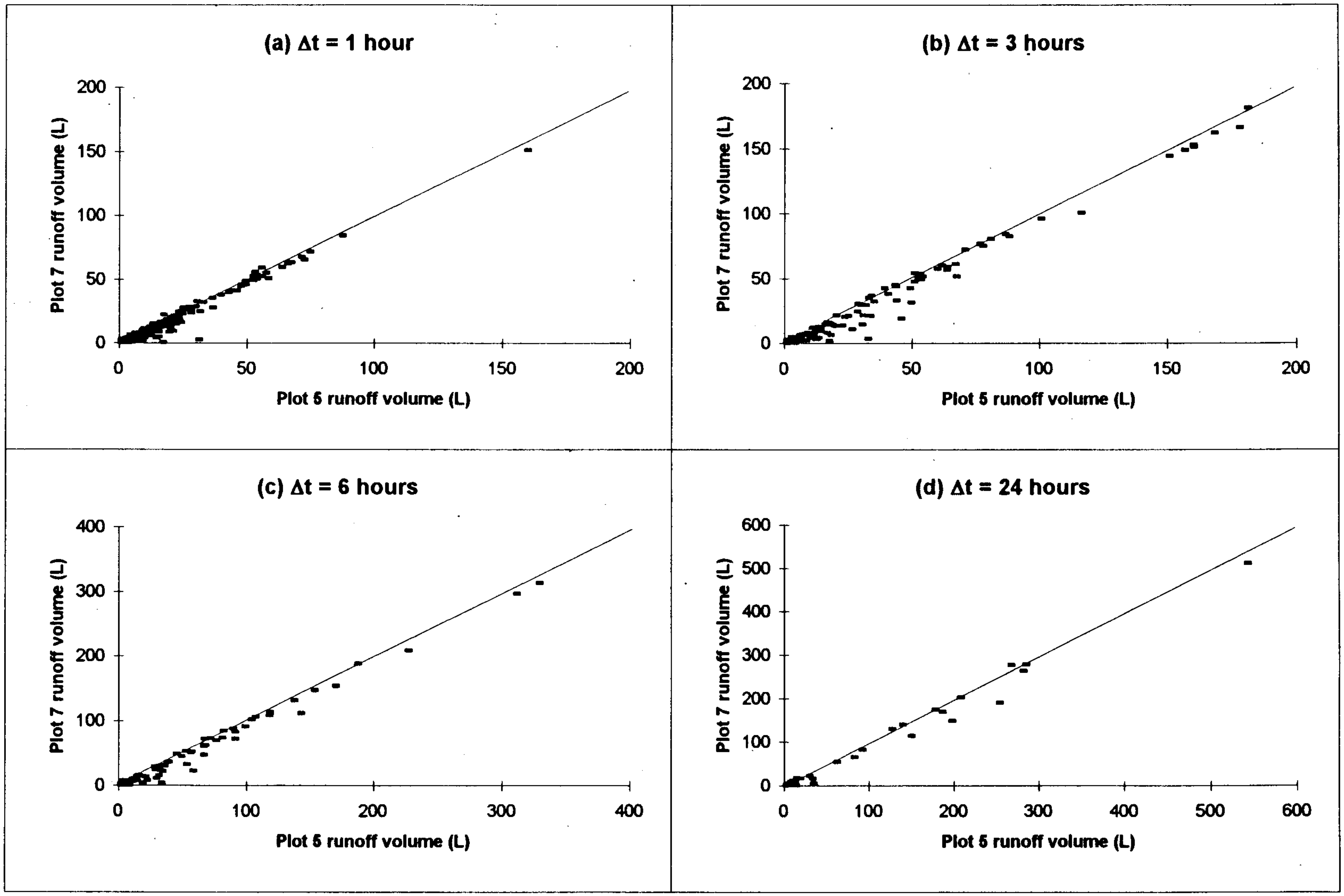

Figure 5-11: Scatterplots of Plot 7 runoff and Plot 5 runoff for four time increments

Chapter 6 - Simulated storms

6.1 Objectives of the storm simulation program

Rainfall simulations were performed to supplement the information gained from monitoring natural events. The simulations allowed for the application of artificial storms with magnitudes higher than those observed from natural storms during the study period. Also, the degree of control over rainfall rates and patterns enable the possibility of repeating the storms in the future to monitor the change in the effectiveness of the amendments over time.

Having observed the responses of the seven plots during several months of natural storms, we decided to perform simulations only on two pairs of plots: Plots 1 and 2 (control and fine wood chip compost), and Plots 5 and 6 (control and sewage sludge compost). Comparisons between these plots provided the clearest indications of the degree to which compost can alter the behavior of till.

The challenges in performing storm simulations primarily involve the generation and measurement of the artificial rain. Ideally, the simulated rainfall would be spatially uniform over the areas of application (at 23.78 square meters, or 256 square feet, per plot) and steady during the duration of the simulation. Constructing a system to these specifications is a daunting task. Many methods have been used by researchers over the years to achieve these objectives, including inverted nozzles and sliding racks, but the degree of effectiveness and level of cost for these attempts ranged widely. The low-cost sprinkler system we chose is described in the following section.

The depth of rainfall delivered to a plot was determined by collecting sprinkler-delivered water both on and around the tested plots and estimating by interpolation the distribution over the remainder of the plot. Design of both the synthetic rain sampling network and the method for interpolating the sampled amounts to the entire plot area are equally important. With the rainfall depth accurately determined and the runoff responses measured, comparisons can be made between the responses of the tested plots.

6.2 Simulation procedure

6.2.1 Sprinkler system design

Specifications for a sprinkler system included the delivery of regional extreme rainfall rates, somewhat uniform coverage, low cost, and simplicity. Drop size and energy were not considered because erosion was not a concern. Because the point of diminishing returns is rapidly approached as the cost of a rainfall simulation system rises, cost was chosen as a primary constraint. A satisfactory combination of low cost and reasonable spray pattern was obtained from Gardena HydroFan 3500 oscillating garden sprinklers purchased from local garden supply outlets. Rainfall distribution tests demonstrated the coverage from the sprinklers was generally adequate for rainfall simulation. Additionally, the areal extent of the coverage was suitable for watering a pair of plots simultaneously. Using several sprinklers with long hoses provided an inexpensive but flexible alternative for producing artificial rain.

The first simulations, on April 24-25, were performed with one sprinkler at high pressure located between Plots 1 and 2 at their midpoint. The water distribution pattern from the single sprinkler was not satisfactory because the long distance from the sprinkler to the far corners of the plots resulted in significantly different water depths between the center and ends of the plots. To remedy this problem, starting May 4 two sprinklers were used with the axes of oscillation oriented parallel to the long dimension of the plots. This configuration assisted in producing water distributions which were more uniform due to the additive effect where the sprinkler coverages overlap. As illustrated in Figure 6-1, the overlap often created a ridge of high water depths at the middle of the plots. However, the areal extent of this region was small and the overall distribution pattern was relatively uniform. The overlap of the sprinkler coverages and wind interference made completely spatially-uniform synthetic rain patters unattainable.

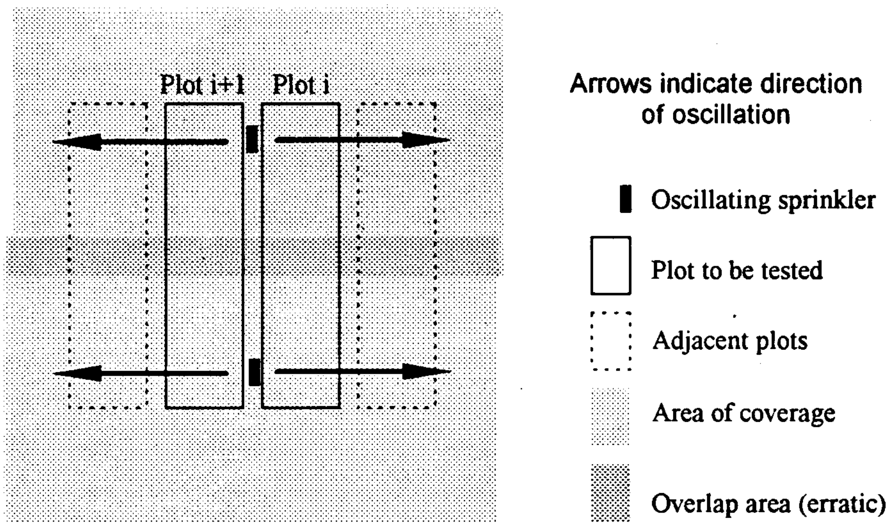

Figure 6-1: Plan view schematic of placement and coverage of sprinklers

A hose fitting was attached to the 51-mm (2-inch) water delivery line. A pressure gauge was installed at the hose fitting to provide an index of the delivery rate of the water. In particular, these pressure gauge readings were used to perform duplicate tests on different pairs of plots at different times. Standard 100-foot, 3/4-inch garden hoses were run from the pressure gauge to the appropriate sprinklers. The sprinklers were placed between the two plots to be tested. They were oriented as indicated in Figure 6-2.

6.2.2 Summary of storm simulations

Nine simulations were performed between April 25 and June 22, 1995. Four of these simulations were conducted over two days, for a total of twelve days of simulations.

Table 6-1 provides the schedule of synthetic storms during the spring and summer of 1995.

Table 6-1: Summary of storm simulations

Date	Plots	Duration (hrs)	#Cans	Pressure(psi)	Comments
April 25-26	1 & 2	8	15	60	Only test with one sprinkler
May 4	1 & 2	1.5 (am), 2 (pm)	15	60,40	Rate too high, overwhelmed buckets
May 12	1 & 2	3	28	25	Experimented w/ sprinkler locations
May 15-16	5 & 6	3, 2	28	25,30	Final trial of test setup
May 24-25	5 & 6	6, 6	28	30	**Used for analysis**
May 27	1 & 2	6	28	30	Data lost from stuck buckets
May 30-31	1 & 2	6, 6	28	30	**Used for analysis**
June 9	1&2/5&6	3/3	28	25	Smaller storms for separate study
June 22	1 & 2	6	53	30	**Used for analysis**; 53 can-network

One sprinkler operated under high pressure was used to generate synthetic rain for the first test. The rainfall depths in fifteen cans after eight hours of sprinkling each day revealed a water application pattern which was mounded around the sprinkler. These results prompted the use of two sprinklers in an attempt to distribute the water more evenly, and the tests from May 4 to May 16 were used to experiment with various water pressures and sprinkler spacings. Beginning May 24 the sprinkler setup was standardized with two sprinklers set 8.5 meters (28 feet) apart and the water pressure at the supply line to the hoses set at 207 kPa (30 psi).

The number of water collection cans used during each simulation are shown in Table 6-1. The dimensions of the cans are given in Chapter 3. The number of cans was increased by adding cans to the previously-used can network. For example, one could obtain the can pattern for the 15-can setups by removing 13 of the cans from the 28-can network. This practice allowed analysis of the size of a smaller network used in previous tests by comparing estimated rain patterns using the full complement of cans to the estimated patterns obtained by hypothetically removing some from consideration. In this manner, the adequacy of the 15-can and 28-can setups were examined using the 53-can network of June 22. The layouts of the cans are shown in Figure 6-2.

Beginning May 15, direct precipitation in the surface collection gutters was prevented by temporary placement of additional pieces of four-inch gutter over the collection gutters which were sloped to direct rainfall away from the tested plots.

Two simulations will be discussed in detail: May 24-25 (Plots 5 and 6) and May 30-31 (Plots 1 and 2). The simulations of April 25 and June 22 will also be used to compare initial responses to rainfall from several separate simulations.

6.2.3 Estimating the Depth of Simulated Rainfall

Rainfall depths from the sprinklers were sampled using discarded food cans from the University of Washington student union kitchens. The #10 galvanized steel cans were obtained in good condition, having been thoroughly cleaned by the kitchen staff. They resemble typical coffee cans and are 178 mm (7 inches) tall with a diameter of 152 mm (6 inches). The rims are thin but are not sharpened. Estimation of the depth of water in the can is performed by measuring the volume of water in the can with a graduated measuring cylinder and converting the volume to a depth using the mouth diameter of the can (152 mm).

The sampling network was designed to provide numerous measurements at the perimeter of the tested plots so the depths within the plots could be estimated by interpolation, with a few cans placed inside the plots. Figure 6-2 illustrates the layout of the cans during the simulations. The solid circles indicates locations of cans when 28 cans were used. The open circles indicate locations where additional cans were placed for the 53-can simulation on June 22, 1995.

Calculation of each storm's rainfall depth was accomplished by generating contours of the rainfall distribution from the measured can depths with commercially-available contouring software. The contouring was performed by using a linear kriging routine which provided contours compatible with qualitative field observations. Other gridding and contouring techniques were less satisfactory and were not used. After defining the areal limits of each plot, the software computed the volume under the estimated rainfall distribution for each plot. Dividing this volume by the plot area (not including the surface water collection gutters) provided a mean rainfall depth for each plot.

Fifty-three cans were placed on and around Plots 1 and 2 during the June 22 simulation to evaluate the adequacy of the 28-can networks that had been used. For comparison, the contour plot generated from all 53 cans and the contour plot generated from only 28 of the 53 cans are provided in Figure 6-3. In overall character the two can densities produced qualitatively similar contour plots, although the 53-can density resulted in more local peaks and valleys. The calculated mean rainfall depth for the 53-can network was 1.90 inches, while the 28-can network resulted in an estimate of 1.95 inches. This difference is not sufficient to conclude that the 28-can network was inadequate for estimating the rainfall amount during a period of sprinkling.

Since the contours were constructed from grids with a spacing of 30 cm (1 foot), a plot of the difference in contours between the 28-can and 53-can networks was generated by subtracting the 297 node depths of the 28-can grid from the corresponding node depths of the 53-can grid. The resulting grid was contoured and contours are shown in Figure 6-4 (the contour for zero difference has been removed for clarity). The contours indicate that the 28-can and 53-can interpolation procedures agreed to within 2.5 mm (0.10 inches) over more than 75% of the area. The most notable differences occur at mid-slope at both edges, where four distinct regions of high differences are clearly evident. These regions are centered about cans which were present in the 53-can network but omitted to construct the hypothetical 28-can network, indicating the tendency of the sprinklers to produce streams of water which may or may not cross a sampling can. The area of these regions is small compared to the total area, however, so their effect on the estimated areal average depth is small; the 28-can rain depth estimates were adequate for the analyses we present below.

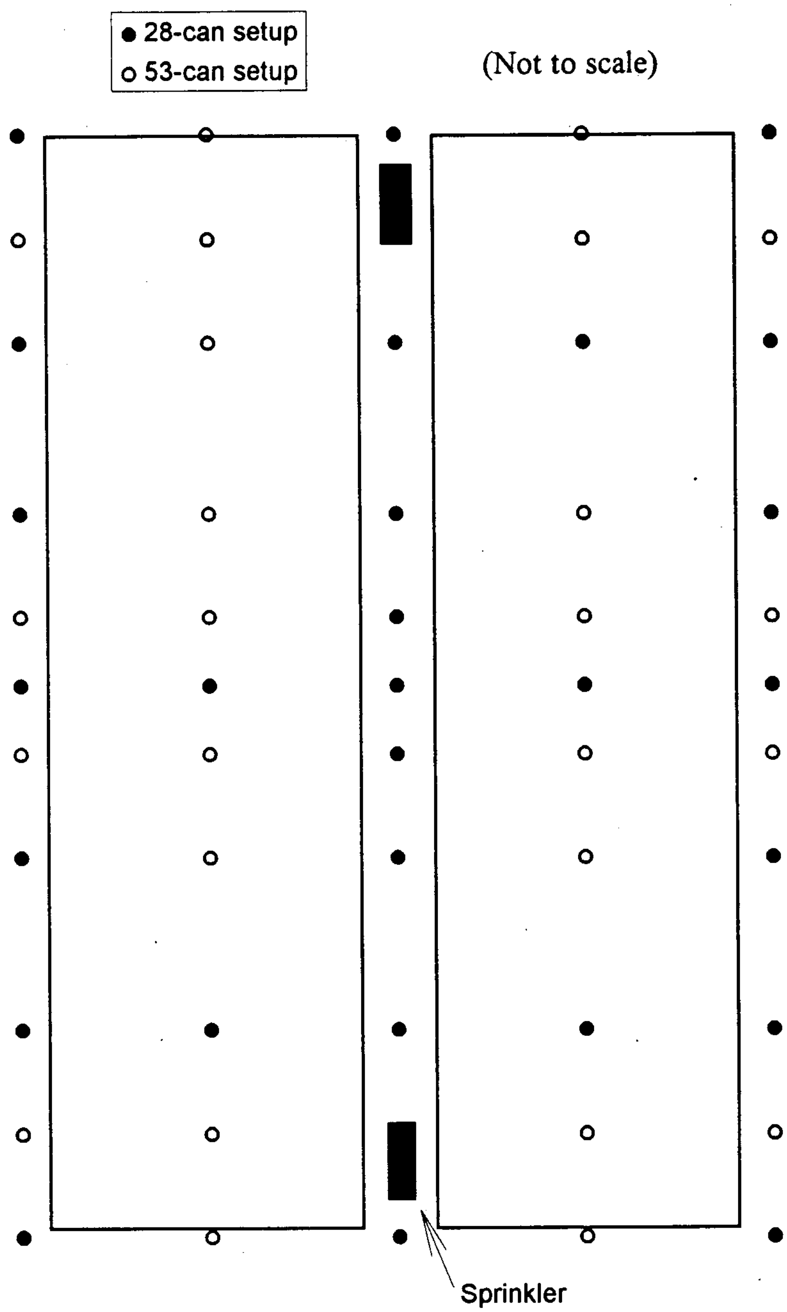

Figure 6-2: Layout of cans for cumulative synthetic rainfall depth recording

(a) Contours generated using depths from all 53 cans

(b) Contours generated using depths from 28 of the 53 cans

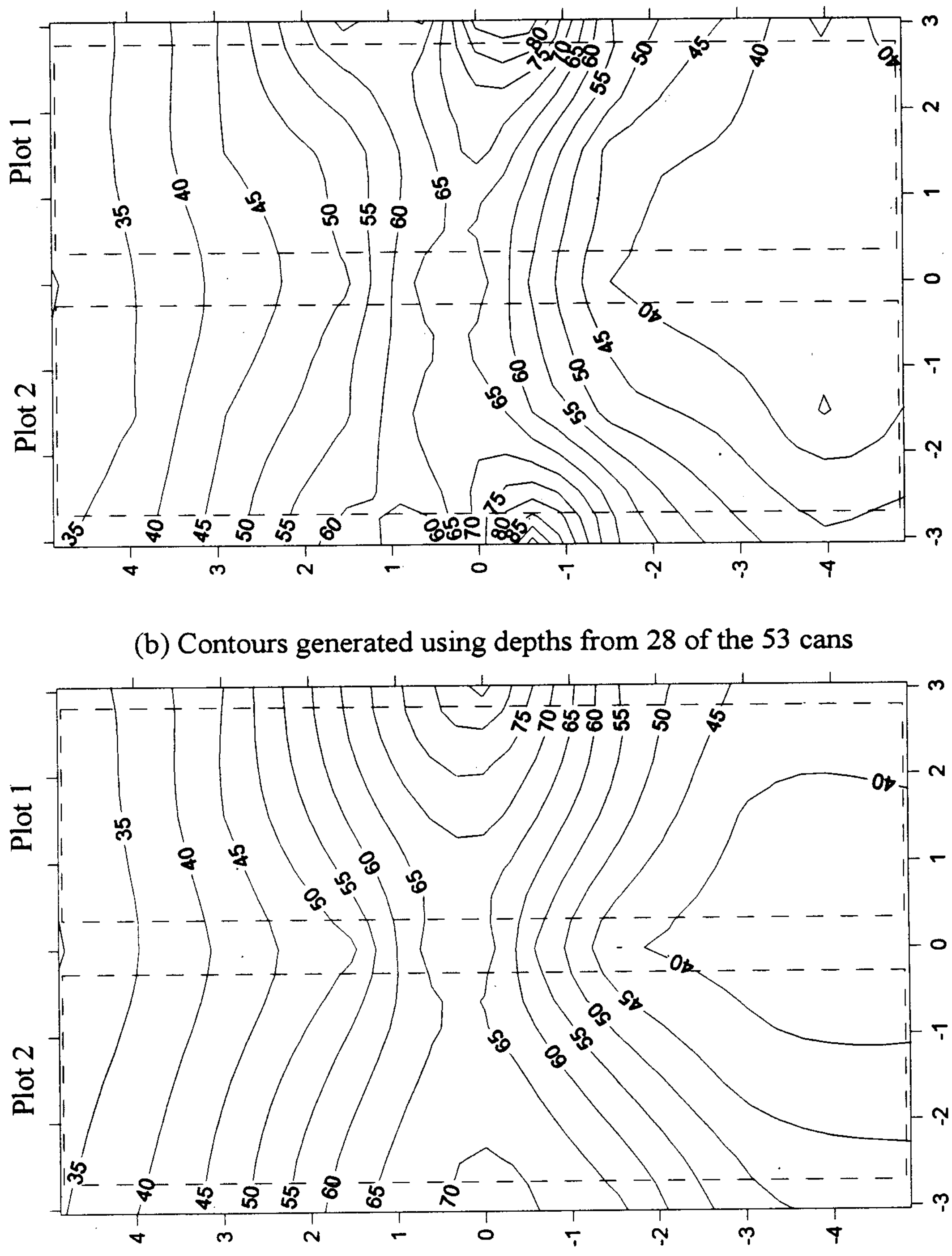

Figure 6-3: Comparison of rain depth contours from June 22 can networks
(Axes in meters, contour interval = 5 mm)

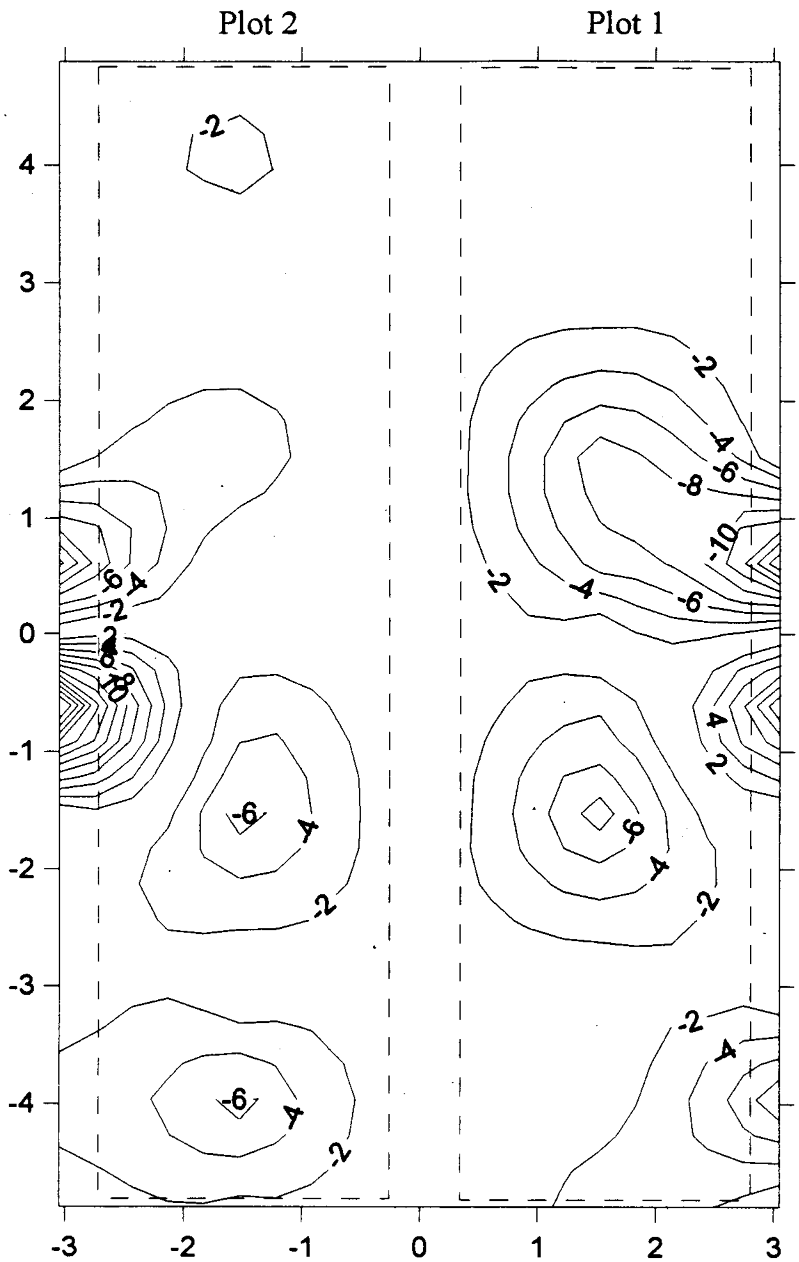

Figure 6-4: Difference in can network rain depth contours
(Axes in meters, contour interval = 2 mm)

6.3 Analysis of simulation results - Plots 5 and 6 (May 24-25)

6.3.1 Observations

The first synthetic storm was begun on May 24 at 12:00. The weather was hot and breezy. The plots were dry (no baseflow and dry piezometers), with the last watering occurring with the simulation of May 16. The rainfall distribution is illustrated in Figure 6-5. The calculated mean rain depth for this six-hour event was 50.3 mm (1.98 inches) for Plot 5 (the till control) and 50.0 mm (1.97 inches) for Plot 6 (with amended till) based on volumes computed from contour plots of water distribution from the sprinklers. Each of these 6-hour rain depths is approximately equivalent to a natural event with a return period of 100 years.

The differences in runoff responses between Plot 5 and 6 were remarkable and not unexpected (Figure 6-7). Flow rates from Plot 5 after one hour of sprinkling were not attained by Plot 6 for another three hours. Plot 5 appeared to approach a steady runoff rate, while Plot 6 continued to store water as the test progressed. The piezometers in Plot 5 remained dry throughout the simulation, indicating the extremely low conductivity of the till. The Plot 6 piezometers rose to 22 cm at the 1.5 meter (5 foot) piezometer and 28 cm at the 4.9 meter (16 foot) piezometer by the end of the simulation as the rain infiltrated and was stored in the soil. Recession flow rates were low from Plot 6 and nonexistent from Plot 5.

At noon the next day a second 6-hour duration synthetic storm was initiated. The water depth contours are provided in Figure 6-6. Estimated mean rain depths were 49.0 mm (1.93 inches) for Plot 5 and 51.1 mm (2.01 inches) for Plot 6. The piezometers in Plot 5 were dry and remained so throughout the test, while those in Plot 6 had fallen overnight and rose with this follow-up storm.

Table 6-2: Plot 6 water table depths during the May 24 - 25 simulations (cm)

Time (hours)	1.5 m (5 ft)	4.9 m (16 ft)
0 - Begin rain	dry	dry
3	dry	dry
6 - End rain	21	28
24 - Begin rain	19	13
27	26	23
30 - End rain	29	25

Plot 6 responded more rapidly to the rainfall with this storm than it had the previous day, reaching a steady rate of runoff about three hours into the storm. The rate of this runoff was about 93% of the steady flow observed from Plot 5. Recession curves were similar to those of the previous day.

Table 6-3: Input and output volumes for the May 24-25 simulation (Liters)

	Plot 5	Plot 6
Rain (L)	2325	2367
Runoff (L)	1733	1279
Runoff/Rain (%)	*75*	*54*

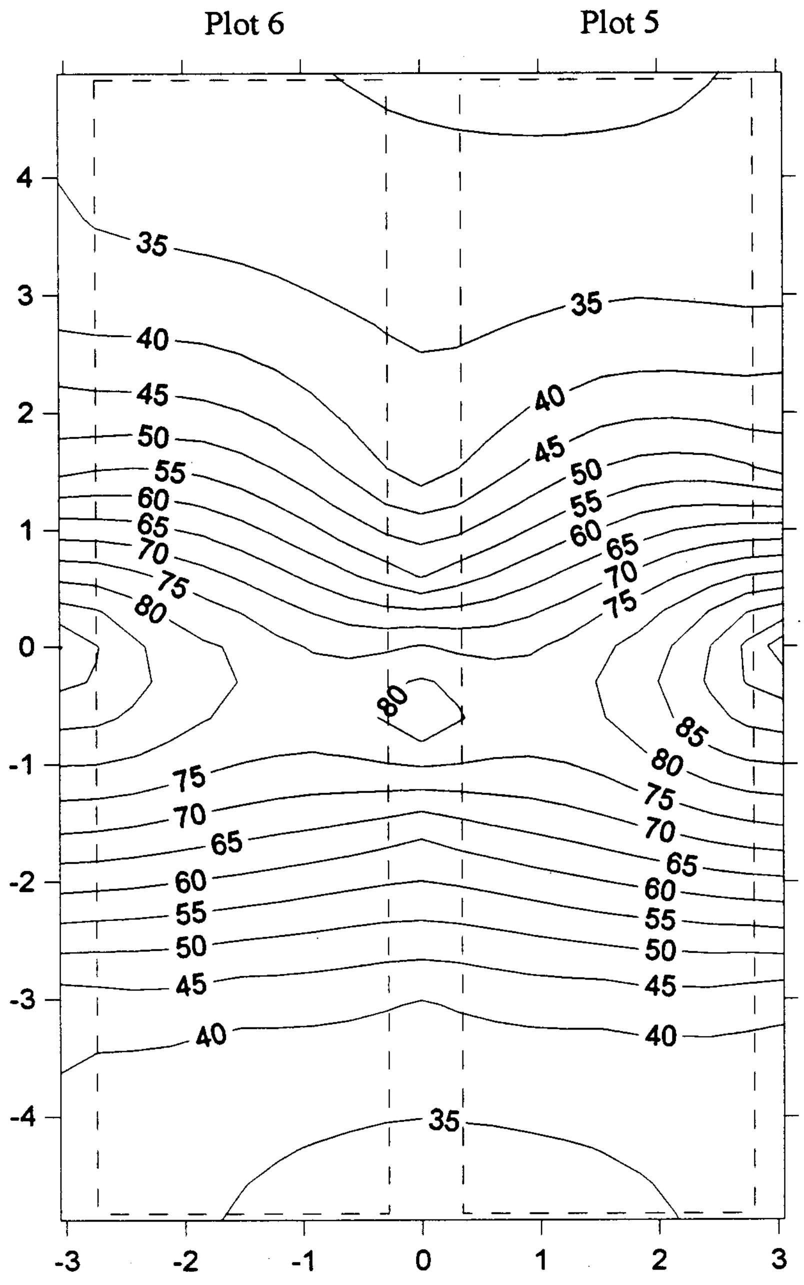

Figure 6-5: Sprinkler coverage contours for the May 24 simulation
(Axes in meters, contour interval = 5 mm)

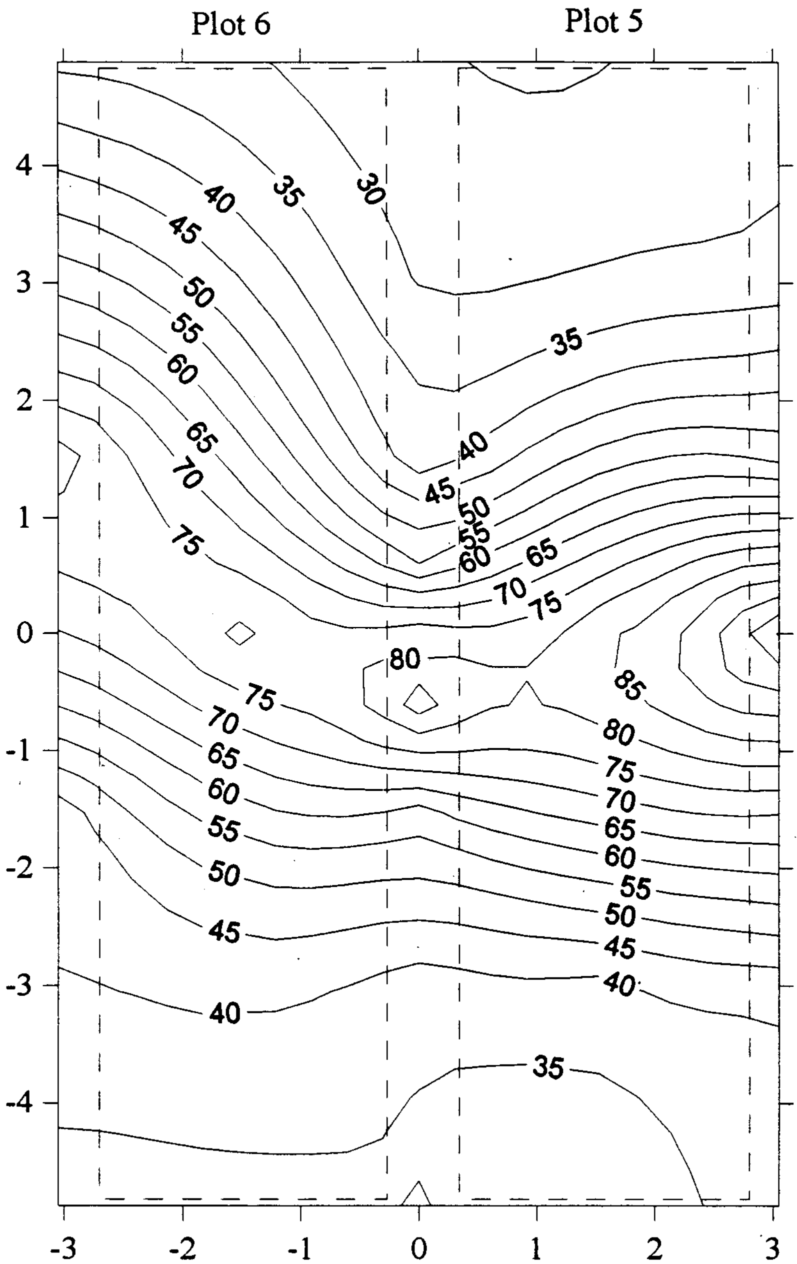

Figure 6-6: Sprinkler coverage contours for the May 25 simulation
(Axes in meters, contour interval = 5 mm)

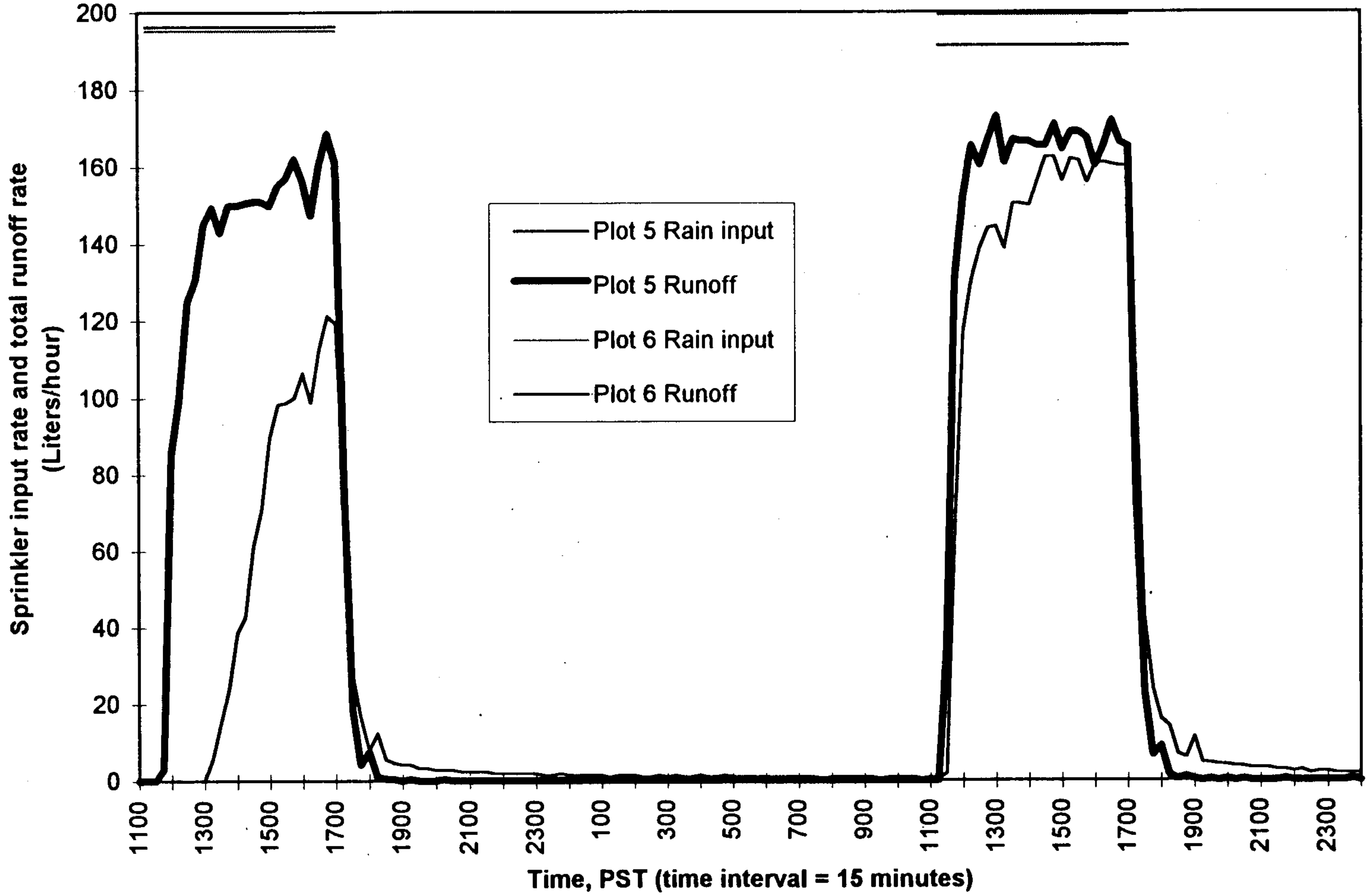

Figure 6-7: Response of Plots 5 and 6 to rainfall simulations of May 24 - 25, 1995

6.3.2 Discussion

The significant difference in response to the initial sprinkling was expected following experience with natural storms, as was the more similar behavior between the plots at the onset of the follow-up storm the next day. The sprinkling rate and duration brought the runoff to a steady rate for both plots by the end of the second day's storm. If the rainfall depth calculation is correct, though, the plots were not at steady state conditions. The rate of rainfall was higher than the constant rate of runoff, indicating a continuing acceptance of water to storage.

This situation may occur for two reasons: if the infiltration rate was limited as a certain ponding depth was reached (thus, water would continue to enter storage even as runoff had reached an approximately constant rate), or if the saturated zone profile continued to evolve as the storm progressed and the full storage capacity of the plots was not reached. Based on the first assumption, the constant infiltration rate averaged over the plot area for Plot 5 was around 0.25 mm/hour (0.010 inches/hour) compared to a sprinkler rate of 8.17 mm/hour (0.32 inches/hour), while the infiltration rate of Plot 6 was around 0.46 mm/hour (0.018 inches/hour). This mechanism is plausible for Plot 5, which was observed to have low conductivity; also, the plot failed to develop a saturated zone during the storm simulation, indicating a conductivity too low to allow water to percolate to the liner within the duration of the simulation.

The reasoning that the saturated zone dynamics complicate the story is more plausible for Plot 6, where the conductivity was observed to be higher and piezometer levels indicated higher levels in the downslope piezometer even as both piezometer levels rose throughout the sprinkling. Also, during field observations during natural rainstorms, it was noticed that the top of the slope was typically the last portion of the plots to pond. The lack of data about the water table at the upper regions of the slope preclude a complete analysis of the internal storage behavior of Plot 6, though it is evident that Plot 6 accepted larger portions of rainfall to storage than Plot 5.

6.4 Analysis of simulation results - Plots 1 and 2 (May 30-31)

6.4.1 Observations

The plots were relatively dry (likely near field capacity) at the outset of this simulation. Although a simulation with six hours of sprinkling had been performed three days earlier, the days had been hot and dry since May 23. Dry piezometers in both plots indicated the dry soil conditions. The first six-hour storm was initiated at 10:00 am in light winds. The sprinkler depth contours are presented in Figure 6-8. From these contours, estimated mean rain depths were 45 mm (1.76 inches) for Plot 1 and 46 mm (1.81 inches) for Plot 2.

Measurements showed no runoff response from the plots for the first hour of rainfall (Figure 6-10). Within 3 hours the runoff from Plot 1 leveled off at a steady flow rate. By the end of the sprinkling the runoff from Plot 2 was continuing to rise to flow rates higher than the runoff flow rates of Plot 1. The piezometers in Plot 1 were generally dry, while those in Plot 2 had risen substantially.

Table 6-4: Water table depths during the May 30 simulation (cm)

	PLOT 1 (meters from gutter)					PLOT 2		
	0.61	1.52	2.74	4.88	7.32	0.61	1.52	4.88
Begin rain	0	0	0	0	0	0	0	0
t = 3 hours	0	0	0	0	0	9	17	20
End rain	0	0	0	0	0	19	25	25

The subsurface bucket in Plot 1 was observed to stick (balance in a neutral position) towards the end of the simulation and was adjusted. The data show the bucket appeared to have failed for about 30 minutes before being freed. The runoff from both plots fell quickly at the termination of the sprinkling. As observed from natural storms, the runoff rate during recession was significantly higher from Plot 2 than from Plot 1.

The follow-up six-hour storm was begun at 10:00 am the next day, 24 hours after the beginning of the previous day's test. The depth contours are shown in Figure 6-9. Calculated mean rain depths were 45 mm (1.76 inches) for Plot 1 and 46 mm (1.83 inches) for Plot 2. Runoff from the first storm had ceased from Plot 1 but baseflow was continuing from Plot 2. Both plots responded to this storm with more rapid increases in runoff and both plots reached steady runoff rates after a shorter period of time: one hour for Plot 1, approximately 2.5 hours for Plot 2.

As the storm progressed the runoff from Plot 2 steadied at a rate about 29% higher than the steady rate from Plot 1, indicating that less water was entering storage in Plot 1, the control. Recession curves were identical to those of the previous day's storm.

The piezometer readings indicate that Plot 2 became mostly saturated within three hours, while any water table rise in Plot 1 was nonexistent or undetected by the piezometers after 3 hours. The water table levels are shown in Table 6-5.

Table 6-5: Water table depths during the May 31 simulation (cm)

	PLOT 1 (meters from gutter)					PLOT 2		
	0.61	1.52	2.74	4.88	7.32	0.61	1.52	4.88
Begin rain	0	0	0	0	0	9.5	16	14
t = 3 hours	0	0	0	0	0	22	g.s.*	g.s.*
End rain	5	4	0	7	0	20	g.s.*	g.s.*

* g.s. indicates water levels observed to be at the ground surface

Table 6-6 provides the total volumes of rainfall and runoff for each plot, where the runoff total includes all runoff produced by the plots until no more baseflow is recorded (a period of several days for Plot 2).

Table 6-6: Input and output volumes for the May 30-31 simulation (Liters)

	Plot 1	Plot 2
Rain (L)	2093	2165
Runoff (L)	1377	1561
Runoff/rain (%)	66	72

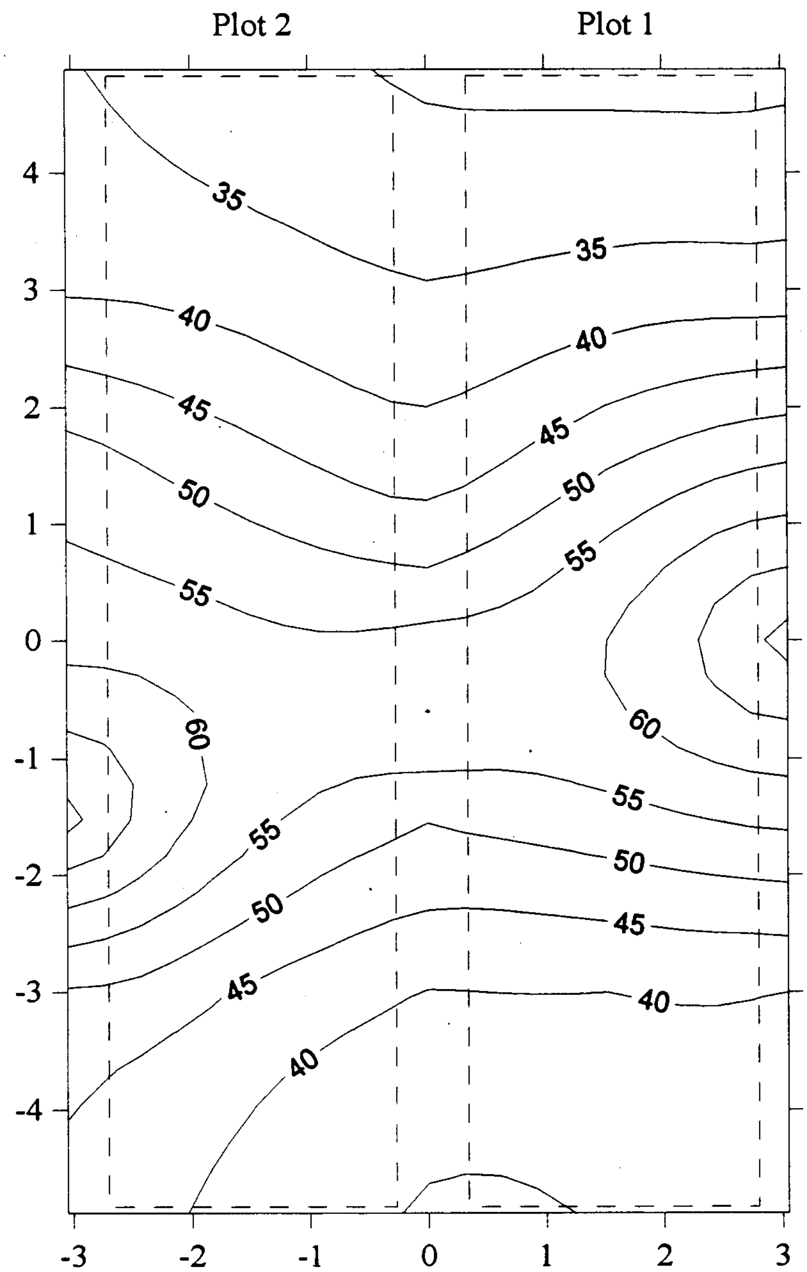

Figure 6-8: Sprinkler coverage contours for the May 30 simulation
(Axes in meters, contour interval = 5 mm)

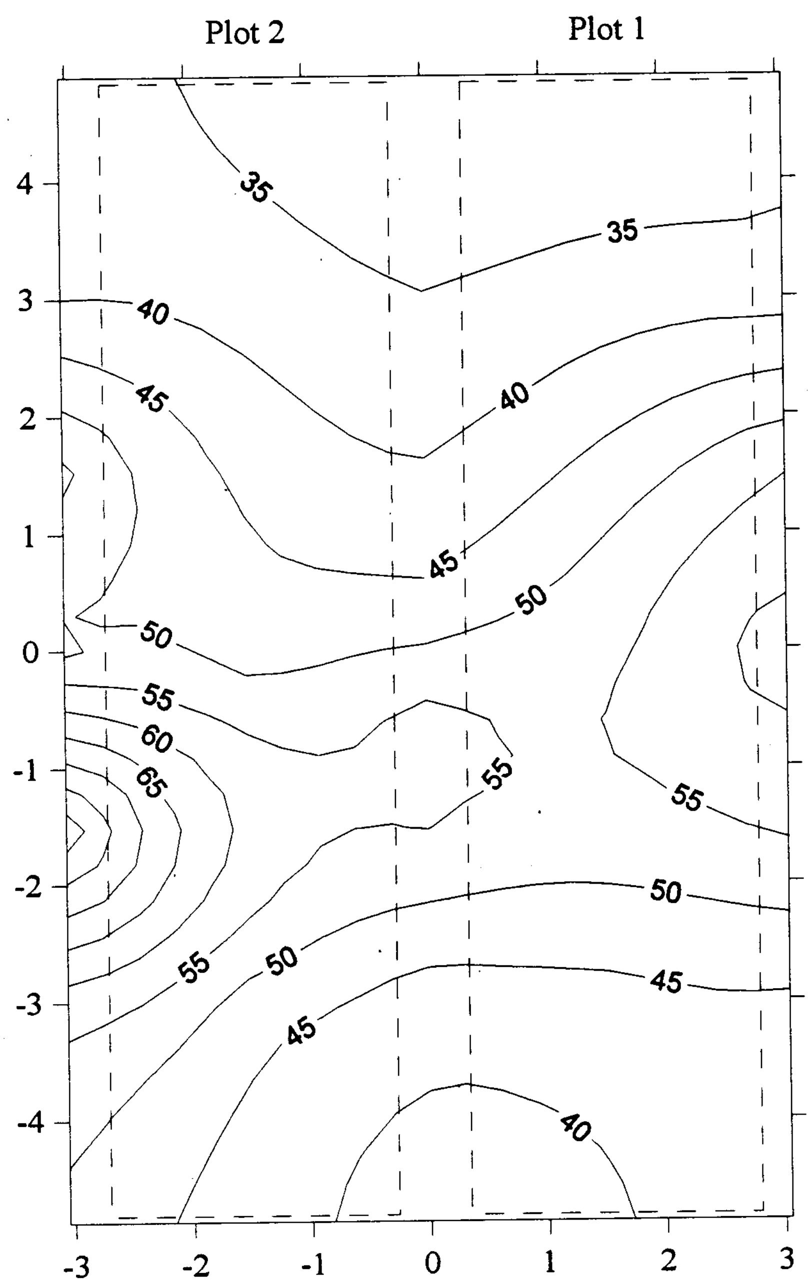

Figure 6-9: Sprinkler coverage contours for the May 31 simulation

(Axes in meters, contour interval = 5 mm)

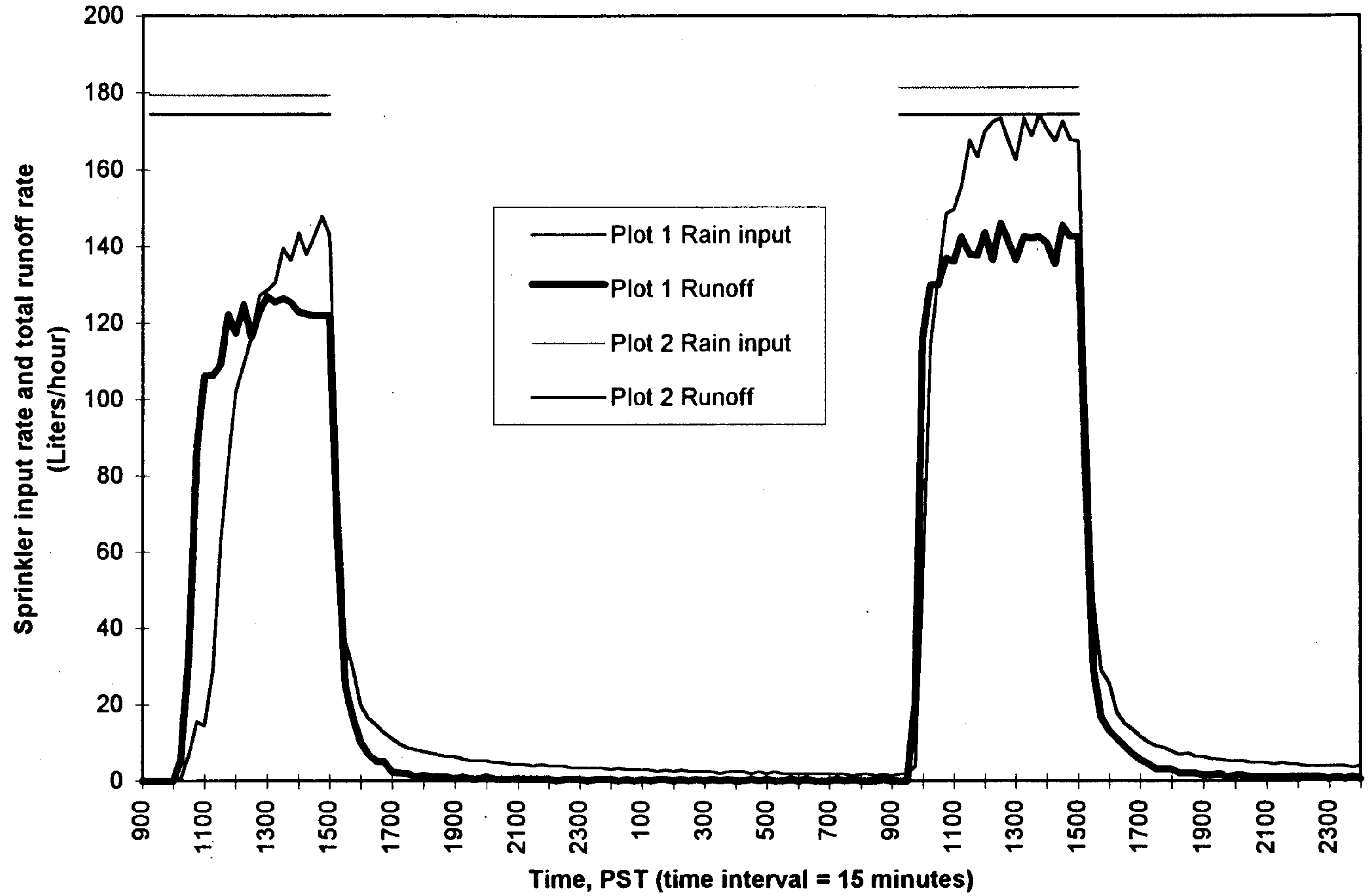

Figure 6-10: Response of Plots 1 and 2 to rainfall simulations of May 30 - 31, 1995

6.4.2 Discussion

As with the May 24-25 simulation, the rainfall rates exceeded the runoff rates of both plots even after the runoff rates leveled off at a constant rate. Thus both plots continued to accept water to storage as the runoff remained steady. As with Plots 5 and 6, the question becomes the manner by which the storm runoff was generated by each plot.

The back-calculated infiltration rates of 0.41 mm/hr (0.016 inches/hour) for Plot 1 and 0.10 mm/hr (0.004 inches/hour) for Plot 2 contradict all other indications that Plot 2 is far more conductive than Plot 1. The surface flow-generating mechanisms of the two plots were evidently different. Plot 1 generated storm runoff by Hortonian processes, infiltrating at the 0.41 mm/hour rate while shedding rainfall in excess of this rate. Hence the piezometers did not indicate the development of a substantial saturated zone although the runoff rates were high.

Plot 2, however, accepted much of the rain from the first storm into storage and the water table rose (Table 6-4). The next day, after the soil column became saturated over significant portions of the plot (Table 6-5), the runoff from Plot 2 increased and nearly equaled the rate of the incoming rain. This behavior was observed because Plot 2 surface runoff was produced by saturated overland flow processes: as more of the plot became saturated, the total runoff approached the rainfall input. The relative quickness by which the water table rose and the high recession flows indicate the high conductivity of the plot, though the conductivity was not high enough to drain the plot at a rate higher than the incoming sprinkled water.

Chapter 7 - Summary and conclusions

7.1 Summary

The preceding chapters detailed the development of a field experiment for examining the hydrologic effects of amending lawns grown on till with compost. Seven lawn-scale plots were constructed with five having various mixes of different types of compost. Continuous monitoring of the rainfall and the runoff from each plot provided nearly five months of data from natural storms. The response tendencies of the plots were determined by examining the hyetographs and hydrographs for several significant storm systems. In addition, basic statistics were computed from the rainfall and runoff data to quantify the behavior observed in the field and from the hydrographs.

Beginning in late April sprinklers were used to produce synthetic rainfall. The resulting runoff was monitored just as it had been during natural storms, and the rainfall depth was estimated using a spatial network of water-catching cans.

7.2 Evaluation of systems and procedures

7.2.1 Data collection and soil characterization

The program of collecting rainfall and runoff data generally met its objectives. Useful data from a number of significant events were collected once the runoff collection and monitoring systems were operational.

Problems with soil structure and turf establishment and the "breaking in" process of the initial designs delayed the start of data collection until after large storms in October, November, and early December, 1994 had already occurred. Reliability of the surface runoff collection gutters and tipping buckets was initially low until problems were identified by observation or examination of the accumulated data. Finally, the necessary refinement of plot construction techniques as experience was gained may have created a differential bias in some of the results. In particular, the difference in compaction technique and surface shaping between the first two plots and the remaining five may complicate comparisons of the hydrologic behavior of Plots 1 and 2 relative to Plots 3 and 4.

In spite of these drawbacks and lessons, however, the field measurements yielded data useful for answering the questions at hand.

7.2.2 Data Analysis

The monitoring program provided excellent information on *what* happened hydrologically, but due to the constraints on what could be measured was less able to provide information about *why* those results were obtained. Therefore the analysis focused on discussing what was observed and inferring its causes rather than investigating each possible mechanism, an endeavor which would have involved a massive and expensive data collection effort well beyond the scope of this work.

The analysis of the hydrographs was begun once all the rain and flow data were assimilated. Concern over the ability of the surface and subsurface collection systems to monitor accurately the above-ground and below-ground fluxes precluded an extensive examination of the source of the runoff. This potential problem had no effect on the accuracy of the measurement of total runoff, so total runoff measurements provided the principal basis for examining the responses of the plots to rainfall.

The simple statistical analysis provided a suitable method for quantifying the observations in the field and from the hydrograph analysis. Cumulative distribution functions of runoff volumes, scatterplots, and examinations of amendment benefit as affected by rainfall depths provided a variety of perspectives in quantitatively determining the difference in behavior between till with and without amendment. The critical assumption in aggregating the data for each plot was that the data were independent, that is, the flow rate in one hour is not correlated to the flow rate of the previous hour. This assumption is erroneous, as successive hours of runoff are affected by the same initial conditions for a single rainfall event. The derived statistics are not coefficients for design or planning, and to apply them in this manner would be erroneous. However, when considered in context with the time series analyses, the statistical analysis corroborates quantitatively some of the observed and measured response behavior of the seven plots.

7.3 Effect of organic amendments on till

7.3.1 Soil properties

As previous research has indicated, amending a soil with compost increases the organic content while decreasing the bulk density. The effect on particle size distribution was limited predominately to particle sizes larger than 0.05 mm (sand and gravel ranges).

7.3.2 Hydrologic response

Application of high amounts of fine, aged compost (2:1 till:compost by loose volume, Cedar Grove 7/16" and Groco composts) resulted in significantly improved hydrologic behavior relative to unamended soil. The higher soil conductivity resulted in increased infiltration and baseflow. The higher porosity improved storage and retention through dry periods. Storm peaks were consistently delayed and reduced. These characteristics were indicated by hydrographs, statistical analyses, and the turf health.

The increased conductivity of amended soils altered the mechanisms of storm flow generation. In till plots Hortonian infiltration-limited runoff was observed, where slow infiltration continued as excess ponded water was shed. In the plot with the highest observed conductivity, Plot 2 (2:1 till:Cedar Grove 7/16" by loose volume), saturation overland flow was the dominant mechanism of surface runoff generation as indicated by piezometer observations during natural and simulated storms.

Application of smaller amounts of amendment reduced the effectiveness of the amendments in improving the hydrologic response of the plots, and in some respects resulted in detrimental characteristics. The lean mix in Plot 4 (4:1 Cedar Grove 7/16") produced a tight soil which shed water quickly during heavy rainfall. Plot 7 (3:1 Cedar Grove 7/16") behaved much like the control throughout the period of analysis, with little improvement in behavior observed.

The coarse compost (2:1 Cedar Grove 3/4" Cathcart) in Plot 3 likewise resulted in marginal improvements in soil response. Storage and conductivity were not substantially increased.

7.3.3 Turf establishment and health

The amended soils clearly aided in the establishment of turf. The higher organic content provided more nutrients for the grass, and longer, more dense root networks were consistently noted in the amended soils. The turf in plots with amended soils also remained green for longer periods of time during dry periods in June and July, 1995.

7.4 Recommendations for future research

This work was designed as a springboard for future research. The use of different composts and application rates was intended to determine if the potential existed for compost to improve the hydrologic behavior of residential lawns in locations of till geology. The data demonstrate the potential for this technology as a stormwater management technique.

Many questions remain:

1. How can one determine whether a proposed amendment is suitable given the properties of the till?

2. Are the effects observed during this study permanent, or will the properties and behavior of the plots change over time as the soil develops and the compost decomposes?

3. What were the runoff mechanisms responsible for generating the observed responses, and how was each mechanism affected by the amendment?

4. What are the ramifications in terms of water quality, stormwater management, and economics if lawns throughout a residential development were amended with compost?

References

Ahrens, C.D., Essentials of Meteorology, West Publishing Company, 1993.

American Society of Civil Engineers, ASCE Manual on Engineering Practice No. 70: Evapotranspiration and Irrigation Water Requirements, 1990.

Andrews, E.D., "Bed-material entrainment and hydraulic geometry of gravel-bed rivers in Colorado," Geological Society of America Bulletin, v. 95, p.371-378, 1994.

Argue, J., "Strategies for coping with urban runoff," Adelaide Greenhouse '88 Conference, South Australian Greenhouse '88 Working Group, the South Australian Department of Environment and Planning and the Commission for the Future, 40-46, 1988.

Bain, R., "Soil Amendment Project," Report prepared for the City of Redmond Department of Public Works, 1989.

Beven, K., "Kinematic subsurface stormflow," Water Resour. Res., 17(5), 1419-1424, 1981.

Beven, K., "On subsurface stormflow: Predictions with simple kinematic theory for saturated and unsaturated flows," Water Resour. Res., 18(6), 1627-1633, 1982.

Binley, A., J. Elgy and K. Beven, "A physically based model of heterogeneous hillslopes (Parts 1 and 2)," Water Resour. Res., 25(6), 1219-1233, 1989.

Carling, P., "The concept of dominant discharge applied to two gravel-bed streams in relation to channel stability thresholds," Earth Surface Processes and Landforms, Vol. 13, 355-367, 1988.

Chow, V.T., D.R. Maidment, and L.W. Mays, Applied Hydrology, McGraw-Hill, 1988.

Conniff, R., "On the lowly earthworm we Earthlings pin our loftiest dreams," Smithsonian, 86-95, 1993.

Dreimanis, A., Tills: Their origin and properties," The Royal Society of Canada Special Publications #12, Ed. R. Legget, 1976.

Dunne, T., and R. Black, "An experimental investigation of runoff production in permeable soils," Water Resour. Res., 6(2), 478 - 490, 1970.

Dunne, T., and L. Leopold, Water in Environmental Planning, W.H. Freeman and Company, 1978.

Epstein, E., J. Taylor, and R. Chaney, "Effects of sewage sludge and sludge compost applied to soil on some soil physical and chemical properties," J. Environ. Qual., 5(4), 422-426, 1976.

Freeze, R.A., "Streamflow generation," Reviews of Geophys. and Space Phys., 12(4), 627-647, 1974.

Gupta, R., R. Rudra, T. Dickinson, N. Patni, and G. Wall, "Stochastic analysis of seasonal hydraulic conductivity," Irrigation and Drainage: Saving a Threatened

Resource - In Search of Solutions, Proceedings of the Irrigation and Drainage Sessions at Water Forum 1992, ASCE, Baltimore, MD, 32-38, 1992.

Gupta, S., R. Dowdy, and W. Larson, "Hydraulic and thermal properties of a sandy soil as influenced by incorporation of sewage sludge," Soil Sci, Soc. Am. J., 41, 601-605, 1977.

Guymon, G. L., Unsaturated Zone Hydrology, Prentice-Hall, 1994.

Harr, R.O., "Water flux in soil and subsoil on a steep forested slope," Journal of Hydrology, 33, 37-58, 1977.

Jamison, V. C., and D. B. Peters, "Slope length of claypan soil affects runoff," Water Resour. Res., 3(2), 471 - 480, 1967.

King County, "King County, Washington, Surface Water Design Manual," , 1992, pp. 4.5.2-1 - 4.

Koide, S., and H. Wheater, "Subsurface flow simulation of a small plot at Loch Chon, Scotland," Hydrological Processes, 6, 299-326, 1992.

Leopold, L.B., "The sediment size that determines channel morphology," Unpublished manuscript, 18 p., 1988.

Linsley, R.K., M.A. Kohler, and J.L.H. Paulhus, Hydrology for Engineers, 3rd Edition, McGraw-Hill, 1982.

Luteneggar, A., T. Kemmis, and G. Hallberg, "Origin and properties of glacial till and diamictons," Special Publication on Geological Environment and Soil Properties, ASCE Convention, Houston, TX, October 17-21, 1983.

Megahan, W. and J. Clayton, "Tracing subsurface flow on roadcuts on steep, forested slopes," Soil Science Society of America Journal, 47(6), 1063-1067, 1983.

Miller, J.F., R.H. Frederick, and R.J. Tracey, Precipitation-Frequency Atlas of the Western United States: Volume IX - Washington, NOAA/NWS, Silver Spring, MD: 1973.

Nyborg, M., "A model for the relationship between the hydraulic conductivity and primary sedimentary structures of till," Nordic Hydrology, 20, 137-152, 1989.

Olmsted, T., "Geological aspects and engineering properties of glacial till in the Puget Lowland, Washington," in *Proc. 7th Annual Eng. Geol. and Soils Eng. Symp.*, Moscow, Idaho, 223-233, 1969.

Pagliai, M., G. Guidi, M. La Marca, M. Giachetti, and G. Lucamante, "Effects of sewage sludges and composts on soil porosity and aggregation," J. Environ. Qual., 10(4), 556-561, 1981.

Pickup, G., and R.F. Warner, "Effects of hydrologic regime on magnitude and frequency of dominant discharge," Journal of Hydrology, 29, 51-75, 1976.

Sidle, R.C., "Bed load transport regime of a small forest stream," Water Resour. Res., 24(2), 207-218, 1988.

Striebe, Sandra, "Environmental effects of using less turfgrass and more mulch in landscaped areas," King County Department of Surface Water Management, 1994.

Tester, C., "Organic amendment effects on physical and chemical properties of a sandy soil," Soil Sci. Soc. Am. J., 54, 827-831, 1990.

Whipkey, R., "Subsurface stormflow from forested slopes," Int. Ass. Sci. Hydrol. Bull., 10(2), 74-85, 1965.

Wigmosta, M., S.J. Burges, and J.M. Meena, "Modeling and monitoring to predict spatial and temporal hydrologic characteristics in small catchments," University of Washington, Department of Civil Engineering, Water Resources Series, Tech. Rept. No. 137, 1994.

Appendix A - Schedule of activities at the research site

The following is a history of the plot construction and instrument installation activities.

1994

June 28	Construction of Plots 1 and 2 begun.
July 15	Plots 1 and 2 seeded.
August 16	Plots 1 and 2 fertilized.
August 19	Fence constructed on site.
August 31	Piezometers installed in Plots 1 and 2.
	Prototype surface water-collection gutter installed in Plot 1.
September 8	Plot 3 filled with amended soil.
	Sod strips placed along edges of Plots 1 and 2.
September 12	Plot 4 filled with amended soil.
	Plots 3 and 4 fertilized and seeded.
September 20	Plot 5 filled with till from second construction site, fertilized, and seeded.
September 22	Plot 6 filled with amended soil, fertilized, and seeded.
September 27	Plot 7 filled with amended soil.
September 29	Plot 7 seeded and fertilized.
October 18	All seven instrument vaults completed, ready for plumbing and tipping buckets.
October 23	Plot 5 soil found to have no structure (wet slurry).
October 25	Weather station operational (rain gage temporarily mounted on stick, pyranometer still covered).
November 2	Pyranometer operational.
	8-inch non-standard gage placed between Plots 3 and 4.
November 3	Plots 4 and 7 observed to have no soil/root structure (wet slurry).
November 6	Rain gage permanently mounted to post.

December 2	Subsurface buckets operational (except Plot 4).
December 8	Gutter installation begins.
December 16	Gutter installation complete.
December 18	Plumbing and surface buckets completed, Plots 2,3,4,6, and 7.
December 20	Gutter installed, Plot 1 (replaced prototype gutter)
	* All subsurface buckets now logging (except Plot 4)
	* All surface buckets (except Plots 3,5) now logging.

1995

January 12	Activated subsurface bucket, Plot 4 now operational.
January 19	Moved 8-inch non-standard gage into fenced enclosure.
	Fixed Plot 2 leak (PVC had popped out).
	Added grass seed to lower end of plots.
	Plot 3 surface bucket made operational, Plot 3 gutter dropped 1.5 inches.
February 2	Surface gutter/soil interfaces sealed with bentonite to improve capture.
February 9	Plot 5: still slurry-like; had replaced subsurface collection system, added surface gutter, and installed tippers: now fully operational.
February 11	Installed piezometers, Plots 3 and 4 (5' and 16' from downslope end).
February 23	Spent 23rd and 24th calibrating all tipping buckets.
February 28	Performed rain gauge calibration check.
	Performed conductivity tests on Plots 1,2,3, and 4.
March 2	Performed rain gauge calibration check.
	Installed piezometers, Plot 6.
March 17	Mounted tippers on patio stones: Plots 1,2,3,5, and 6.
April 22	Calibrated tippers in Plots 1,2,3,5, and 6.
April 25,26	First storm simulations.
May 10	Installed piezometers, Plot 5.

Appendix B: Rainfall depths and events

Table B-1: Daily rainfall totals recorded at the site

(All rainfall amounts in inches)

Date	Nov	Dec	Jan	Feb	Mar	Apr	May	Jun
1	0.03	0.21	0	0.21	0	0.18	0.09	0
2	0.11	0	0	0	0	0	0.54	0
3	0.09	0	0	0.04	0	0	0	0
4	0.47	0	0	0	0.04	0.12	0	0.13
5	0.01	0	0	0	0.03	0	0.02	0.39
6	0.20	0.10	0	0	0	0.08	0	0.01
7	0	0	0.26	0	0	0.64	0	0
8	0.54	0.11	0.24	0	0.54	0.02	0.04	0
9	0.30	0	0.39	0	0.52	0	0.10	0
10	0	0.10	0.18	0	0.63	0.30	0.01	0.34
11	0.21	0.12	0.17	0.09	0.20	0.01	0.42	0
12	0.15	0	0.24	0	0	0.35	0	0.20
13	0	0	0.21	0	0.36	0.53	0	0.03
14	0.04	0.21	0.33	0.01	0.41	0.04	0	0.05
15	0.33	0.36	0	0.35	0	0	0	0
16	0.74	0.15	0.04	0.33	0	0	0	0
17	0.42	1.01	0.08	0.26	0.12	0.33	0.03	0.25
18	0	0.16	0.13	0.97	0.27	0.29	0	0.02
19	0.30	1.36	0.01	0.78	0.12	0	0	0.01
20	0	0.77	0	0.07	0.30	0.13	0	0.02
21	0.01	0	0	0	0.04	0	0	0
22	0.05	0.01	0	0	0.03	0	0	0
23	0.24	0	0	0	0.43	0	0	0
24	0.04	0.08	0	0.07	0.29	0	0	0
25	0.17	0.29	0	0.02	0	0	0	0
26	0.01	1.18	0.03	0	0	0	0	0
27	0.21	0.74	0	0	0	0	0	0
28	0.11	0	0.38	0	0	0	0	0
29	0.15	0	0.57	*	0	0.30	0	0
30	0.97	0	0.64	*	0	0	0	0
31	*	0.01	0.87	*	0.04	*	0	*
Monthly Total:	5.91	6.97	4.77	3.18	4.40	3.33	1.26	1.46

Table B-2: Recorded rainfall depths ranked by magnitude
Period of record: December 19, 1994 to June 26, 1995

(a) Hourly rainfall depths

Rank	Date	Time	Depth (in)
1	Apr 13	1900	0.27
2	May 2	600	0.25
3	May 11	1600	0.24
4	Apr 17	2200	0.18
5	Jan 30	800	0.17
6	Apr 18	2200	0.17
7	Mar 23	400	0.16

(b) 6-hour rainfall depths

Rank	Date	Time	Depth (in)
1	Dec 26	500	0.61
2	Dec 27	400	0.58
3	Feb 18	1600	0.58
4	May 2	700	0.51
5	Jan 30	1100	0.50
6	Apr 13	1900	0.49
7	Feb 19	1800	0.48
8	Jan 31	1100	0.43
9	Jan 29	600	0.39
10	Jun 5	600	0.38
11	Mar 14	1100	0.36

Depth is recorded rainfall in previous 6 hours

(c) 24-hour rainfall depths

Rank	Date	Time	Depth (in)
1	Dec 27	1000	1.33
2	Feb 18	2400	0.97
3	Jan 31	2200	0.93
4	Jan 29	1200	0.91
5	Mar 9	1100	0.77
6	Feb 20	100	0.76

Depth is recorded rainfall in previous 24 hours

Appendix C - Periods of operation for the flow measuring tipping buckets

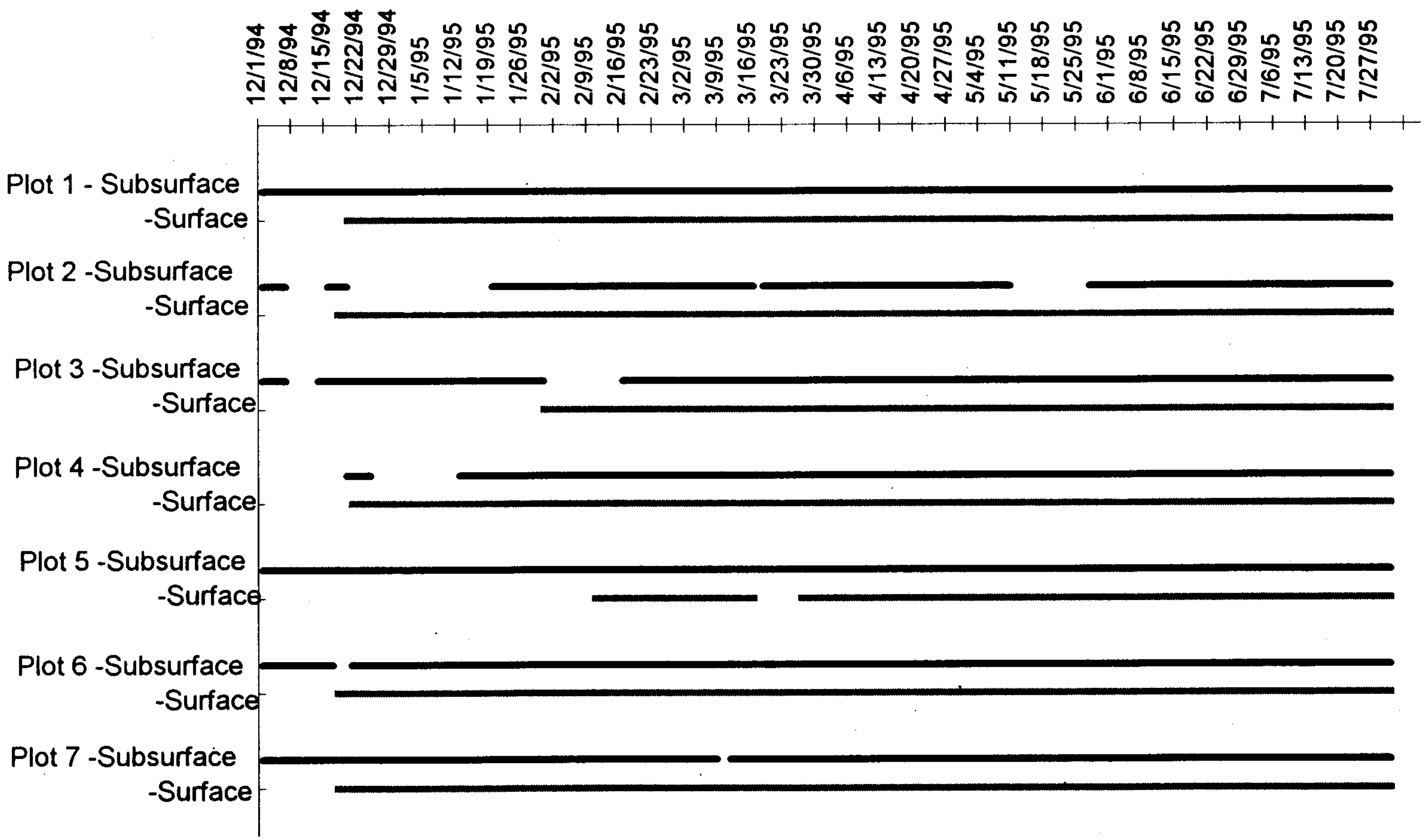

Figure C-1: Periods of operation for the flow-measuring tipping buckets

Appendix D: Soil analyses from August 31 and December 13, 1994

Table D-1: Soil analysis of August 31, 1994

Sample source	Total C %	Total N %	Field Capacity g/g %	Field Capacity ml/ml %	Total porosity %	Bulk density g/cm3	Particle density g/cm3	% particles in size category (mm) by weight			
								2-0.02 %	0.02-0.005 %	0.005-0.002 %	<0.002 %
Plot 1	0.2	0.12	20	28	48	1.37	2.63	76.3	12.5	1.3	10.0
	0.3	0.14	18	22	52	1.22	2.54	76.3	11.3	3.8	8.8
	0.3	0.13	18	21	56	1.15	2.64	76.3	12.5	1.3	10.0
	0.3	0.15	18	24	42	1.38	2.39	75.0	13.8	3.8	7.5
	0.2	0.12	16	20	49	1.28	2.53	76.3	13.8	2.5	7.5
	0.3	0.10	16	22	46	1.35	2.50	76.3	13.8	1.3	8.8
	0.5	0.12	16	20	52	1.23	2.54	76.3	13.8	1.3	8.8
	0.2	0.11	28	35	50	1.26	2.54	76.3	12.5	1.3	10.0
Plot 2	2.2	0.26	37	41	47	1.12	2.12	73.8	12.5	6.3	7.5
	2.6	0.27	39	39	56	0.98	2.23	77.5	10.0	5.0	7.5
	3.4	0.28	34	33	52	0.95	1.97	77.5	10.0	5.0	7.5
	2.7	0.25	32	36	49	1.14	2.25	77.5	10.0	5.0	7.5
	2.8	0.24	33	37	47	1.14	2.13	77.5	10.0	5.0	7.5
	2.0	0.22	32	35	53	1.07	2.29	73.8	12.5	6.3	7.5
	2.5	0.30	46	49	48	1.06	2.03	76.3	10.0	6.3	7.5
	4.5	0.36	27	30	44	1.14	2.05	73.8	12.5	6.3	7.5

Appendix E - Evapotranspiration rate estimation procedures

E.1 Background

Evapotranspiration depths for the field study were estimated using the Penman-Monteith equation. This equation determines the rate of exchange of heat from a wet surface to the surrounding air [*Monteith*, 1990, pp. 183 - 185]. In this case the wet surface may be either bare ground or a grass blade.

$$\lambda E_t = \frac{\Delta}{\Delta + \gamma^*}(R_n - G) + \frac{\gamma}{\Delta + \gamma^*} K_1 \frac{0.622\lambda\rho}{P}\frac{1}{r_a}(e_z^o - e_z) \qquad \text{[Jensen, 1990]}$$

where the variables are as follows:

λ	Latent heat of vaporization of water
E_t	Potential evaporation from vegetation
Δ	Slope of the saturation vapor pressure curve for water
γ	Psychrometric constant
γ^*	Apparent psychrometric constant
R_n	Net radiation
G	Soil heat flux density
K_1	Dimensionless coefficient for unit conversion
ρ	Air density
P	Air pressure
r_a	Aerodynamic resistance to vapor transfer
$(e_z^o - e_z)$	Air vapor pressure deficit

The equation determines the change in latent heat of the wet surface, so it is solved for the rate of evaporation by dividing by the latent heat of vaporization of water (λ). This form of the equation is given below with some additional modifications based on the Ideal Gas Law and the definition of the psychrometric constant [*Campbell Scientific documentation*].

$$ET_o = \frac{\Delta(R_n - G)}{\lambda(\Delta + \gamma^*)} + \frac{\gamma^* M_w(e_a - e_d)}{R\Theta r_v(\Delta + \gamma^*)}$$

where the variables with their units are as follows:

ET_o	Potential evaporation (kg m^{-2} s^{-1} = mm/s)
R_n	Net radiation (kW/m^2)
G	Soil heat flux density (kW/m^2)
M_w	Molecular mass of water (0.018 kg/mol)
R	Gas constant (8.31 x 10^{-3} kJ mol^{-1} K^{-1})
Θ	Approximate temperature (293 Kelvin)
$(e_a - e_d)$	Air vapor pressure deficit (Pa)
λ	Latent heat of vaporization of water (2450 kJ/kg)
r_v	$= r_c + r_a$ = canopy + boundary layer resistance for vapor (s/m)
Δ	Slope of the saturation vapor pressure curve for water (Pa/°C)
γ^*	Apparent psychrometric constant (Pa/°C)

The first term involves solar heat input and absorption which warm the surface and increase the rate of evaporation. The second term accounts for the gain in heat from convection and loss through evaporation in an adiabatic process. [*Monteith*, 1990].

The calculated value for *potential evapotranspiration*, ET_0, is not necessarily equal to the *potential evaporation* [*Brutsaert*, 1982, p. 214]. The potential evaporation rate is achieved only when a large, uniform surface is evenly supplied with sufficient moisture to keep the air at the surface saturated. Potential evapotranspiration includes the effects of actively growing vegetation on vapor transfer and surface roughness, which are generally difficult to measure. However, for short, non-wet vegetation the difference between potential evapotranspiration and potential evaporation is small.

Another complication in the concept of potential evapotranspiration lies in the measurement of atmospheric parameters for calculating potential evapotranspiration. The levels of energy and moisture in the atmosphere near the ground and the availability of moisture on the ground are interdependent. Thus measurements may be taken and used to estimate potential evapotranspiration, although in actuality the conditions required in the concept of potential evaporation (a large, uniform, moisture-supplied surface) do not exist; if they did, the observed atmospheric conditions would be different [*Brutsaert* 1982, pp. 214-215]. These considerations are important conceptually, but as yet there is no practical method available to compensate for them.

E.2 Algorithm for estimating potential evapotranspiration

Variables used in the algorithm to estimate potential evapotranspiration are listed below in the order in which they are encountered when using the algorithm. Variables in **bold** are collected by the weather station. Variables in *italics* are site parameters which are assumed to be constant for every computation period. The rest of the variables are computed.

Lnic	Atmospheric radiant emittance minus the crop emittance in clear skies (kW/m^2)
T	**Air temperature (°C) at 2 meters**
d	Solar declination angle
DOY	**Day of year**
j	Day of year divided by 100
L_c	Longitude correction
L_s	*Standard meridian (0, 15, 30, ..., 345 degrees)*
L	*Site longitude*
t_e	"Equation of time"
t_o	Time of solar noon
t	**Datalogger time (hour)**
ϕ	Elevation angle of the sun
Lat	*Site latitude*
S_o	Potential solar radiation on a horizontal surface outside the Earth's atmosphere (kW/m^2)
L_{ni}	Atmospheric radiant emittance minus the crop emittance at air temperature (kW/m^2)
S_t	**Incident solar radiation measured by the weather station pyranometer (kW/m^2) (400 to 1000 nanometer wavelength)**
a_s	*Absorptivity of the crop for solar radiation*

d	Crop (grass) boundary layer displacement height (m)
H	Mean height of the crop canopy (m)
z_{om}	Roughness length for momentum transfer (m)
z_{oh}	Roughness length for vapor transfer (m)
r_a	Convective resistance for heat transfer (sec/meter)
u_3	**Wind speed at 3 meters (m/s)**
r_c	*Canopy resistance (sec/meter)*
A	*Site altitude (m)*
RH	**Relative humidity (fraction)**

All evapotranspiration depths were calculated on an hourly basis, the time step at which the procedure is most accurate [*Jensen*, 1990, p. 96]. The steps taken to estimate the potential evapotranspiration rate given the site parameters and hourly climatic data are given below.

(1) $Lnic = 0.0003\ T - 0.107$

(2) $\sin d = -0.37726 - 0.10564j + 1.2458j^2 - 0.75478j^3 + 0.13627j^4 - 0.00572j^5$

(3) $\cos d = (1 - \sin d^2 d)^{1/2}$

(4) $L_c = (L_s - L)/15$

(5a) $t_e = -0.04056 - 0.74503j + 0.08823j^2 + 2.0516j^3 - 1.8111j^4 + 0.42832j^5$

day < 180, j = (day of year)/100

(5b) $t_e = -0.05039 - 0.33954j + 0.04084j^2 + 1.8928j^3 - 1.7619j^4 + 0.4224j^5$

day > 180, j = (day of year - 180)/100

(6) $t_o = 12 - L_c - t_e$ [hours]

(7) $\sin\phi = (\sin d)(\sin Lat) + (\cos d)(\cos Lat)(\cos[15(t-t_o)])$

(8) $S_o = 1.36 \sin\phi$

(9) $$L_{ni} = \left(1 - \frac{1}{1 + 0.034 \exp\{7.9 S_t / S_o\}}\right) L_{nic}$$

(10) $R_n = a_s S_t + L_{ni}$

(11a) $G = 0.1 R_n$ for $S_t > 0$

(11b) $G = 0.5R_n$ for $S_t = 0$ (night)

(12) $\Delta = 45.3 + 2.97T + 0.0549T^2 + 0.00223T^3$ [Pa/° C] for $-5 < T < 45$ °C

(see also Equation 5-24a, *Linsley et al*, 1982]).

(13a) $$r_a = \frac{\ln\left(\frac{z_u - d}{z_{om}}\right)\ln\left(\frac{z_t - d}{z_{oh}}\right)}{k^2 u_3}$$ where $d = (2/3)H$, $z_{om} = 0.12H$, $z_{oh} = 0.1\ z_{om}$

(13b) $r_a = 240/u_3$ (Simplification of 13a; see text below)

(14) $r_v = r_a + r_c$

(15) $\gamma = 67.3 \exp\{-A/8500\}$

(16) $\gamma^* = \gamma\ (r_v/r_a) = \gamma\ (1 + r_c/r_a)$

(17) $$e_a = \exp\left\{\frac{-M_w\lambda}{R}\left(\frac{1}{T+273} - \frac{1}{273}\right) + \ln(0.601)\right\}$$ (Pa)

(18) $e_d = e_a * RH$

(19) Campbell Scientific approximation to Penman-Monteith Equation:

$$ET_o = \frac{\Delta(R_n - G)}{\lambda(\Delta + \gamma^*)} + \frac{\gamma * M_w(e_a - e_d)}{R\Theta r_v(\Delta + \gamma^*)}$$ (mm/sec)

The estimated evapotranspiration rate ET_0 is then multiplied by 3600 to obtain the evapotranspiration depth in mm for the previous hour.

E.3 Sample results and sensitivity analysis

To demonstrate the variability of evapotranspiration rates depending on atmospheric conditions, estimated evapotranspiration rates are shown in Table E-1 for three days: February 18, April 3, and June 9, 1995. February 18 was cool, cloudy, and rainy (25 mm in 24 hours). April 3 was partly cloudy and warm and was followed by a week of rain. June 9 was clear, sunny, and warm. Table E-1 shows the parameters for the Penman-Monteith equation and the results of the calculation procedures. All evapotranspiration estimates are for the period of 12:00 to 13:00 Pacific Standard Time. (Site parameters:

latitude = 46.5°, longitude = 122°, standard meridian =120°, altitude = 6 meters, r_c = 80 s/c, a_s = 0.77.)

Table E-1: Sample evapotranspiration estimates for two days at 13:00

Conditions	February 18	April 3	June 9
Temp, °C (°F)	11 (51)	18 (64)	26 (79)
RH, %	97	51	35
u_3, m/s (mph)	1.8 (4)	0.9 (2)	1.8 (4)
S_t , kW/m^2	0.194	0.697	0.880
Day of year	49	93	160
Time (PST)	1300	1300	1300
ET (mm/hr)	0.08	0.38	0.60

The first term of the Penman-Monteith equation was more significant in both of these calculations. The fist term accounted for 97% of the ET on February 18 and 84% of the ET on June 6. The second term becomes more significant when the relative humidity is low.

Equation (13b) was used rather than Equation (13a) to simplify the calculations. Equation (13a) is derived from Equation (13a) when the following values are assumed: z_t = 3 m, H = 0.12 m. During an hour with typical input parameter values (the base case described in the next paragraph) the estimated evapotranspiration rate is 0.262 mm/hr. Using the same input parameters but the actual values z_t = 1.5 m and H = 0.05 m, the estimated evapotranspiration rate is 0.264 mm/hr. The error is less than 1% so the simplification is acceptable.

To check the validity of the Campbell Scientific modification of the Penman-Monteith equation, the original form of the equation [*Jensen*, 1990] was used to estimate the potential evapotranspiration rates in the three sample cases of Table E-1. The air pressure was assumed to be equal to 101.3 kPa, standard atmospheric pressure at sea level. The air density was calculated as a function of the air pressure, air temperature, and mixing ratio (*Jensen*[1990], Eq. 2.4 and p. 285). The apparent psychrometric constant was also calculated differently, using Eq. 6.19 from *Jensen* [1990], $\gamma^* = \gamma(1 + r_c/r_a)$. The estimated potential evapotranspiration rates agreed to within 0.01 mm/hr with the estimates from Campbell Scientific's modified equation.

The sensitivity of the Penman-Monteith equation to the various input parameters was examined by estimating the hourly evapotranspiration rate for a set of typical input parameters. The input values and resulting potential evapotranspiration rate make up the base case. The effect of each parameter on the potential evapotranspiration estimate was determined by altering the values of each of the parameters while keeping the other parameters constant. The resulting potential evapotranspiration rates were compared to the rate calculated from the base case.

Figure E-1 shows the percent change in the evapotranspiration rate caused by changes in each of the input parameters. Temperature and solar radiation had the greatest effect on the ET rate with the relationships nearly linear through the range of values tested. The effects of relative humidity and the day of year were small, and wind speed was nearly irrelevant with the base conditions chosen for the examination.

E.4 References

Brutsaert, W., Evaporation into the Atmosphere, D. Reidel Publishing Company, Dordrecht, Holland, 1982.

Campbell Scientific, Inc., and G.S. Campbell, "Online estimation of grass reference evapotranspiration with the Campbell Scientific Automated Weather Station," product documentation.

Jensen, M.E., R.D. Burman, and R.G. Allen, Evapotranspiration and Irrigation Water Requirements, ASCE Manuals and Reports on Engineering Practice, No. 70, 1990.

Linsley, R.K., M.A. Kohler, and J.L.H. Paulhus, Hydrology for Engineers, 3rd Edition, McGraw-Hill, 1982.

Monteith, J.L., and M.H. Unsworth, Principles of Environmental Physics, Second Edition, Distributed in USA by Routledge, Chapman, and Hall, Inc., 1990.